AD_____
(Leave blank)

Award Number: W81XWH-06-1-0010
(Enter Army Award number assigned to research, i.e., DAMD17-00-1-0296)

TITLE: Molecular modulation of inhibitors of apoptosis as a novel approach for radiosensitization of human prostate cancer

PRINCIPAL INVESTIGATOR: Liang Xu, M.D., Ph.D.

CONTRACTING ORGANIZATION:
University of Michigan
Ann Arbor, MI 48109-5637

REPORT DATE: November 2008

TYPE OF REPORT: Annual report

PREPARED FOR: U.S. Army Medical Research and Materiel Command
Fort Detrick, Maryland 21702-5012

DISTRIBUTION STATEMENT: (Check one)

X Approved for public release; distribution unlimited

☐ Distribution limited to U.S. Government agencies only; report contains proprietary information

REPORT DOCUMENTATION PAGE

Form Approved
OMB No. 0704-0188

1. REPORT DATE *(DD-MM-YYYY)*	2. REPORT TYPE	3. DATES COVERED *(From - To)*
11-14-2008	Annual report	15 OCT 2007 - 14 OCT 2008

4. TITLE AND SUBTITLE

Molecular modulation of inhibitors of apoptosis as a novel approach for radiosensitization of human prostate cancer

5a. CONTRACT NUMBER
W81XWH-06-1-0010

5b. GRANT NUMBER

5c. PROGRAM ELEMENT NUMBER

6. AUTHOR(S)

Liang Xu, M.D., Ph.D.

Email: liangxu@umich.edu

5d. PROJECT NUMBER

5e. TASK NUMBER

5f. WORK UNIT NUMBER

7. PERFORMING ORGANIZATION NAME(S) AND ADDRESS(ES)

University of Michigan
4424E Med Sci I
1301 Catherine St.
Ann Arbor, MI 48109-5637

8. PERFORMING ORGANIZATION REPORT NUMBER

9. SPONSORING / MONITORING AGENCY NAME(S) AND ADDRESS(ES)

U.S. Army Medical Research and Materiel
Fort Detrick, Maryland 21702-5012

10. SPONSOR/MONITOR'S ACRONYM(S)

11. SPONSOR/MONITOR'S REPORT NUMBER(S)

12. DISTRIBUTION / AVAILABILITY STATEMENT

13. SUPPLEMENTARY NOTES

14. ABSTRACT

The major goal of the project is to investigate the radiosensitization activity and mechanism of action of novel IAP-inhibitors in prostate cancer. In the third year of the project, we have investigated the *in vivo* radiosensitization activity of our lead IAP-inhibitors, SH-130 and Embelin, and mechanism of action in human prostate cancer xenograft model. IAP-inhibitors potently enhanced radiation-induced tumor growth inhibition, together with increased induction of apoptosis. In nude mouse xenograft models, IAP-inhibitors Embelin and SH-130 potently sensitized the DU-145 tumors to X-ray radiation. Mechanism studies show that NK-kB pathway activation was also inhibited in the combination therapy. Interestingly, we also observed anti-angiogenic effect of the combination treatment. Due to the lab move in March, 2008, together with our animal room moved and more importantly the move of our X-ray irradiator at the same time, our animal experiments were delayed. We have requested and obtained approval a one year no-cost extension for finish the planned animal and MOA studies.

15. SUBJECT TERMS
apoptosis, radiation, IAP

16. SECURITY CLASSIFICATION OF:			17. LIMITATION OF ABSTRACT	18. NUMBER OF PAGES	19a. NAME OF RESPONSIBLE PERSON
a. REPORT	b. ABSTRACT	c. THIS PAGE			Liang Xu
Unclassified	Unclassified	Unclassified	Unlimited	74	19b. TELEPHONE NUMBER *(include area code)* 734-615-7017

Table of Contents

I. Introduction:

In this project, we will investigate in vitro and in vivo radiosensitization activity and the mechanism of action of IAP-inhibitors in human prostate cancer with IAPs overexpression. Our basic hypothesis to be tested is that (1) The IAPs play a critical role in radiation resistance of human prostate cancer overexpressing IAPs; (2) Inhibition of the anti-apoptotic function of IAPs by small molecule IAP inhibitors will overcome radioresistance rendered by the overexpressed IAPs, that in turn will enhance tumor response and restore sensitivity of prostate cancer cells to ionizing irradiation. Our goal is to investigate and validate that IAPs are promising novel targets for radiosensitization of human prostate cancer with IAP-overexpression, with the ultimate goal to establish the molecular modulation of IAPs by potent small molecule IAP inhibitors as a novel approach for overcoming radiation resistance of human prostate cancer with high levels of IAPs.

II. Research progress and key research accomplishments:

This is the third year of the project. We have finished the part of the tasks proposed in the *approved* Statement of Work for the corresponding period of time. Due to the lab move from Kresge to Med Sci I Building in March, 2008, together with our animal room moved from Kresge to MSRB II and more importantly the move of our X-ray irradiator at the same time, our animal experiments (which requires X-ray radiation for the tumors in nude mice) were delayed, and many animals had to be ordered after our move. We have requested and obtained approval a one year no-cost extension for finish the planned animal and MOA studies.

Specifically, we have finished the following tasks:

A. Task 3. To investigate in vivo radiosensitization activity of small molecule inhibitors of IAP in human prostate cancer animal models with IAP overexpression. (months 13-36)

A.1. Employ nude mouse xenograft model of human prostate cancer to investigate radiosensitization efficacy of IAP inhibitors in vivo (months 15-24)

To evaluate whether our Smac-mimetic IAP-inhibitors can radiosensitize human prostate cancer with high levels of IAPs *in vivo*, we carried out animal studies using human prostate cancer PC-3 and DU-145 xenograft models in nude mice. The PC-3 and DU-145 tumor models were established as we previously described. When the tumors reached a size of 120mm^3 for PC-3 model, the mice were randomized (6-8 mice/12-16 tumors/group) and treated with our lead Smac-mimetic IAP-inhibitor, Embelin, 60mg/kg p.o. via oral gavage, q.d.5 x 3, or X-ray irradiation, 2 Gy q.d.5 x 2, or Embelin followed with radiation within 30min as combination therapy. The irradiation was performed as we recently described, with only tumor area exposed while the main body of a mouse was shielded. Although Embelin alone had moderate effect on tumor growth, it significantly enhanced PC-3 tumor response to X-ray irradiation ($p<0.01$, two-way ANOVA, n=12).

For DU-145 tumor model, when the tumors reached a size of 60-80mm^3, the mice were randomized (5-8 mice/10-16 tumors/group) and treated with our lead Smac-mimetic IAP-inhibitor, **SH-130**, 50mg/kg i.v. q.d.5 x 2, or X-ray irradiation, 2 Gy q.d.5 x 2, or SH-130 followed with radiation within 30min. DU-145 tumor model is more resistant to radiation, consistent with our earlier reports. However, SH-130 potently sensitized the DU-145 tumors to X-ray irradiation, without increasing toxicity to the animals. The combination therapy inhibited the tumor growth, significantly more effective than either treatment alone ($p<0.001$, n=14). No obvious animal toxicity was observed. Notably, 5 out of 14 tumors in the combination group showed complete regression that did not grow back 5 months after the therapy, whereas radiation alone had only 2 out of 10 tumors with complete regression, no complete regression in SH-130 alone or vehicle control groups.

The above studies are summarized in our paper in press in **Clin Cancer Res** (2008), attached below.

These preliminary *in vivo* radiation studies provide us a strong proof-of-principle that a potent IAP-inhibitor can indeed sensitize a radioresistant tumor to radiation therapy, although the dose, schedule, and sequence of

the two treatments are yet to be optimized in the combination therapy. The latter will be investigated in detail in the current proposal in multiple animal tumor models. Interestingly, in both *in vivo* studies, SH-130 alone showed no obvious effect on tumor growth; this is consistent with our *in vitro* data that SH-130 does not have single agent activity in terms of cytotoxicity. Having potent radiosensitizing activity without direct cytotoxicity to cells may be the unique feature for our lead compound SH-130 to be developed as a novel molecularly targeted radiosensitizer for cancers with IAP overexpression.

A.2. Immuohistological study of apoptosis induction and biomarkers in above animal models in response to IAP inhibitors and radiation therapy. (months 15-36)

We have collected the samples in our efficacy studies and processed for immunohistological analysis. IAP inhibitors enhanced radiation induced apoptosis as indicated with significantly increased TUNEL+ cells. The data are included in two manuscripts in preparation.

B. Task 4. To investigate the mechanism of action of small molecule inhibitors of IAP in overcoming radiation resistance of prostate cancer. (months 13-36)

B.1. Molecular target selectivity analysis using transfected cells.

We have established a series of clones of IAP transfected cells. The evaluations of these clones are still ongoing.

B.2. **IAP-inhibitors inhibit NF-κB activation**

A recent study suggests that IAP-inhibitor, Embelin, also inhibits NF-κB activation by TNFα. We confirmed this finding in prostate cancer cells. To investigate whether this is true only for natural compound such as Embelin that may have multiple targets, we analyzed the effect of SH-130, our more potent and specific IAP-inhibitor, on the NF-κB activation in prostate cancer cells. SH-130 inhibited TNFα-induced IκBα degradation, an indication of NF-κB activation by the canonical pathway. The negative control compound SH-123 that does not bind to IAPs has no effect on NF-κB. SH-130-mediated NF-κB inhibition is partial and dose-dependent, without significant change of Rel A translocation, suggesting that SH-130-mediated inhibition of NF-κB activation is indirect.

Above data were confirmed by a quantitative, luciferase-based NF-κB reporter assay. SH-130 and Embelin inhibited TNFα-induced NF-κB activation in NF-κB luciferase reporter assay. This inhibition could not be blocked by Pan-Caspase inhibitor zVAD, indicating that the IAP-inhibitor-mediated NF-κB inhibition does not involve Caspases. This NF-κB inhibition is partial, even at high doses of IAP-inhibitors, comparing with celastrol, a natural proteosome inhibitor that completely blocked NF-κB activation, consistent with the recent literature. In a separate qRT-PCR assay of NF-κB target gene expression, Embelin also partially block NF-κB activation.

The above studies are summarized in our paper in press in **Clin Cancer Res** (2008), and a manuscript under review, both are attached below.

Taken together, our preliminary data with NF-κB activation studies demonstrate that IAP-inhibitors Embelin and SH-130 can block NF-κB activation without involving Caspases. This partial and apparently indirect inhibition of NF-κB activation indicates a potential role of IAP – Smac in NF-κB pathway other than classical apoptosis pathway. Based on these exciting new finding and recent publications in the literature, we propose a potential link or crosstalk between IAP-apoptosis pathway and NF-κB pathway: the TRAF-cIAP–(Act1)–NEMO loop. Delineation of this link/crosstalk is beyond the current funded project and is one of the aims in the R01 proposal to be submitted.

III. Reportable outcomes:

A. Three papers published/in press.

1. Meng Y, Tang W, Dai Y, Wu X, Liu M, Ji Q, Ji M, Pienta K, Lawrence TS, and **Xu L**. Natural BH3-mimetic chemosensitizes human prostate cancer via Bcl-xL inhibition accompanied by increase of Puma and Noxa. *Mol Cancer Ther* 2008; **7**(7):2192-2202.
2. Dai Y, Lawrence TS and **Xu L**. Overcoming cancer therapy resistance by targeting inhibitors of apoptosis proteins and nuclear factor-kappa B. *Am J Transl Res* 2009; 1(1):4-18. (http://www.ajtr.org/V1_No1.html)
3. Dai Y, Liu M, Tang W, DeSano J, Burstein E, Pienta K, Lawrence TS, **Xu L**. Molecularly targeted radio-sensitization of human prostate cancer by modulating inhibitor of apoptosis. *Clin Cancer Res* 2008 (in press).

B. One manuscript is under review and one manuscript on Embelin radiosensitization will be submitted soon.

Yao Dai, Meilan Liu, Kenneth Pienta, Theodore Lawrence, and **Liang Xu**. A Smac-mimetic sensitizes prostate cancer cells to TRAIL-induced apoptosis via modulating both IAPs and NF-κB. (Submitted to BMC Cancer)

C. Funded from this PRCP grant, two abstracts were presented in national or international meetings, and one abstract will be submitted to 2008 AACR annual meeting.

- Dai, et al. Molecularly targeted cancer radiosensitization of prostate cancer by modulating IAP. *The American Association for Cancer Research 99th Annual Meeting*, San Diego, California, April 14-18, 2008. (**Oral presentation**)
- **Xu L**, et al. Molecular radiosensitization of prostate cancer by modulating cell death pathways. The First SANTRO (Sino-American Therapeutic Radiation Oncology) Conference, Beijing, China, August 26-29, 2008. (**Oral presentation**)

IV. Conclusions:

The major goal in the thirdyear of the project is to investigate the radiosensitization activity in vivo and the mechanism of action of novel IAP-inhibitors in prostate cancer models. We have investigated the *in vivo* radiosensitization activity of our lead IAP-inhibitors, SH-130 and Embelin, in human prostate cancer xenograft models. In nude mouse xenograft models, IAP-inhibitors Embelin and SH-130 potently sensitized the DU-145 tumors to X-ray radiation. Bioluminescence imaging confirmed SH-130 plus radiation resulted in complete tumor regression in 6 out of 10 tumors, comparing 2/10 tumors with radiation alone, and 0/10 tumors with SH-130 alone. Mechanism studies show that IAP-inhibitors increased radiation-induced apoptosis in vivo. NK-kB pathway activation was also inhibited in the combination therapy.

Due to the lab move in March, 2008, together with our animal room moved and more importantly the move of our X-ray irradiator at the same time, our animal experiments were delayed. We have requested and obtained approval a one year no-cost extension for finish the planned animal and MOA studies. In the requested 12-month extension, we will carry out the animal studies proposed in the original Statement of Work for third year in our proposal, without changing the scope and content of our original Statement of Work.

VI. APPENDICES:

1. One paper in press: Clin Cancer Res 2008.
2. One paper published: Mol Cancer Ther 2008; **7**(7):2192-2202.
3. One paper published: *Am J Transl Res* 2009; 1(1):4-18. (http://www.ajtr.org/V1_No1.html).
4. One manuscript under review: BMC Cancer.

Molecularly Targeted Radiosensitization of Human Prostate Cancer by Modulating Inhibitor of Apoptosis

Yao Dai,[1] Meilan Liu,[1] Wenhua Tang,[1] Jeffrey DeSano,[1] Ezra Burstein,[2] Mary Davis,[1] Kenneth Pienta,[2,3] Theodore Lawrence,[1] and Liang Xu[1]

Abstract

Purpose: The inhibitor of apoptosis proteins (IAP) are overexpressed in hormone-refractory prostate cancer, rendering the cancer cells resistant to radiation. This study aims to investigate the radiosensitizing effect of small-molecule IAP inhibitor both *in vitro* and *in vivo* in androgen-independent prostate cancer and the possible mechanism of radiosensitization.

Experimental Design: Radiosensitization of SH-130 in human prostate cancer DU-145 cells was determined by clonogenic survival assay. Combination effect of SH-130 and ionizing radiation was evaluated by apoptosis assays. Pull-down and immunoprecipitation assays were employed to investigate the interaction between SH-130 and IAPs. DU-145 xenografts in nude mice were treated with SH-130, radiation, or combination, and tumor suppression effect was determined by caliper measurement or bioluminescence imaging. Nuclear factor-κB activation was detected by luciferase reporter assay and quantitative real-time PCR.

Results: SH-130 potently enhanced radiation-induced caspase activation and apoptosis in DU-145 cells. Both X-linked IAP and cIAP-1 can be pulled down by SH-130 but not by inactive SH-123. Moreover, SH-130 interrupted interaction between X-linked IAP/cIAP-1 and Smac. In a nude mouse xenograft model, SH-130 potently sensitized the DU-145 tumors to X-ray radiation without increasing systemic toxicity. The combination therapy suppressed tumor growth more significantly than either treatment alone, with over 80% of complete tumor regression. Furthermore, SH-130 partially blocked tumor necrosis factor-α- and radiation-induced nuclear factor-κB activation in DU-145 cells.

Conclusions: Our results show that small-molecule inhibitors of IAPs can overcome apoptosis resistance and radiosensitize human prostate cancer with high levels of IAPs. Molecular modulation of IAPs may improve the outcome of prostate cancer radiotherapy.

Androgen-independent disease is the main obstacle to improved survival and quality of life in patients with advanced prostate cancer. There is an urgent need for novel therapeutic strategies to overcome radioresistance in the treatment of advanced prostate cancer by specifically targeting the fundamental molecular basis of androgen-independent prostate cancer.

Authors' Affiliations: Departments of [1]Radiation Oncology, [2]Internal Medicine, and [3]Urology, University of Michigan Comprehensive Cancer Center, Ann Arbor, Michigan

Received 1/23/08; revised 6/13/08; accepted 7/5/08.

Grant support: Department of Defense Prostate Cancer Research Program grants W81XWH-04-1-0215 and W81XWH-06-1-0010 and NIH grant R01 CA121830-01 and R21 CA128220-01 (L. Xu) and NIH through the University of Michigan Cancer Center support grant 5 P30 CA46592. J. DeSano is a University of Michigan Undergraduate Research Opportunity Program student.

The costs of publication of this article were defrayed in part by the payment of page charges. This article must therefore be hereby marked *advertisement* in accordance with 18 U.S.C. Section 1734 solely to indicate this fact.

Note: Supplementary data for this article are available at Clinical Cancer Research Online (http://clincancerres.aacrjournals.org/).

Requests for reprints: Liang Xu, Division of Cancer Biology, Department of Radiation Oncology, University of Michigan Comprehensive Cancer Center, Room 4131, 1331 East Ann Street, Ann Arbor, MI 48109-0582. Phone: 734-615-7017; Fax: 734-615-3422; E-mail: liangxu@umich.edu.

doi:10.1158/1078-0432.CCR-08-0188

Most of the current anticancer therapies work, at least in part, through inducing apoptosis in cancer cells, including ionizing irradiation (1). Lack of appropriate apoptosis due to defects in the normal apoptosis machinery plays a crucial role in the resistance of cancer cells to a wide variety of current anticancer therapies. Radioresistance markedly impairs the efficacy of cancer radiotherapy and involves antiapoptotic signal transduction pathways that prevent radiation-induced cell death (2). The aggressive cancer cell phenotype is the result of a variety of genetic and epigenetic alterations leading to deregulation of intracellular signaling pathways, including an impaired ability of the cancer cell to undergo apoptosis (3). Primary or acquired resistance of hormone-refractory prostate cancer to current treatment protocols has been associated with apoptosis resistance in cancer cells and is linked to therapy failures (4, 5).

Current and future efforts toward designing new therapies to improve survival rates and quality of life for cancer patients will include strategies that specifically target cancer cell resistance to apoptosis. The inhibitors of apoptosis proteins (IAP) is an important class of intrinsic cellular apoptosis inhibitors (6, 7). IAPs potently suppress apoptosis against a large variety of apoptotic stimuli, including chemotherapeutics, radiation, and immunotherapy in cancer cells (8). The IAPs function as potent endogenous apoptosis inhibitors by directly binding to and effectively inhibiting three members of the caspase family of

Translational Relevance

Despite initial response to local therapy with surgery or radiation, many prostate cancer patients experience recurrence with advanced disease. Androgen ablation therapy produces only temporary responses because of the development of androgen independence. Failure to respond to radiation represents a critical problem in radiotherapy of hormone-refractory human prostate cancer. HRPC is resistant to apoptosis and IAPs have been shown to play a key role in apoptosis resistance. This study aims to investigate the radiosensitizing potential of a novel small-molecule IAP inhibitor both *in vitro* and *in vivo* in androgen-independent prostate cancer and the possible mechanism of radiosensitization. Our results show that the small-molecule IAP inhibitor radiosensitizes HRPC partly due to the enhanced apoptosis and inhibition of NF-κB induced by radiation. The data suggest that functional down-modulation of IAPs may be a promising approach for overcoming radiation resistance of HRPC. More importantly, the success of this strategy will pave the way to develop the small-molecule IAP inhibitors as an entirely new class of anticancer therapy for radiosensitizing human prostate cancer. The combination of IAP targeting molecular therapy and conventional radiotherapy may become a promising novel strategy to enhance the radiation efficacy and ultimately improve the survival of HRPC patients.

enzymes: two effector caspases (caspase-3 and -7) and one initiator caspase-9 (9). The X-linked IAP (XIAP) is perhaps the best characterized IAP member due to its potent activity (10). XIAP effectively inhibits both intrinsic and extrinsic apoptosis pathways by binding and inhibiting both initiator and effector caspases, whose activity is crucial for the execution of apoptosis (7, 11). Because effector caspase activity is both necessary and sufficient for irrevocable programmed cell death, XIAP functions as a gatekeeper to this final stage of the process. XIAP is widely expressed in cancer cell lines and tumor tissues and a high level of XIAP makes cancer cells apoptosis-resistant to a wide variety of therapeutic agents (12). cIAP-1/2 also inhibits both caspase-3 and caspase-7 although not as powerfully as XIAP (13).

Most components of the major cell death regulatory pathways have been implicated in radiation-induced cell death (14). It has been well established that IAPs, which are highly expressed in many types of cancer, including prostate cancer, appear to play a pivotal role in resistance to apoptosis induced by cancer therapy. Accumulating evidences show that XIAP and cIAP-1, two IAP members that are mostly studied for antiapoptosis and cell survival signaling, play a crucial role in chemoresistance or radioresistance (7). Specifically, radiation triggers apoptosis mediated by mitochondria, resulting in the release of mitochondrial proteins into cytoplasm, including Smac (15). The released Smac binds to XIAP and other IAP proteins and abolishes their antiapoptotic function. Because IAPs block apoptosis at the downstream effector phase, a point where multiple apoptosis signaling pathways converge, strategies targeting IAPs may prove to be highly effective in overcoming apoptosis resistance of human prostate cancer overexpressing IAPs. This link between radiation resistance and IAPs is supported by recent studies in which the suppression of XIAP levels by RNA interference or antisense indeed sensitized XIAP-overexpressing cancer cells to death receptor-induced apoptosis as well as radiation (16, 17).

Smac-based peptide inhibitors effectively overcome apoptosis resistance in different types of cancer cells with high levels of IAP and sensitize cancer cells to current therapeutic agents *in vitro* and *in vivo*, providing an important proof-of-concept for molecular therapy targeting IAPs (15, 18). Recently, we have designed Smac peptido-mimetics and nonpeptidic mimetics (Smac-mimetics) based on Smac peptide and the high-resolution experimental three-dimensional structures of Smac in complex with the XIAP BIR3 domain, called SH compounds (19, 20). These Smac mimetics are cell-permeable and have a much higher binding affinity to XIAP than the natural Smac peptide. Our preliminary results with newer and more potent Smac-mimetic IAP inhibitors show a 1 to 20 nmol/L binding affinity to XIAP BIR3 as well as potent cellular activity. These studies provide us with a solid foundation to determine if the IAPs are valid molecular targets for radiosensitization of human prostate cancer with IAP overexpression.

In this study, we evaluated the radiosensitizing effects of one of the Smac-mimetic IAP inhibitors, SH-130, in human prostate cancer cells with high levels of IAPs. We hypothesized that a Smac-mimetic targeting the IAP family of proteins would be highly effective in overcoming prostate cancer resistance to radiation therapy. We also investigated the potential molecular targets and mechanisms involved in the SH-130-mediated radiosensitization.

Materials and Methods

Reagents. Smac-mimetic compound SH-130, its negative control compound SH-123, and their biotin-labeled derivatives were dissolved in DMSO, stored as small aliquots at -20°C, and then diluted as needed in a cell culture medium. Recombinant human tumor necrosis factor-α (TNF-α) was obtained from Roche Applied Science. MG132 was provided by Biomol. High-glucose DMEM, fetal bovine serum, penicillin, streptomycin, and LipofectAMINE 2000 were purchased from Invitrogen. Pan-caspase inhibitor zVAD, caspase-3 substrate DEVD-AFC, and anti-Smac polyclonal antibody were purchased from Biovision. Crystal violet and β-actin antibody were purchased from Sigma-Aldrich. Antibodies against poly(ADP-ribose) polymerase (PARP), pro-caspase-3, p65/RelA, IκBα, and β-tubulin were purchased from Santa Cruz Biotechnology. Anti-XIAP and cIAP-1/2 antibodies were purchased from BD Biosciences. Survivin antibody was supplied by Novus Biologicals.

Cell culture. Human prostate cancer cell lines PC-3 and DU-145 and human normal fibroblast cell line WI-38 were purchased from the American Type Culture Collection. Luciferase stably transfected DU-145 cells (DU-145^{Lux}) were established as described previously (21). All types of cell lines were routinely cultured in high-glucose DMEM supplemented with 10% fetal bovine serum in a 5% CO_2 humidified incubator at 37°C. All media were also supplemented with 100 units/mL penicillin and 100 μg/mL streptomycin. Human normal prostate epithelial cell line PrEC was purchased from Lonza and maintained following the manufacturer's instruction.

Clonogenic cell survival assay. DU-145 cells were seeded in six-well plates at different cell densities (100-10,000 per well) and treated with SH-130 or SH-123 and X-ray radiation individually or in combination.

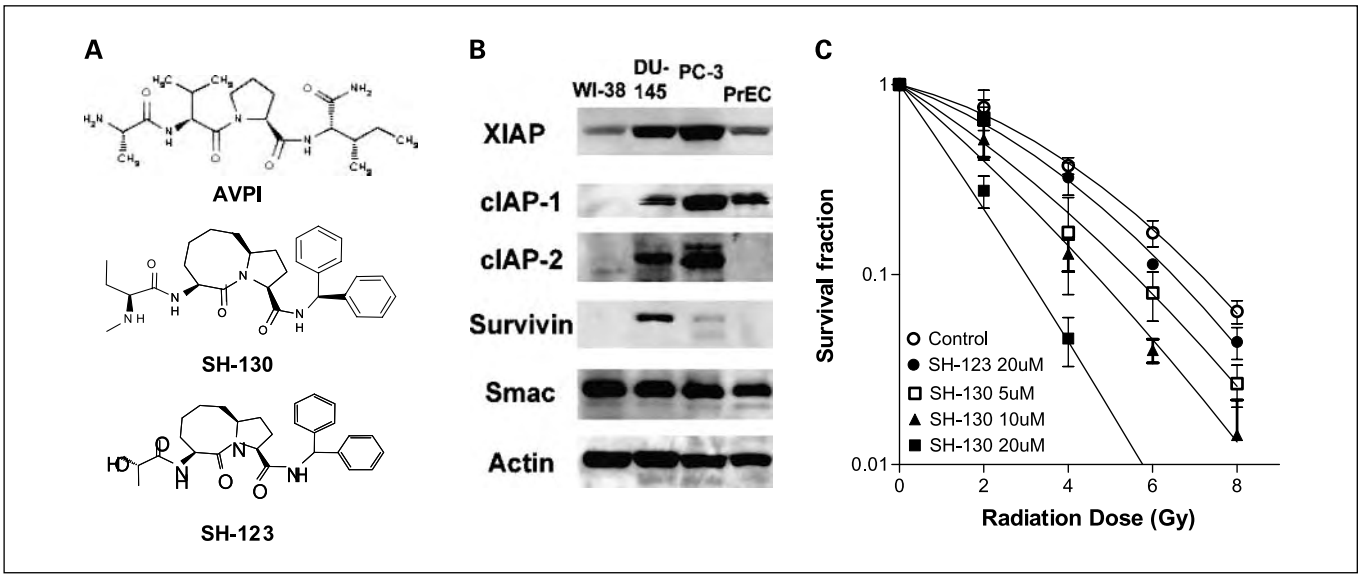

Q4

Fig. 1. *A,* structure of the Smac-mimetic compound SH-130 and an inactive control compound, SH-123. *B,* Western blot analysis of the expression of IAPs in human prostate cancer cells DU-145 and PC-3, with normal prostate epithelial cells PrEC and human fibroblast WI-38. *C,* SH-130–mediated radiosensitization of DU-145 cells by clonogenic survival assay. Cells seeded in six-well plates were treated with 5, 10, or 20 μmol/L SH-130 or 20 μmol/L SH-123, respectively, followed by 2, 4, 6, or 8 Gy X-ray radiation within 1 h. Each sample was tested in triplicate. After 14 d of incubation, colonies were stained by crystal violet and counted manually. Data were normalized and expressed as mean ± SD (n = 3). One of three independent experiments.

Solvent DMSO was used as a vehicle control. Each sample was tested in triplicate, and the cell medium was replaced 7 days later. After another 5 to 7 days of incubation, the plates were gently washed with PBS and stained with a 0.1% crystal violet solution. Colonies with over 50 cells were manually counted. The cell survival enhancement ratio was calculated as we described previously (22).

Western blot analysis. To determine the levels of protein expression in prostate cancer cell lines, cells were harvested and lysed in a radioimmunoprecipitation assay lysis buffer [50 mmol/L Tris-HCl (pH 8.0), 150 mmol/L NaCl, 0.1% SDS, 1% NP-40, 0.25% sodium deoxycholate, and 1 mmol/L EDTA] with freshly added protease inhibitor cocktail (Roche) for 15 min on ice and then centrifuged at 13,000 rpm for 10 min. Whole-cell extract was measured for total protein concentration using Bradford reagent (Bio-Rad), and proteins were resolved by SDS-PAGE (Bio-Rad). For nonreducing and non-denaturing SDS-PAGE, samples were mixed with loading buffer (no reducing agent) and directly loaded on a gel without boiling. After electrophoresis, the proteins were electrotransferred to nitrocellulose membranes (Bio-Rad), probed with the relevant primary antibody followed by horseradish peroxidase-conjugated secondary antibody (Pierce), and detected with the SuperSignal West Pico chemiluminescence substrate (Pierce). Intensity of the desired bands was analyzed using TotalLab software (Nonlinear Dynamics).

Apoptosis assay. To detect apoptosis, we used an Annexin V-FITC and propidium iodide double staining kit (Trevigen). In brief, DU-145 cells were seeded into six-well plates and treated with SH-130 or negative control SH-123 with or without pretreatment with the pan-caspase inhibitor zVAD (Biovision). X-ray irradiation was done immediately after drug addition. Twenty-four hours after radiation, the cells were collected, gently washed twice with cold PBS, stained with Annexin V and propidium iodide as per manufacturer's instruction, and analyzed with a flow cytometer (FACSCalibur; BD Biosciences) in the Flow Cytometry Core at the University of Michigan Cancer Center. Other aliquoted samples were processed for caspase function and Western blot analysis.

Caspase-3 function assay. Caspase activation of treated DU-145 cells was determined following the instructions of a caspase-3 detection kit (BioVision). Cells were lysed in a lysis buffer, and whole-cell lysates (20 μg) were incubated with 25 μmol/L fluorogenic substrate DEVD-AFC in a reaction buffer (containing 5 mmol/L DTT) at 37°C for 2 h. Proteolytic release of AFC was monitored at λ_{ex} = 405 nm and λ_{em} = 500 nm using a microplate reader (BMG Labtech). Fold increase of the fluorescence signal was calculated for each treated sample by dividing its normalized signal activity by that of the untreated control.

Pull-down and immunoprecipitation assay. DU-145 cells were washed with ice-cold PBS, harvested, and resuspended in a lysis buffer

Table 1. Radiobiological variables from surviving curves

	Mean inactivation dose	Enhancement ratio	Survival fraction (2 Gy)	Gy (1%)
Control	3.66		0.70	10.83
SH-123 (20 μmol/L)	2.96	1.24	0.57	10.49
SH-130 (5 μmol/L)	2.53	1.45	0.49	9.53
SH-130 (10 μmol/L)	2.05	1.79	0.40	8.42
SH-130 (20 μmol/L)	1.28	2.86	0.21	5.63

NOTE: Radiobiological variables were calculated from survival curves in Fig. 1C based on linear-quadratic model. Enhancement ratio was calculated from mean inactivation dose in control group divided by that in treated group. Gy (1%), radiation dose leading to 1% cell survival.

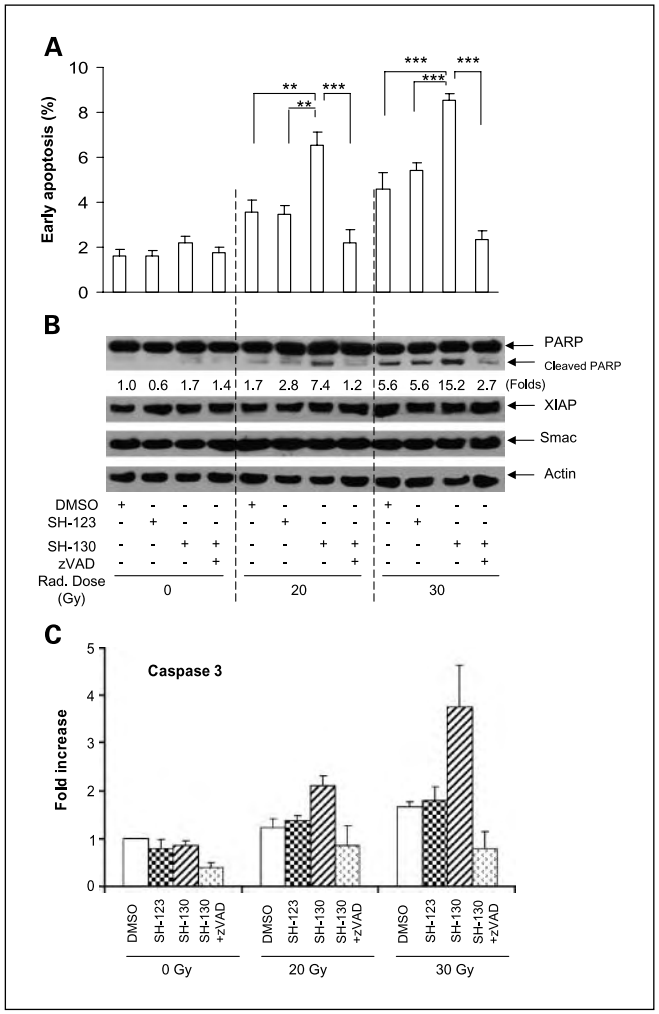

Fig. 2. SH-130 enhances radiation-induced apoptosis. DU-145 cells were seeded into six-well plates at the concentration of 2×10^5/mL, pretreated with zVAD (2.5 μmol/L) for 1 h, incubated with 10 μmol/L SH-130 or SH-123, and irradiated at doses of 0, 20, or 30 Gy, respectively. Twenty-four hours after incubation, cells were harvested and processed for further detection. One of three independent experiments. *A,* early apoptotic cell populations after treatment. DU-145 cells were stained with Annexin V-FITC and propidium iodide (Trevigen) and determined by flow cytometry. Mean ± SD ($n = 3$). **, $P < 0.01$; ***, $P < 0.001$, Student's t test. *B,* Western blot analysis of apoptosis-related proteins. Samples were probed with antibodies against PARP, caspase-3, XIAP, and Smac. Actin is shown as a loading control. Band intensity of cleaved PARP was normalized to actin. *C,* caspase-3 activation after treatment. Whole-cell lysates (20 μg) were reacted with fluorogenic substrate DEVD-AFC. After incubation at 37°C for 2 h, released AFC was monitored by a microplate reader (BMG Labtech). Mean ± SD ($n = 3$). Fold increase of fluorescence signal was expressed by normalizing activity to untreated control.

[50 mmol/L Tris-HCl (pH 7.5), 150 mmol/L NaCl, 1% NP-40, 0.5% sodium deoxycholate, and protease inhibitor tablet (Roche)]. For pull-down assay, after preclearing the streptavidin agarose gel (Invitrogen) at 4°C for 2 h, whole-cell lysate (1 mg total proteins) was incubated with biotin-labeled SH-130 (20 μmol/L) with or without the addition of an unlabeled SH-130 competitor (200 μmol/L). DMSO was used as a solvent control. After rotation at 4°C for 3 h, the lysate was incubated overnight with the gel (50 μL) at 4°C. For immunoprecipitation assay, the lysate (1 mg total proteins) was incubated with 1 and 10 μmol/L SH-130 or 10 μmol/L SH-123 at 4°C for 1 h. Antibody (10 μL) was then added, and the sample was incubated for 1 h before an overnight incubation with 50 μL protein A/G-agarose gel (Invitrogen). The immunoprecipitates were washed five times with desired wash buffer (Roche), eluted with SDS-PAGE sample buffer, and analyzed by Western blot.

Animal studies. The general procedure for *in vivo* experiments was described previously (22). Briefly, female athymic NCr-*nu*/*nu* nude mice (5-6 weeks old) were inoculated s.c. on both sides of the lower back above the tail with 3×10^6 per 0.2 mL DU-145 cells. When tumors reached 50 to 100 mm^3, the mice were randomized into four groups (8 mice per group) and treated with either SH-130 i.v. injected with 50 mg/kg for q.d. × 5 × 2 weeks, X-ray irradiation with 2 Gy daily for q.d. × 5 × 2 weeks, or a combination of SH-130 and radiation. The vehicle control and radiation-only groups received the same amount of DMSO solvent. Tumor size and body weight were measured twice a week. Tumor volume was calculated using the formula: $V = a \times b^2 / 2$, where a and b represented both the long and the vertical short diameter of the tumor. For *in vivo* imaging experiments, mice were transplanted s.c. with 5×10^6 cells per 0.2 mL DU-145^{Lux} cells. Treatment started (day 0) when the average tumor volume reached 50 mm^3 using the following regimen: SH-130 50 mg/kg i.v. q.o.d. × 3 weeks, X-ray irradiation 2 Gy q.d. × 5 × 3 weeks, or a combination of SH-130 and radiation. On days 0, 8, 17, 24, 41, and 120, mice were imaged 12 min after i.p. injection of luciferin using the Xenogen Bioluminescence Imaging (BLI) System in the University of Michigan Small Animal Imaging Core. Light intensity was quantified using LivingImage software on a red (high intensity/cell number) to blue (low intensity/cell number) visual scale. All animal experiments were done according to protocols approved by the University of Michigan Committee for Use and Care of Animals.

Nuclear factor-κB activity assay. Two independent assays were done to determine the effect of SH-130 on TNF-α-induced nuclear factor-κB (NF-κB) activation as shown below.

NF-κB reporter assay. DU-145 cells were seeded into a 24-well plate 24 h before transfection. For each well, cells were transiently cotransfected with 0.4 μg of a NF-κB reporter construct (pNF-κB; Panomics) or a control reporter plasmid (pControl; Panomics), together with 0.2 μg of a β-galactosidase reporter vector (Promega), which was used to normalize NF-κB reporter gene activity, using LipofectAMINE 2000 (Invitrogen). Twenty-four hours after transfection, cells were pretreated with SH-130 with or without the caspase inhibitor zVAD or SH-123 for 1 h followed by TNF-α stimulation for 4 h. The proteasome inhibitor MG132 was used as a positive control. Cell lysates were prepared using Reporter Lysis Buffer (Promega). For luciferase and β-galactosidase assays, the samples were measured on a microplate luminometer (BMG Labtech) using the Bright-Glo luciferase kit (Promega) and β-galactosidase enzyme assay kit (Promega), respectively, according to the manufacturer's instructions. Fold increase was calculated for each treated sample by dividing normalized luciferase activity by that of the untreated control.

Quantitative real-time PCR. Quantitative PCR was done to determine the expression level of the TNF gene as a NF-κB target gene (23). Total RNA was extracted from DU-145 cells using TRIzol reagent (Invitrogen) according to the manufacturer's instructions. Reverse transcription reaction with 1 μg total RNA in 100 μL was done following the instructions of the TaqMan Reverse Transcription Kit (Applied Biosystems). For quantitative PCR, FAM probe TNF primer (Applied Biosystems) was used for detection of target gene expression, and SYBR Green-labeled actin (Applied Biosystems) was used as an internal control, with the primers designed as forward 5′-ATGCAGAAG-GAGATCACTGC-3′ and reverse 5′-TCATAGTCCGCCTAGAAGCA-3′. All reactions with TaqMan PCR Master Mix (Applied Biosystems) were done on the Mastercycler realplex system (Eppendorf). Fold increase of gene expression was calculated for each treated sample by dividing normalized TNF expression activity with that from the untreated control.

Statistical analysis. Two-tailed Student's t test and two-way ANOVA were employed to analyze the *in vitro* and *in vivo* data, respectively, using Prism 5.0 software (GraphPad Prism). A threshold of $P < 0.05$ was defined as statistically significant.

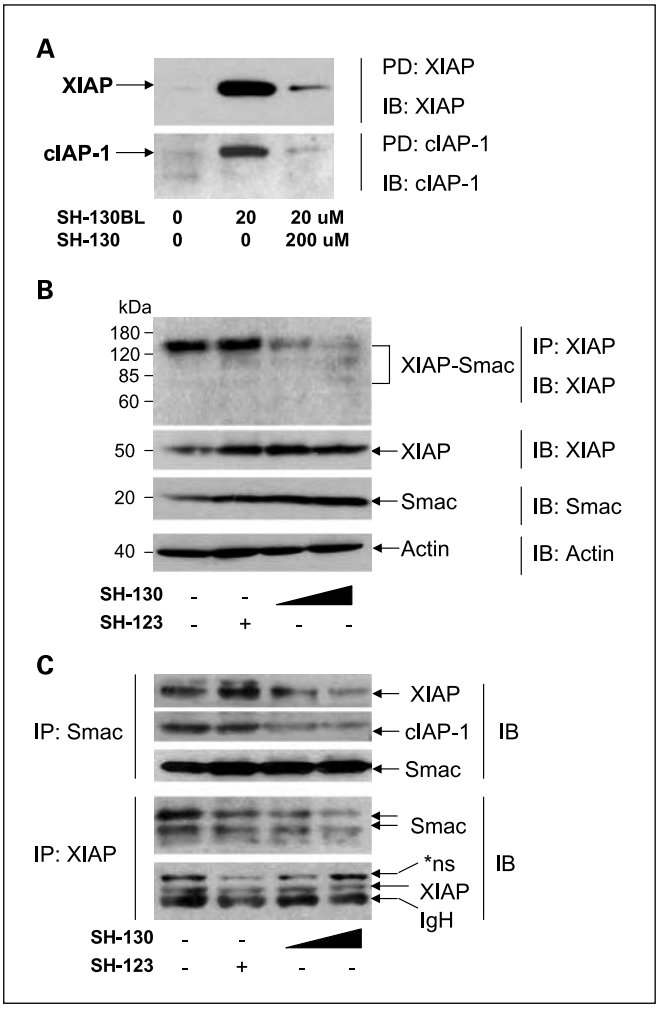

Fig. 3. SH-130 interrupts interaction between XIAP/cIAP-1 and Smac. DU-145 cells were collected and disrupted in a lysis buffer. Pull-down or immunoprecipitation was done as described in Materials and Methods. Immunoprecipitates were analyzed by Western blot. Endogenous XIAP, cIAP-1, and Smac were visualized by relevant antibodies. *A,* biotin-labeled SH-130 (SH-130BL) was incubated with cell lysates with or without nonlabeled SH-130 followed by incubation with precleared streptavidin-agarose beads. *B,* cell lysates were incubated with 1 and 10 μmol/L SH-130 or 10 μmol/L SH-123 for 1 h. Lysates were mixed with a sample buffer (Bio-Rad; without reducing agent) and directly analyzed by Western blot without boiling. Actin was used as a loading control. *C,* cell lysates from *B* were incubated with an anti-Smac or an anti-XIAP antibody and mixed with protein A/G-agarose beads. Eluents were analyzed by Western blot and probed with specified antibodies. IgG heavy chain (*IgH*) was probed as a control. One of three independent experiments. *PD,* pull-down; *IP,* immunoprecipitation; *IB,* immunoblotting; *ns,* nonspecific.

Results

Synergistic induction of radiation-induced cancer cell growth inhibition by the small-molecule IAP inhibitor. As reported previously (19, 20), a series of compounds were designed to mimic AVPI, the critical NH_2-terminal tetrapeptide on the active Smac protein (Fig. 1A). SH-130, a lead compound of these Smac-mimetics, was found to be 20 to 30 times more potent in binding to XIAP than the cell-permeable Smac peptide pSMAC-8c, a positive control for serial SH compounds used previously (Fig. 1A). Another analogue, SH-123, which was almost 1,000 times less active than SH-130, was used as an inactive control (Fig. 1A). Human prostate cancer DU-145 and PC-3 cell lines have medium to high levels of most of IAPs, whereas the normal human fibroblast cell line WI-38 and normal human prostate epithelial cells PrEC show low levels of IAPs (Fig. 1B).

To determine whether the Smac-mimetic compound could potentiate radiation-induced inhibition of cancer cell growth, we examined the radiosensitization of SH-130. SH-130 promoted radiation-induced clonogenic cell death dose-dependently, whereas SH-123 exhibited much less effect even at a high dose (Fig. 1C). Radiobiological variables were calculated and summarized in Table 1. The radiosensitizing activity of SH-130 was not observed in normal cells PrEC and WI-38 that have low IAPs (data not shown). We have also carried out MTT-based cytotoxicity assay (22) and SH-130 alone showed IC_{50} > 100 μmol/L in prostate cancer DU-145 and PC-3 cells as well as WI-38 cells, indicating that SH-130 is not a cytotoxic compound, consistent with other small-molecule Smac-mimetics we reported earlier (19, 20).

Enhancement of radiation-induced apoptosis by inhibition of IAPs. Preliminary data indicated that in cell-free systems SH-130, but not SH-123, abolished the inhibitory action of IAPs on both caspase-9 and caspase-3 in a dose- and time-dependent manner, showing a potent effect on competing IAPs and thus activating caspases. To provide further evidence for the role of SH-130 in mediating radiation-induced apoptosis, DU-145 cells were treated with SH-130 or SH-123 with or without X-ray radiation. As shown in Fig. 2A, induction of early apoptotic events (Annexin V positive) became evident when cells were treated with either 20 or 30 Gy together with 10 μmol/L SH-130. A 4- to 5-fold increase was seen compared with the untreated control and a 2-fold increase over radiation alone ($P < 0.01$). Pretreatment with the pan-caspase inhibitor zVAD abolished this increase in radiation-induced early apoptosis by SH-130 ($P < 0.001$; Fig. 2A), indicating that SH-130-mediated radiosensitization is caspase dependent. In contrast, neither SH-130 nor SH-123 alone induced significant apoptosis, suggesting a nontoxic profile of these compounds. We also evaluated total (early plus late) apoptotic events and obtained similar results (Supplementary Fig. S1). Furthermore, in the cells treated with radiation plus SH-130, a clear PARP cleavage was observed (Fig. 2B) compared with the cells treated with radiation alone. Because PARP is one of the substrates of caspase-3, our functional assay also showed similar profile on caspase-3 activation (Fig. 2C). Here again, zVAD efficiently blocked the SH-130 effect on caspase-3 activation and PARP cleavage. For all the samples tested (Fig. 2B), the expression level of XIAP and Smac did not change significantly, indicating that SH-130 acts on the apoptosis pathway, not by inhibiting the expression of IAPs.

Blockade of XIAP/cIAP-1 and Smac interaction by the IAP inhibitor. To further examine whether the small-molecule IAP inhibitor, SH-130, binds to the IAP family of proteins in cells as designed, we carried out IAP pull-down assays using biotin-labeled compounds. SH-130 was labeled with biotin (SH-130BL) via chemical synthesis. A fluorescence polarization-based binding assay confirmed that SH-130BL had the same binding affinity to XIAP as unlabeled SH-130.[4] SH-130BL successfully pulled down both XIAP and cIAP-1 in DU-145 cells

[4] Unpublished data.

(Fig. 3A). Competition with unlabeled SH-130 effectively blocked the pull-down of both XIAP and cIAP-1 by SH-130BL. Furthermore, we conducted immunoprecipitation assays to see if SH-130 interfered with XIAP (or cIAP-1) and Smac interaction. Interestingly, under nonreducing and nondenaturing conditions, XIAP and Smac formed a complex at molecular weight ranging from ~80 to 160 kDa (Fig. 3B), consistent with the tetramer model (24). XIAP-Smac complex levels were decreased by the addition of SH-130, but not SH-123, with increasing levels of free XIAP and Smac (Fig. 3B). Furthermore, SH-130 dose-dependently interrupted interaction between Smac and XIAP or cIAP-1 (Fig. 3C). Interestingly, when mature Smac was pulled down together with XIAP, two bands always seemed to be visualized by Western blot (Fig. 3C). The upper band (~28 kDa) level showed the same alteration as the lower band (~21 kDa), which is thought to be the cleaved or activated Smac. Compared with the artificial transfection with tag-labeled system (25), our condition is more likely to mimic the native intracellular protein behavior. These data confirm that the IAP inhibitors can bind to XIAP/cIAP-1, thus interrupting the interaction between endogenous XIAP/cIAP-1 and Smac in prostate cancer cells.

In vivo *tumor suppression effect of the IAP inhibitor with radiation.* To evaluate the radiosensitization potential of SH-130 *in vivo*, a DU-145 tumor model was established as we described previously (4, 22). The DU-145 tumors were resistant to radiation, and SH-130 alone did not show tumor suppression effect (Fig. 4A). However, SH-130 synergistically sensitized the DU-145 tumors to radiation without showing systemic toxicity (Fig. 4B). The combination therapy inhibited tumor growth significantly more effectively than either treatment alone ($P < 0.001$, $n = 14$), and no obvious animal toxicity was observed. Notably, 5 of 14 tumors in the combination group showed complete regression that did not grow back 5 months after the therapy, whereas the radiation-alone group had only 2 of 10 tumors with complete regression. No complete regression in the SH-130-alone or vehicle control groups was observed.

In the second experiment, we wished to extend the treatment period to a more clinically relevant 3-week course of therapy. For this experiment, we used the DU-145^{Lux} tumor model and employed BLI to evaluate tumor response. SH-130 plus radiation led to complete tumor regression (undetectable signal in BLI in Fig. 4C). By quantification, the combination therapy resulted in a 2-log reduction in bioluminescence signal compared with the radiation-alone group and a 4- to 5-log reduction compared with the vehicle control group (Fig. 4D). BLI was also conducted on days 0, 24, and 120 (Supplementary Fig. S2), and percentage of complete tumor regression is summarized in Fig. 4D. The percentage of complete tumor regression in the radiation-alone group was highest (35%) on day 41 and dropped to 33.3% on day 120, indicating tumor recurrence over time. For the combination therapy group, the

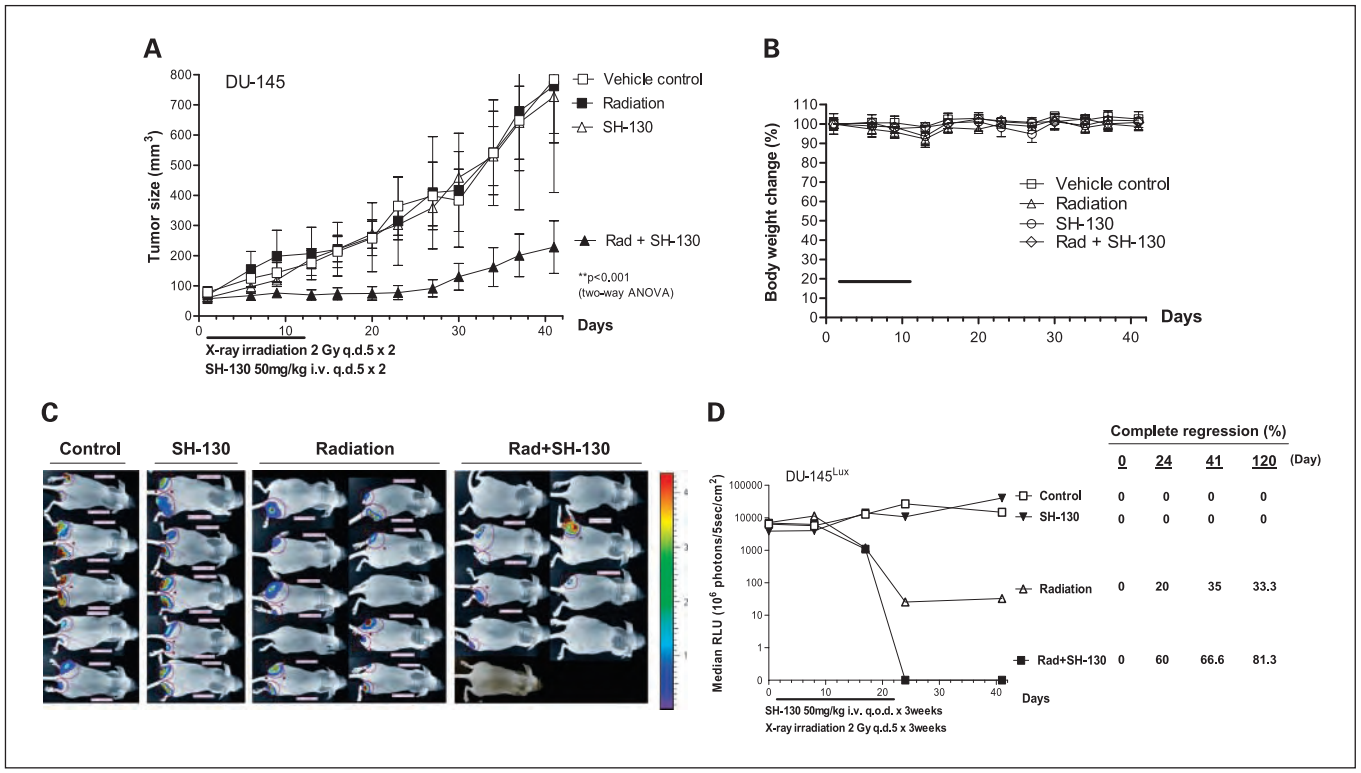

Fig. 4. SH-130 potentiates DU-145 tumor regression induced by X-ray radiation with caliper measurement (*A* and *B*) or BLI (*C* and *D*). Nude mice bearing DU-145 cells were treated with either SH-130, or X-ray irradiation, or a combination. Tumor size (*A*) and body weight (*B*) were measured twice a week, and curves were plotted up to day 41. Mean ± SE ($n = 16$) for tumor volume (*A*) and mean ± SE ($n = 8$) for body weight (*B*). *C* and *D,* SH-130 combined with radiation eradicated DU-145 tumors by BLI. Nude mice bearing DU-145^{Lux} cells were treated as described in Materials and Methods. Imaging was carried out to visualize bioluminescent tumors on days 0, 8, 17, 24, 41, and 120, respectively. *C,* BLI of DU-145^{Lux} on day 41. The light intensity of each photo was quantified to an optimized visual scale (from *red* to *blue*). *D,* summary of quantitative data of bioluminescence intensity. Absolute photon counts of tumors were measured and expressed as a median of relative light unit (*RLU*). Percentage of complete regression was calculated by dividing the number of eradicated tumors with total tumors. *Rad,* X-ray radiation.

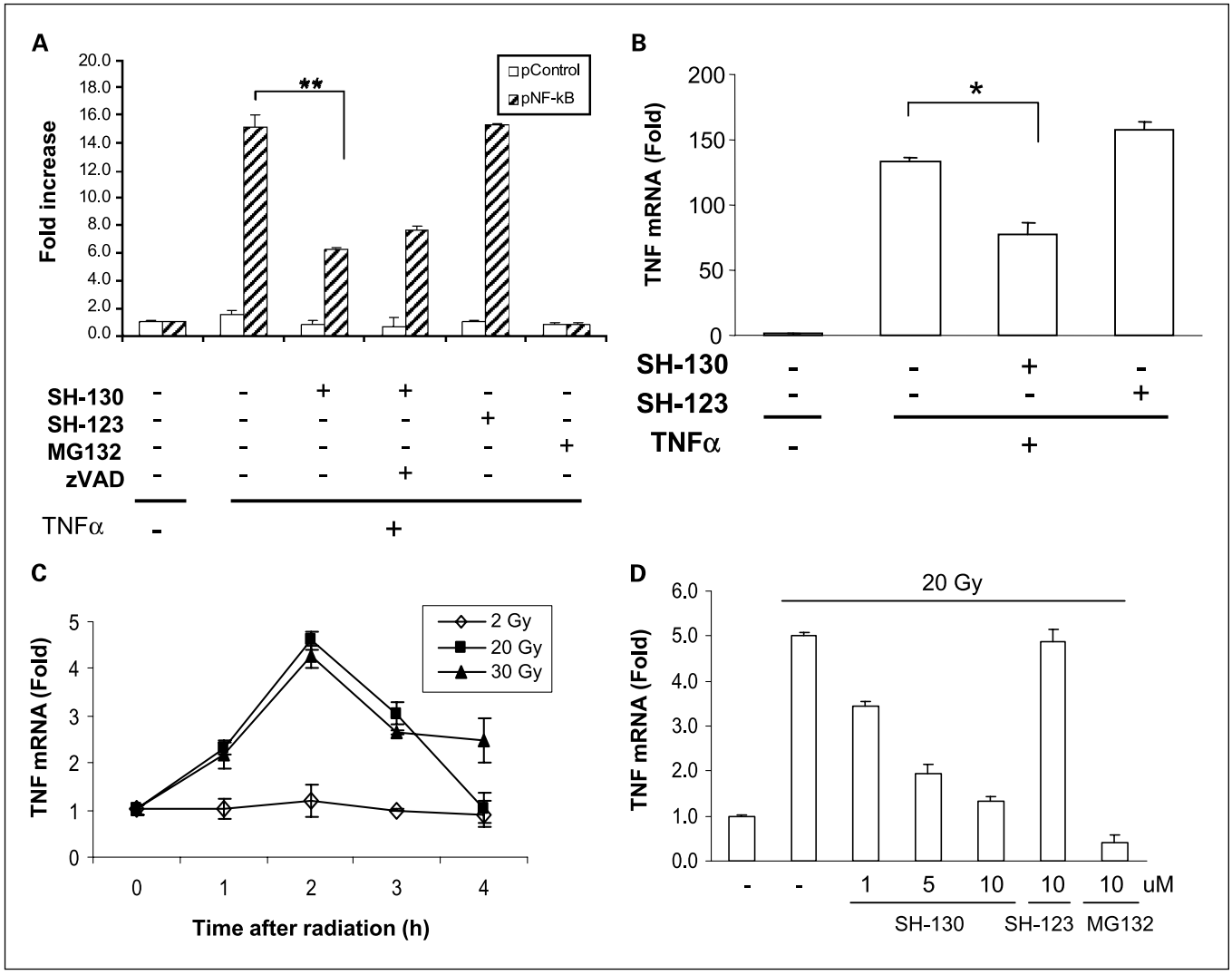

Fig. 5. SH-130 inhibits NF-κB activation induced by TNF-α (*A* and *B*) and radiation (*C* and *D*). *A,* DU-145 cells were transiently cotransfected with pNF-κB or pControl (0.4 μg/well) together with β-galactosidase plasmid (0.2 μg/well). Cells were then pretreated with SH-130 (20 μmol/L) with or without zVAD (2.5 μmol/L) or SH-123 (20 μmol/L) for 1 h followed by TNF-α stimulation for 4 h. MG132 (10 μmol/L) was used as a positive control. Luciferase and β-galactosidase activities were measured as described in Materials and Methods. Fold increase was calculated as mean ± SD ($n = 2$). One of three independent experiments. **, $P < 0.01$. *B,* cells were pretreated with 20 μmol/L SH-130 or SH-123 for 1 h before 10 min pulse stimulation of TNF-α. Total RNA was extracted and quantitative PCR was done as described in Materials and Methods. Fold increase was calculated by dividing the normalized TNF expression activity by that of the untreated control. *Columns,* mean; *bars,* SD ($n = 3$). *, $P < 0.05$. *C,* cells were irradiated with the indicated doses of X-ray radiation. TNF mRNA expression level at desired time points was detected and normalized as described in *B*. *D,* cells were pretreated with the indicated doses of compounds for 1 h and TNF mRNA expression level was determined 2 h after 20 Gy radiation. MG132, positive control.

percentage of complete tumor regression continued to increase up to day 120 (81.3%), indicating a potent and long-term efficacy of the combination treatment. Thus, two *in vivo* studies showed a similar and promising *in vivo* radiosensitization efficacy of the IAP inhibitor.

Suppression of NF-κB activation by inhibiting IAPs. To test the hypothesis that SH-130 may also work on the NF-κB pathway, we analyzed the effects of SH-130 on NF-κB activation induced by TNF-α and X-ray radiation in DU-145 cells. Using luciferase-based NF-κB reporter assay (26), SH-130 inhibited TNF-α-induced NF-κB activation by >50% ($P < 0.01$) and the inhibition could not be blocked by zVAD (Fig. 5A), indicating that the IAP inhibitor-mediated NF-κB inhibition is caspases independent. Moreover, SH-130 partially inhibited NF-κB activation, even at a high concentration, compared with MG132 (Fig. 5A). SH-130 inhibited TNF-α-induced IκBα degradation (Supplementary Fig. S3), yet without a significant change in RelA nuclear translocation (data not shown), suggesting that SH-130-mediated inhibition of NF-κB activation is indirect. Quantitative real-time PCR assay further confirmed that TNF gene expression was down-regulated 50% by SH-130 ($P < 0.05$), but not by negative control compound SH-123, after TNF-α stimulation (Fig. 5B), indicating that SH-130 clearly although partially blocked NF-κB target gene expression.

Next, we examined if SH-130 has similar suppression effect on X-ray radiation-induced NF-κB target gene expression. Radiation (20 Gy) was employed to trigger NF-κB activation as high radiation doses (20 and 30 Gy) exhibited activation of TNF gene expression by 4- to 5-fold more than low dose (2 Gy; Fig. 5C). Similar to TNF-α, radiation-induced TNF gene expression could also be partially suppressed by SH-130 in a

dose-dependent manner (Fig. 5D) compared with its negative analogue, SH-123. These data show that SH-130 can block both TNF-α- and radiation-induced NF-κB activation in terms of inhibiting NF-κB target gene expression.

Discussion

In this study, we have found that a small-molecule IAP inhibitor potently sensitizes prostate cancer DU-145 cells to X-ray irradiation and increases radiation-induced cell death and tumor growth delay both *in vitro* and *in vivo*. Such effects may be due to activation of the apoptosis pathway. Moreover, the IAP inhibitor SH-130 also blocked activation of the NF-κB partially and indirectly, suggesting a potential cross-talk between apoptosis and NF-κB pathways (Fig. 6). The data confirmed our hypothesis that molecular modulation of IAP family proteins may improve the outcome of prostate cancer radiotherapy and represents a promising molecularly targeted therapy for hormone-refractory prostate cancer.

Small-molecule inhibitors of IAPs are a promising choice for functionally blocking IAPs and overcoming chemoresistance/radioresistance of cancer cells with high levels of IAPs. Our previous studies showed that the Smac-mimetic tetrapeptide pSmac-8c (used as the positive control) significantly sensitized both androgen-independent DU-145 and PC-3 cells to chemotherapeutic agents (19, 20), indicating that IAP is a valid target for overcoming chemoresistance in prostate cancer cells, and our current study supports that modulating IAPs is a promising approach on radiosensitization. Future work will focus on comparing androgen-dependent LNCaP and its androgen-independent derivative cell line CL-1 on their response to radiation and SH-130. Expected data on this isogenic cell model will further support that IAPs may play an essential role in the transition from androgen-dependent to androgen-independent prostate cancer, and overcoming resistance of radiation-induced apoptosis can be achieved by down-regulating IAPs.

Our *in vivo* studies showed consistently that IAP inhibition exhibits promising radiosensitivity in the DU-145 xenografted model, although IAP inhibitor itself is nontoxic and shows no tumor suppression effect alone. Data from regular tumor volume measurement and BLI imaging are consistent in exhibiting a synergistic efficacy when SH-130 is used together with X-ray radiation. By BLI, mice in the combination group showed an increasing trend toward complete tumor regression that lasted up to 4 months after treatment, indicating the long-term tumor-suppressing efficacy of combination therapy over radiation alone. Using BLI for the efficacy study is critically important, especially when the tumor disappears as a complete tumor regression. Conventional tumor measurement by hand will still detect a scar or nodule, but no live tumor cells are detectable, as the BLI will detect no light emission. On the other hand, some tumors may appear to have completely disappeared and will not be detectable by hand, but BLI can still detect light emission and reveal the presence of live tumor cells. Therefore, the more sensitive and quantitative BLI will yield robust and quantitative efficacy data, especially when evaluating the complete tumor regression in the current study.

Ionizing radiation activates the NF-κB signaling pathway, and blocking this pathway can sensitize cancer cells response to radiation (27, 28). Classically, cytokines such as TNF-α trigger NF-κB activation, typically mediated by TNF receptor-associated factor 2. It has been shown that TNF receptor-associated factor 2 physically interacts with cIAP-1, another IAP protein that is commonly studied along with XIAP (29). In addition, embelin, a natural IAP inhibitor first reported by us (30), sequentially inhibits NF-κB activation at multiple levels (26). Moreover, XIAP could induce TAK1-dependent NF-κB activation (31). Thus, it is reasonable to postulate that IAPs may function as "bridging" molecules mediating cross-talk between apoptosis and NF-κB pathways. Our data show that SH-130 indeed inhibits NF-κB activation, partially and indirectly, by TNF-α and X-ray radiation. This partial effect of an IAP inhibitor on NF-κB activation is consistent with an earlier report showing that partial NF-κB inhibition by another class of Smac-mimetics (32). Inhibition of IκBα degradation by SH-130 reflects an effect at the level of the IκBα kinase complex as shown by embelin (26). Currently, we are delineating the detailed signaling pathways and molecules involved in the cross-talk either via cIAP-1 or XIAP. This may have important implications for the rational design of novel therapies targeting IAPs and optimal recruitment of the patient population that will benefit the most from such therapy.

DU-145 cells are highly resistant to radiation potentially due to high levels of IAPs as well as constitutive active NF-κB pathway (33). It is conceivable that the dose of radiation used might affect NF-κB activation as well as radiation-induced cell death, where the high and low doses may stimulate different cellular responses. In the clinic, the dose of radiation therapy on patients is 1.8 to 2 Gy daily fractionation with total doses of 20 to 70 Gy. Thus, in the current study, we followed the clinical regimen with totaling 20 and 30 Gy in two animal studies. Consistent with previous reports that a relative high dose (15-20 Gy) of X-ray radiation could induce NF-κB activation in

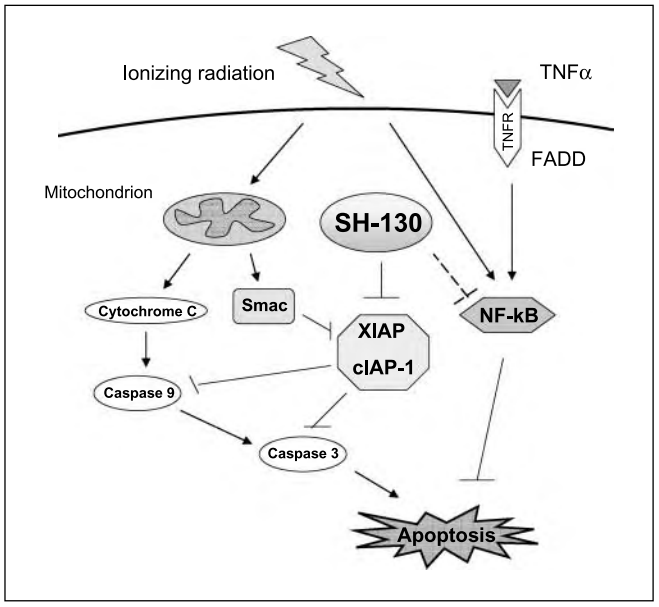

Fig. 6. Working model of the Smac-mimetic IAP inhibitors in radiosensitization. SH-130 enhances ionizing radiation-induced apoptosis via the intrinsic (mitochondrion) pathway by inhibiting XIAP/cIAP-1 activity and blocking caspase activation. On the other hand, SH-130 blocks NF-κB activation induced by TNF-α as well as ionizing radiation, indicating the suppression effect of radiation-mediated prosurvival signaling that attenuates apoptosis.

human tumor cells *in vitro* (34, 35), we found that, in our system, high-dose radiation (20 and 30 Gy) effectively induced apoptosis as well as NF-κB activation but not the low doses (2-4 Gy). Furthermore, RelA was clearly observed at doses >15 Gy (data not shown). Taken together, the radiosensitization effect of Smac-mimetic SH-130 is due, at least in part, to the simultaneous inhibition of IAPs and the NF-κB survival signaling pathway, which is constitutively active in androgen-independent prostate cancer cells.

Very recently, three groups reported that several Smac-mimetic IAP inhibitors can induce TNF-α-dependent apoptosis in sensitive cell lines via cIAP-1 down-regulation and NF-κB activation (36–38). However, most of the androgen-independent prostate cancer cells are resistant to TNF-α and have constitutive active NF-κB signaling (33). How these resistant cancer cells respond to IAP inhibitors remains to be investigated. In our hands, those cells, including DU-145, PC-3, and CL-1, are highly resistant to our Smac-mimetic IAP inhibitors such as SH-130, which has a IAP-binding affinity comparable with that of the compounds used in the three reports (36–38). To our knowledge, this is the first report that an IAP inhibitor blocks radiation-induced NF-κB activation in these TNF-α-resistant cells. Moreover, SH-130 treatment does not induce cIAP-1 down-regulation, TNF-α up-regulation, and NF-κB activation in these resistant cells (Supplementary Fig. S4). This mode of action is distinct from that in TNF-α-sensitive cells reported recently (36–38). Our study has significant clinical implications and provides important impetus for using IAP inhibitors as an adjuvant therapy for the TNF-α-resistant, NF-κB constitutively active cancers that account for the majority of patients who are refractory to conventional therapy.

In conclusion, our data provide strong support that modulating IAPs may be a promising novel approach to radiosensitization of human prostate cancer, especially among hormone-refractory, locally advanced, high-risk patients. In a clinical context, although hormone-refractory prostate cancer still exerts response to high-dose palliative radiation therapy to achieve the local control in patients (39), the patient population that could benefit the most would be those with a high Gleason score (>8) and high prostate-specific antigen (>20) without metastatic disease and with a high failure rate even with high-dose radiation. Showing a reasonable relevance to prostate cancer therapy in clinic, our reported small-molecule IAP inhibitor has a promising implication on overcoming radiation resistance of human prostate cancer with high levels of IAPs.

Disclosure of Potential Conflicts of Interest

L. Xu is coinventor of the related compound. Q3

Acknowledgments

We thank Drs. Dian Wang, Jiaxin Zhang, and Mu Li for technical support in the experiments; Dr. Shaomeng Wang for kindly providing IAP inhibitors in our study; Dr. Lori Roberts (University of Michigan Comprehensive Cancer Center Unit of Laboratory Animal Medicine) for measuring tumor sizes; Susan Harris for help with the article; the University of Michigan Comprehensive Cancer Center Flow Cytometry Core for flow cytometry analysis; and the University of Michigan Biomedical Imaging Core for BLI of animals.

SF4

References

1. Szostak MJ, Kyprianou N. Radiation-induced apoptosis: predictive and therapeutic significance in radiotherapy of prostate cancer [review]. Oncol Rep 2000;7:699–706.
2. Lawrence TS, Davis MA, Hough A, Rehemtulla A. The role of apoptosis in 2′,2′-difluoro-2′-deoxycytidine (gemcitabine)-mediated radiosensitization. Clin Cancer Res 2001;7:314–9.
3. Denmeade SR, Lin XS, Isaacs JT. Role of programmed (apoptotic) cell death during the progression and therapy for prostate cancer. Prostate 1996;28:251–65.
4. Xu L, Frederik P, Pirollo KF, et al. Self-assembly of a virus-mimicking nanostructure system for efficient tumor-targeted gene delivery. Hum Gene Ther 2002; 13:469–81.
5. DiPaola RS, Patel J, Rafi MM. Targeting apoptosis in prostate cancer. Hematol Oncol Clin North Am 2001; 15:509–24.
6. Amantana A, London CA, Iversen PL, Devi GR. X-linked inhibitor of apoptosis protein inhibition induces apoptosis and enhances chemotherapy sensitivity in human prostate cancer cells. Mol Cancer Ther 2004;3:699–707.
7. Devi GR. XIAP as target for therapeutic apoptosis in prostate cancer. Drug News Perspect 2004;17:127–34.
8. Salvesen GS, Duckett CS. IAP proteins: blocking the road to death's door. [Review] [154 refs]. Nat Rev Mol Cell Biol 2002;3:401–10.
9. Schimmer AD. Inhibitor of apoptosis proteins: translating basic knowledge into clinical practice. Cancer Res 2004;64:7183–90.
10. Deveraux QL, Takahashi R, Salvesen GS, Reed JC. X-linked IAP is a direct inhibitor of cell-death proteases. Nature 1997;388:300–4.
11. Tenev T, Zachariou A, Wilson R, Ditzel M, Meier P. IAPs are functionally non-equivalent and regulate effector caspases through distinct mechanisms. Nat Cell Biol 2005;7:70–7.
12. Notarbartolo M, Cervello M, Poma P, Dusonchet L, Meli M, D'Alessandro N. Expression of the IAPs in multidrug resistant tumor cells. Oncol Rep 2004;11: 133–6.
13. Deveraux QL, Roy N, Stennicke HR, et al. IAPs block apoptotic events induced by caspase-8 and cytochrome *c* by direct inhibition of distinct caspases. EMBO J 1998;17:2215–23.
14. Zhou L, Yuan R, Serggio L. Molecular mechanisms of irradiation-induced apoptosis. Front Biosci 2003;8: d9–19.
15. Du C, Fang M, Li Y, Li L, Wang X. Smac, a mitochondrial protein that promotes cytochrome *c*-dependent caspase activation by eliminating IAP inhibition. Cell 2000;102:33–42.
16. Ohnishi K, Scuric Z, Schiestl RH, Okamoto N, Takahashi A, Ohnishi T. siRNA targeting NBS1 or XIAP increases radiation sensitivity of human cancer cells independent of TP53 status. Radiat Res 2006;166: 454–62.
17. Yamaguchi Y, Shiraki K, Fuke H, et al. Targeting of X-linked inhibitor of apoptosis protein or survivin by short interfering RNAs sensitize hepatoma cells to TNF-related apoptosis-inducing ligand- and chemotherapeutic agent-induced cell death. Oncol Rep 2005;14:1311–6.
18. Srinivasula SM, Datta P, Fan XJ, Fernandes-Alnemri T, Huang Z, Alnemri ES. Molecular determinants of the caspase-promoting activity of Smac/DIABLO and its role in the death receptor pathway. J Biol Chem 2000;275:36152–7.
19. Sun H, Nikolovska-Coleska Z, Yang CY, et al. Structure-based design, synthesis, and evaluation of conformationally constrained mimetics of the second mitochondria-derived activator of caspase that target the X-linked inhibitor of apoptosis protein/caspase-9 interaction site. J Med Chem 2004;47:4147–50.
20. Sun H, Nikolovska-Coleska Z, Yang CY, et al. Structure-based design of potent, conformationally constrained Smac mimetics. J Am Chem Soc 2004; 126:16686–7.
21. Kalikin LM, Schneider A, Thakur MA, et al. *In vivo* visualization of metastatic prostate cancer and quantitation of disease progression in immunocompromised mice. Cancer Biol Ther 2003;2:656–60.
22. Xu L, Yang D, Wang S, et al. (-)-Gossypol enhances response to radiation therapy and results in tumor regression of human prostate cancer. Mol Cancer Ther 2005;4:197–205.
23. Maine GN, Burstein E. COMMD proteins and the control of the NF κB pathway. Cell Cycle 2007;6: 672–6.
24. Srinivasula SM, Hegde R, Saleh A, et al. A conserved XIAP-interaction motif in caspase-9 and Smac/DIABLO regulates caspase activity and apoptosis [comment]. Nature 2001;410:112–6. Erratum in Nature 2001;411:1081.
25. Liu Z, Sun C, Olejniczak ET, et al. Structural basis for binding of Smac/DIABLO to the XIAP BIR3 domain. Nature 2000;408:1004–8.
26. Ahn KS, Sethi G, Aggarwal BB. Embelin, an inhibitor of X chromosome-linked inhibitor-of-apoptosis protein, blocks nuclear factor-κB (NF-κB) signaling pathway leading to suppression of NF-κB-regulated antiapoptotic and metastatic gene products. Mol Pharmacol 2007;71:209–19.

27. Magne NTR, Bottero V, Didelot C, Houtte PV, Gerard JP, Peyron JF. NF-κB modulation and ionizing radiation: mechanisms and future directions for cancer treatment. Cancer Lett 2006;231:158–68.

28. Voboril R, Weberova-Voborilova J. Constitutive NF-κB activity in colorectal cancer cells: impact on radiation-induced NF-κB activity, radiosensitivity, and apoptosis. Neoplasma 2006;53:518–23.

29. Wang CY, Mayo MW, Korneluk RG, Goeddel DV, Baldwin AS, Jr. NF-κB antiapoptosis: induction of TRAF1 and TRAF2 and c-IAP1 and c-IAP2 to suppress caspase-8 activation. Science 1998;281:1680–3.

30. Nikolovska-Coleska Z, Xu L, Hu Z, et al. Discovery of embelin as a cell-permeable, small-molecular weight inhibitor of XIAP through structure-based computational screening of a traditional herbal medicine three-dimensional structure database. J Med Chem 2004;47:2430–40.

31. Lu M, Lin SC, Huang Y, et al. XIAP induces NF-κB activation via the BIR1/TAB1 interaction and BIR1 dimerization. Mol Cell 2007;26:689–702.

32. Li L, Thomas RM, Suzuki H, De Brabander JK, Wang X, Harran PG. A small molecule Smac mimic potentiates TRAIL- and TNFα-mediated cell death. Science 2004;305:1471–4.

33. Suh J, Rabson AB. NF-κB activation in human prostate cancer: important mediator or epiphenomenon? J Cell Biochem 2004;91:100–17.

34. Jung M, Dritschilo A. NF-κB signaling pathway as a target for human tumor radiosensitization. Semin Radiat Oncol 2001;11:346–51.

35. Brach MA, Hass R, Sherman ML, Gunji H, Weichselbaum R, Kufe D. Ionizing radiation induces expression and binding activity of the nuclear factor κB. J Clin Invest 1991;88:691–5.

36. Varfolomeev E, Blankenship JW, Wayson SM, et al. IAP antagonists induce autoubiquitination of c-IAPs, NF-κB activation, and TNFα-dependent apoptosis. Cell 2007;131:669–81.

37. Vince JE, Wong WW, Khan N, et al. IAP antagonists target cIAP1 to induce TNFα-dependent apoptosis. Cell 2007;131:682–93.

38. Petersen SL, Wang L, Yalcin-Chin A, et al. Autocrine TNFα signaling renders human cancer cells susceptible to Smac-mimetic-induced apoptosis. Cancer Cell 2007;12:445–56.

39. Hindson B, Turner S, Do V. Palliative radiation therapy for localized prostate symptoms in hormone refractory prostate cancer. Australas Radiol 2007;51:584–8.

Natural BH3 mimetic (-)-gossypol chemosensitizes human prostate cancer via Bcl-xL inhibition accompanied by increase of Puma and Noxa

Yang Meng,[1] Wenhua Tang,[1] Yao Dai,[1] Xiaoqing Wu,[3] Meilan Liu,[1] Qing Ji,[1] Min Ji,[3] Kenneth Pienta,[2] Theodore Lawrence,[1] and Liang Xu[1]

Departments of [1]Radiation Oncology and [2]Urology, University of Michigan Comprehensive Cancer Center, Ann Arbor, Michigan and [3]School of Chemistry and Chemical Engineering, Southeast University, Nanjing, Jiangsu, People's Republic of China

Abstract

Antiapoptotic members of the Bcl-2 family proteins are overexpressed in prostate cancer and are promising molecular targets for modulating chemoresistance of prostate cancer. (-)-Gossypol, a natural BH3 mimetic, is a small-molecule inhibitor of Bcl-2/Bcl-xL/Mcl-1 currently in phase II clinical trials as an adjuvant therapy for human prostate cancer. Our objective is to examine the chemosensitization potential of (-)-gossypol in prostate cancer and its molecular mechanisms of action. (-)-Gossypol inhibited cell growth and induced apoptosis through mitochondria pathway in human prostate cancer PC-3 cells and synergistically enhanced the antitumor activity of docetaxel both *in vitro* and *in vivo* in PC-3 xenograft model in nude mouse. (-)-Gossypol blocked the interactions of Bcl-xL with Bax or Bad in cancer cells by fluorescence resonance energy transfer assay and overcame the Bcl-xL protection of FL5.12 model cells on interleukin-3 withdrawal. Western blot and real-time PCR studies showed that a dose-dependent increase of the proapoptotic BH3-only proteins Noxa and Puma contributed to the cell death induced by (-)-gossypol and to the synergistic effects of (-)-gossypol and docetaxel. The small interfering RNA knockdown studies showed that Noxa and Puma are required in the (-)-gossypol-induced cell death. Taken together, these data suggest that (-)-gossypol exerts its antitumor activity through inhibition of the antiapoptotic protein Bcl-xL accompanied by an increase of proapoptotic Noxa and Puma. (-)-Gossypol significantly enhances the antitumor activity of chemotherapy *in vitro* and *in vivo*, representing a promising new regime for the treatment of human hormone-refractory prostate cancer with Bcl-2/Bcl-xL/Mcl-1 overexpression. [Mol Cancer Ther 2008;7(7):2192–202]

Introduction

Androgen deprivation therapy is the cornerstone treatment for men with *de novo* or recurrent metastatic prostate cancer (1). Unfortunately, androgen deprivation therapy is primarily palliative, with nearly all patients progressing to an androgen-independent or hormone-refractory state, for which there is currently no effective therapy (1). Despite several hundred clinical studies of both experimental and approved antitumor agents, chemotherapy has limited activity, with an objective response rate of <50% and no demonstrated survival benefit (2). Thus, androgen-independent disease is the main obstacle to improving the survival and quality of life in patients with advanced prostate cancer and has been the focus of extensive studies (3). There is an urgent need for novel therapeutic strategies for the treatment of advanced prostate cancer by specifically targeting the fundamental molecular basis of progression to androgen independence and the resistance of androgen-independent disease to chemotherapy.

Bcl-2 family proteins are crucial regulators of apoptosis and were first isolated as the products of an oncogene (4). This family of proteins includes both antiapoptotic molecules such as Bcl-2, Bcl-xL, and Mcl-1 and proapoptotic molecules such as Bax, Bak, Bid, Bad, Noxa, and Puma (5, 6). Bcl-2 and Bcl-xL are closely related proteins and both are highly overexpressed in many types of cancers (7). Overexpression of Bcl-2 is observed in 30% to 60% of prostate cancer at diagnosis and in ~100% of hormone-refractory prostate cancer (8, 9). The expression level of Bcl-2 protein also correlates with resistance to a wide spectrum of chemotherapeutic agents and radiation therapy (9–12). Bcl-xL is also overexpressed in ~100% of hormone-refractory prostate cancer and is associated with advanced disease, poor prognosis, recurrence, metastasis, and shortened survival (13, 14). The transition of prostate cancer from androgen dependent to androgen independent is accompanied by several molecular genetic changes, including overexpression of Bcl-2 and Bcl-xL (10, 15). Noxa and Puma are proapoptotic BH3-only proteins, work upstream of Bax

Received 4/7/08; revised 5/8/08; accepted 5/18/08.

Grant support: Department of Defense Prostate Cancer Research Program W81XWH-04-1-0215 and W81XWH-06-1-0010 (L. Xu), NIH/National Cancer Institute Prostate Cancer SPORE in University of Michigan Developmental Project 2P50 CA069568-06A1 (L. Xu), NIH grants R01 CA121830-01 and R21 CA128220-01 (L. Xu), and NIH through the University of Michigan Cancer Center Support Grant 5 P30 CA46592.

The costs of publication of this article were defrayed in part by the payment of page charges. This article must therefore be hereby marked *advertisement* in accordance with 18 U.S.C. Section 1734 solely to indicate this fact.

Requests for reprints: Liang Xu, Department of Radiation Oncology, Division of Cancer Biology, University of Michigan Comprehensive Cancer Center, 4424E Med Sci I/SPC5637, 1301 Catherine Street, Ann Arbor, MI 48109-5637. Phone: 734-615-7017; Fax: 734-615-3422. E-mail: liangxu@umich.edu

doi:10.1158/1535-7163.MCT-08-0333

and Bak to promote mitochondrial depolarization and apoptosis. The BH3-only proteins are classified as activator and sensitizer. Puma is an activator that binds directly to Bax and Bak and promotes their activation, whereas Noxa as a sensitizer binds to the prosurvival proteins and displaces Bim or tBid, allowing them to directly activate Bax and Bak (16). Noxa also engages Mcl-1 and is found to promote Mcl-1 degradation (17, 18).

We have been investigating small-molecule inhibitors of the Bcl-2 family proteins as novel therapeutics for cancer. Recently, (-)-gossypol, a natural product from cottonseed with the BH3 mimetic structure, is identified as small-molecule inhibitor of Bcl-2/Bcl-xL/Mcl-1 and potently induces apoptosis in various cancer cell lines (19, 20). (-)-Gossypol is now in phase II clinical trials for hormone-refractory prostate cancer and other types of cancer at multiple centers in the United States, as one of the world's first small-molecule Bcl-2 inhibitors entered into clinical trial.[4] In the current study, we investigated the therapeutic potential of (-)-gossypol in combination with docetaxel in human hormone-refractory prostate cancer cells *in vitro* and *in vivo*. Our hypothesis is that (-)-gossypol may improve the efficacy of chemotherapy by overcoming apoptosis resistance rendered by Bcl-2/Bcl-xL overexpression, thereby making the prostate cancer cells more sensitive to chemotherapy. Our results should not only facilitate the rational design of clinical trials but also refine the selection of patients who will benefit the most from Bcl-2 molecular therapy.

Materials and Methods

Cell Culture and Reagents

Human prostate cancer cell lines PC-3, DU-145, and LNCaP and human lung fibroblast cell line WI-38 were obtained from the American Type Culture Collection. PC-3 cells were routinely maintained in RPMI 1640 (HyClone), whereas DU-145, LNCaP, and WI-38 were maintained in DMEM (HyClone) supplemented with 10% fetal bovine serum (HyClone). Murine pro-B lymphoid cell line FL5.12 stably transfected with Bcl-xL or vector were kindly provided by Dr. Gabriel Nunez and were maintained in IMEM (Life Technologies) supplemented with 10% fetal bovine serum and 10% WEHI-3B (D-)-conditional medium as a source of interleukin-3 (IL-3; ref. 32). The cell cultures were maintained in a humidified incubator at 37°C and with 5% CO_2. (-)-Gossypol was purified from natural racemic gossypol. Briefly, racemic gossypol was reacted with L-phenylalanine methyl ester hydrochloride overnight at room temperature and sodium bicarbonate was added to yield gossypol Schiff's base as a yellow solid. After silica gel column chromatography purification, the solution of the resolved (±)-gossypol-phenylalanine methyl ester Schiff's base was hydrolyzed by a mixture of tetrahydrofuran, glacial acetic acid, and hydrochloric acid at room temperature for 2 h. The solution was extracted with acetic ether four times and then washed and dried. The (-)-gossypol was collected by filtration and evaporation. Some of the (-)-gossypol used for initial *in vitro* studies was kindly provided by Dr. Shaomeng Wang (University of Michigan) and Dr. Dajun Yang through the National Cancer Institute RAID program. For *in vitro* experiments, (-)-gossypol was dissolved in DMSO at 20 mmol/L as a stock solution. For *in vivo* studies, (-)-gossypol was suspended in carboxymethyl cellulose and then sonicated for 30 min and mixed before each administration. Docetaxel (Taxotere) was purchased from Sanofi-Aventis and diluted in PBS for *in vivo* studies.

MTT-Based Cell Viability Assay

Cell viability was determined by the MTT-based assay using Cell Proliferation Reagent WST-1 (Roche) according to the manufacturer's instruction. Cells (5,000 per well) were plated in 96-well culture plates, and various concentrations of (-)-gossypol or docetaxel were added to the cells in triplicates. Four days later, WST-1 was added to each well and incubated for 1.5 h at 37°C. Absorbance was measured with a plate reader at 450 nm with correction at 650 nm. The results are expressed as the percentage of absorbance of treated wells versus that of vehicle control. IC_{50}, the drug concentration causing 50% growth inhibition, was calculated via sigmoid curve fitting using GraphPad Prism 5.0 (GraphPad).

Apoptosis Assays

For the detection of apoptotic cells using 4′,6-diamidino-2-phenylindole staining, PC-3 cells were plated in six-well plates and treated with various concentrations of (-)-gossypol and then stained with 3 mmol/L 4′,6-diamidino-2-phenylindole for 10 min. The cells with the nuclei showing morphologic characteristics of apoptosis (nuclear karyopyknosis and fragmentation) were counted as positive under a fluorescent microscope as described (22). For mitochondrial transmembrane potential ($\Delta\Psi_m$) assay, PC-3 were cultured in a chamber slide; after wash with PBS, cells were incubated with the MitoCapture solution at 37°C for 15 min according to the manufacturer's protocol (BioVision). The fluorescence was detected and recorded using a Zeiss LSM-510 confocal microscope. For apoptosis analysis of tumors in animal studies, tumor tissues were excised and stained for terminal deoxynucleotidyl transferase–mediated dUTP nick end labeling using the ApopTag kit (Chemicon) according to the manufacturer's instructions.

Fluorescence Resonance Energy Transfer Assay

(-)-Gossypol-mediated disruption of Bcl-xL heterodimerization with Bax and Bad was analyzed with fluorescence resonance energy transfer (FRET) assay as described (23) with modification. Briefly, DU-145 cells were transiently transfected with Bcl-xL-CFP together with either Bax-YFP or Bad-YFP (kindly provided by Dr. Junyin Yuan) using FuGene 6 reagent (Roche). Twenty-four hours later, the cells were treated with increasing doses of (-)-gossypol or DMSO vehicle control for another 15 h. Cells were then harvested and fixed in 2% paraformaldehyde. The cells

[4] http://ClinicalTrials.gov

were plated in 96-well black plates (0.2×10^6 per well) and fluorescence was measured in a Tecan multimode plate reader and calculated based on Dr. Yuan's method as described (23).

Western Blot Analysis

Cells were washed with PBS and lysed in an ice-cold radioimmunoprecipitation assay lysis buffer: 1% NP-40, 0.5% sodium deoxycholate, 0.1% SDS, and Complete Protease Inhibitor cocktail (100 μg/mL) in PBS. Tumor tissues were incubated with 200 μL lysis buffer in an ice-cold French Douncer for 15 min after homogenization by 40 strokes. The cell lysates and homogenates were cleared by centrifugation at 13,000 × *g* for 10 min at 4°C. The supernatants were collected. Protein concentrations were determined with the Bradford method (Bio-Rad); 60 μg protein was electrophoresed by 12% SDS-PAGE. Separated proteins were transferred to polyvinylidene difluoride membranes (Bio-Rad). After blocking with 5% milk, blots were probed with anti-Mcl-1, anti-Bcl-2, anti-Bim, anti-β-actin, and anti-glyceraldehyde-3-phosphate dehydrogenase (purchased from Santa Cruz Biotechnology), anti-Bcl-xL (BD Biosciences), anti-Puma and anti-caspase-3 (Cell Signaling Technology), and anti-Noxa (Calbiochem).

Subcellular Fractionation and Immunoblotting

PC-3 cells were harvested and washed with PBS. Cell pellets were suspended at 3×10^7/mL in mitochondrial resuspension buffer: 250 mmol/L sucrose, 10 mmol/L KCl, 1.5 mmol/L $MgCl_2$, 1 mmol/L EDTA, 1 mmol/L DTT, 1 mmol/L phenylmethylsulfonyl fluoride, and 100 μg/mL cocktail. Digitonin was added to 200 μg/mL. The cells were incubated in digitonin-supplemented mitochondrial resuspension buffer for 5 min on ice. Cell lysates were then centrifuged for 10 min at 13,000 × *g*. Proteins from the supernatant (cytosolic fraction) were respun at 13,000 × *g* for 10 min to clear any remaining debris, and pellet (membrane fraction) was washed twice with mitochondrial resuspension buffer. The pellet was solubilized in radioimmunoprecipitation assay buffer and incubated on ice for 10 min. The cytosolic and mitochondria extracts were analyzed by SDS-PAGE. Antibodies used for immunoblotting were anti-cytochrome *c* (BD PharMingen), anti-apoptosis-inducing factor (AIF; Santa Cruz Biotechnology), and anti-cyclooxygenase IV (Molecular Probes).

Quantitative Real-time PCR

Total RNA was extracted from the treated cells using TRIZOL (Invitrogen) according to the manufacturer's instructions. Reverse transcription was done using SuperScript III First-Strand kits (Invitrogen). Each quantitative real-time PCR (95°C for 10 min, 40 cycles of 95°C for 15 s, 60°C for 1 min, and 72°C for 10 s) was done using TaqMan Universal PCR Master Mix (Applied Biosystems). Primers were designed as *Mcl-1* forward 5′-CTCATTTCTTTTGGTGCCTTT-3′ and reverse 5′-CCAGTCCCGTTTTGTCCTTAC-3′, *Noxa* forward 5′-CTGCAGGACTGTTCGTGTTC-3′ and reverse 5′-TTCTGCCGGAAGTTCAGTTT-3′, and *Puma* forward 5′-TCCTCAGCCCTCGCTCTCGC-3′ and reverse 5′-CCGATGCTGAGTCCATCAGC-3′.

Small Interfering RNA Transfections

Small interfering RNA (siRNA) oligonucleotides were purchased from Dharmacon with the sequences for *Noxa* (NM_021127): 5′-CUUCCGGCAGAAACUUCUG-3′ (24) and *Puma* (NM_014417): 5′-UCUCAUCAUGGGACUCCUG-3′ (25); PC-3 cells were transfected 24 h after being seeded in six-well plates. siRNA (100 pmol) were dissolved in 200 μL serum-free, antibiotic-free medium; Lipofectamine 2000 transfection reagent (5 μL; Invitrogen) was dissolved in 200 μL of the same medium; the above two solutions were mixed and allowed to stand at room temperature for 20 min. The resulting 400 μL transfection complexes were then added to each well containing 1.6 mL medium. Six hours later, the cultures were replaced with fresh medium supplemented with 10% fetal bovine serum and antibiotics. (-)-Gossypol was added to the cells 24 h after transfection as indicated. For Western blot, cells were collected after an additional 24 h; for cell survival assay, cells were collected after 4 days.

Animal Tumor Model and *In vivo* Experiments

Double-blinded *in vivo* experiments were carried out with 5- to 6-week-old male athymic NCr-*nu/nu* nude mice purchased from the National Cancer Institute. After alcohol preparation of the skin, mice were inoculated s.c. with 0.1 mL PC-3 cell suspension (5×10^6 cells) on both flanks using a sterile 22-gauge needle. When tumors reached 100 mm^3, the mice were randomized into six groups with 5 to 8 mice per group. Group 1 was given carboxymethyl cellulose as vehicle control; group 2 was given docetaxel 7.5 mg/kg i.v. once weekly × 3 weeks; groups 3 and 4 were given (-)-gossypol 10 and 20 mg/kg p.o. q.d. 7 weeks, respectively; groups 5 and 6 were given a combination of docetaxel 7.5 mg/kg i.v. once weekly × 3 weeks and (-)-gossypol 10 or 20 mg/kg p.o. q.d. 7 weeks, respectively. The tumor sizes and animal body weights were measured twice weekly. Three weeks after the first treatment, one mouse from each group was sacrificed and the tumors were dissected. Tumor tissues with a size of ~8 mm^3 were prepared for Western blot as described above. All animal experiments were done according to the protocol approved by University of Michigan Guidelines for Use and Care of Animals.

Statistical Analysis

Two-tailed Student's *t* test and two-way ANOVA were employed to analyze the *in vitro* and *in vivo* data, respectively, using Prism 5.0 software (GraphPad Prism).

Results

(-)-Gossypol Induces Apoptosis through Mitochondria Pathway in Human Prostate Cancer Cells

To evaluate the antitumor activity of (-)-gossypol in prostate cancer cells, we carried out the MTT-based cell viability assay. Human prostate cancer cell lines PC-3 (p53-null) and LNCaP (p53 wild-type) as well as human lung fibroblast cell line WI-38 were exposed to (-)-gossypol. As shown in Fig. 1A, (-)-gossypol potently inhibited the growth of PC-3 and LNCaP cells but had minimal effect on normal fibroblast WI-38 cells. The IC_{50} was 3.5 μmol/L

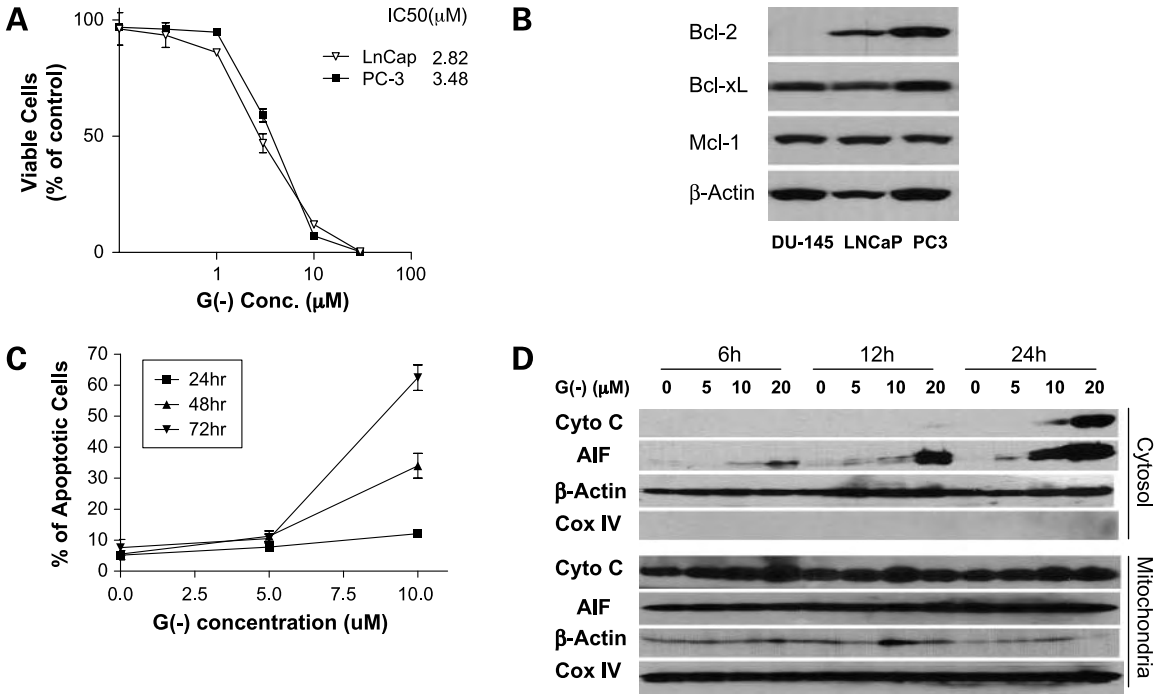

Figure 1. (-)-Gossypol causes cell death and induces apoptosis through mitochondria pathway in human prostate cancer cell line PC-3. **A,** MTT-based cell viability assay of (-)-gossypol in PC-3 and LNCaP cells. Cells were seeded in 96-well plates and treated in triplicates. Mean ± SE normalized to their respective controls (n = 3). **B,** Western blot analysis showed the difference of Bcl-2, Bcl-xL, and Mcl-1 protein levels in three prostate cell lines (60 μg/lane). **C,** apoptotic cells were counted with 4′,6-diamidino-2-phenylindole staining. Cells were counted in five different fields. Mean ± SE. **D,** cytochrome *c* and AIF release from mitochondria to cytosol. PC-3 cells were treated with (-)-gossypol for indicated times and then subjected to a digitonin-based subcellular fractionation as described in Materials and Methods. Cytosolic fractions (~120 μg/lane) and mitochondria fractions (~60 μg/lane) were subjected to SDS-PAGE followed by immunoblotting with the indicated antibodies. The cyclooxygenase IV marker was used to determine cross-contamination of cytosolic fractions with mitochondrial proteins.

for PC-3 cells, 2.8 μmol/L for LNCaP cells, and 17.4 μmol/L for WI-38 cells (Fig. 1A). It was noted that the protein expression of Bcl-2, Bcl-xL, and Mcl-1 differed among these cell lines. PC-3 cells have higher levels of Bcl-2, Bcl-xL, and Mcl-1 (Fig. 1B) than LNCaP cells and form good xenograft tumors in nude mice. Therefore, PC-3 is an appropriate cell line for studying the (-)-gossypol activity and mechanism in prostate cancer.

(-)-Gossypol-induced apoptosis was also assessed by 4′,6-diamidino-2-phenylindole staining and counting the cells with karyorrhexis, a typical apoptotic change of cells (22). PC-3 cells treated with 10 μmol/L (-)-gossypol for 48 and 72 h showed dramatically increased apoptosis (Fig. 1C). Cytochrome *c* and AIF released from the intermembrane space of mitochondria contribute to caspase-dependent and caspase-independent apoptosis (26, 27). We separated the mitochondria from cytosol and examined the cytochrome *c* and AIF release in (-)-gossypol-treated PC-3 (Fig. 1D). Cytochrome *c* translocated from mitochondria to cytosol 24 h after (-)-gossypol treatment. Interestingly, AIF was released from mitochondria into cytosol at 6 h, preceding the cytochrome *c* release, suggesting that AIF-mediated, caspase-independent apoptosis might also be involved in (-)-gossypol-induced cell death. By using MitoCapture staining, we observed the loss of $\Delta\Psi_m$, one of the early events in apoptosis induction via mitochondrial pathway (28), associated with (-)-gossypol-induced apoptosis. As shown in Supplementary Fig. S1,[5] in control cells, consistent with mitochondrial localization, the bright punctuated yellow/orange fluorescence was found mostly in granular structures distributed throughout the cytoplasm. Exposure of PC-3 cells to 20 μmol/L (-)-gossypol for 6 h induced a marked change in $\Delta\Psi_m$ as evidenced by the disappearance of bright yellow/orange fluorescence and an increase of green fluorescence in most cells with a predominantly perinucleic distribution.

(-)-Gossypol Sensitizes PC-3 Cells to Docetaxel-Induced Growth Inhibition and Apoptosis

To investigate whether (-)-gossypol sensitizes the prostate cancer cells to chemotherapy, we examined the cytotoxic effect of the combination of (-)-gossypol and docetaxel, a first-line chemotherapy currently used for hormone-refractory prostate cancer. Figure 2A shows that, as the (-)-gossypol dose increased, there was an obvious left shift of the cytotoxicity curves, indicating that the PC-3 cells

[5] Supplementary material for this article is available at Molecular Cancer Therapeutics Online (http://mct.aacrjournals.org/).

were sensitized to docetaxel by (-)-gossypol. To assess whether the combined effects were synergistic or additive, the combination index value was calculated and isobologram was plotted (Fig. 2B) as we described previously (20). Combination index < 1 is considered synergistic of the combination treatment (20). The combination treatment of 0.5 nmol/L docetaxel with 0.63, 1.25, or 2.5 μmol/L (-)-gossypol resulted in synergistic effects (combination indices = 0.286, 0.412, or 0.538, respectively).

We next investigated the changes of several Bcl-2 family members at protein level. As shown in Fig. 2C and D, no significant change was observed in Bcl-2 and Bcl-xL proteins. This is consistent with an earlier report (29) in large cell lymphoma and supports that (-)-gossypol is a functional inhibitor of Bcl-2 and Bcl-xL via binding to the BH3 domain of the proteins without affecting protein levels directly. (-)-Gossypol-treated PC-3 cells showed an increase of Noxa and Puma as well as a decrease of Bim and a dose-dependent increase of Mcl-1 (both full-length and a shortened form; Fig. 2C and D). Combination with docetaxel reversed the Bim decrease and further increased Puma levels in a time- and dose-dependent manner (Fig. 2C and D), which might contribute to the synergistic effect of the combination therapy.

Noxa and Puma Knockdown by siRNA Attenuates (-)-Gossypol Effects on PC-3 Cells

To further investigate the role of Bcl-2 family members in (-)-gossypol-induced apoptosis, we examined the BH3-only proteins Noxa and Puma in (-)-gossypol-treated PC-3 cells by Western blot. Here again, PC-3 cells treated with (-)-gossypol for 24 and 48 h showed a dose-dependent increase of Noxa and Puma proteins as well as Mcl-1 (both full-length and a shortened form; Fig. 3A). This increase was not accompanied by clear and robust increase of their mRNA levels as assessed by quantitative real-time PCR (Fig. 3C), indicating that Mcl-1 increase was post-translational. It is not clear at the present what the shortened form Mcl-1 is. It could be either the alternatively spliced Mcl-1 or the caspase-cleaved Mcl-1, both of which have been reported to be proapoptotic and associated with apoptosis

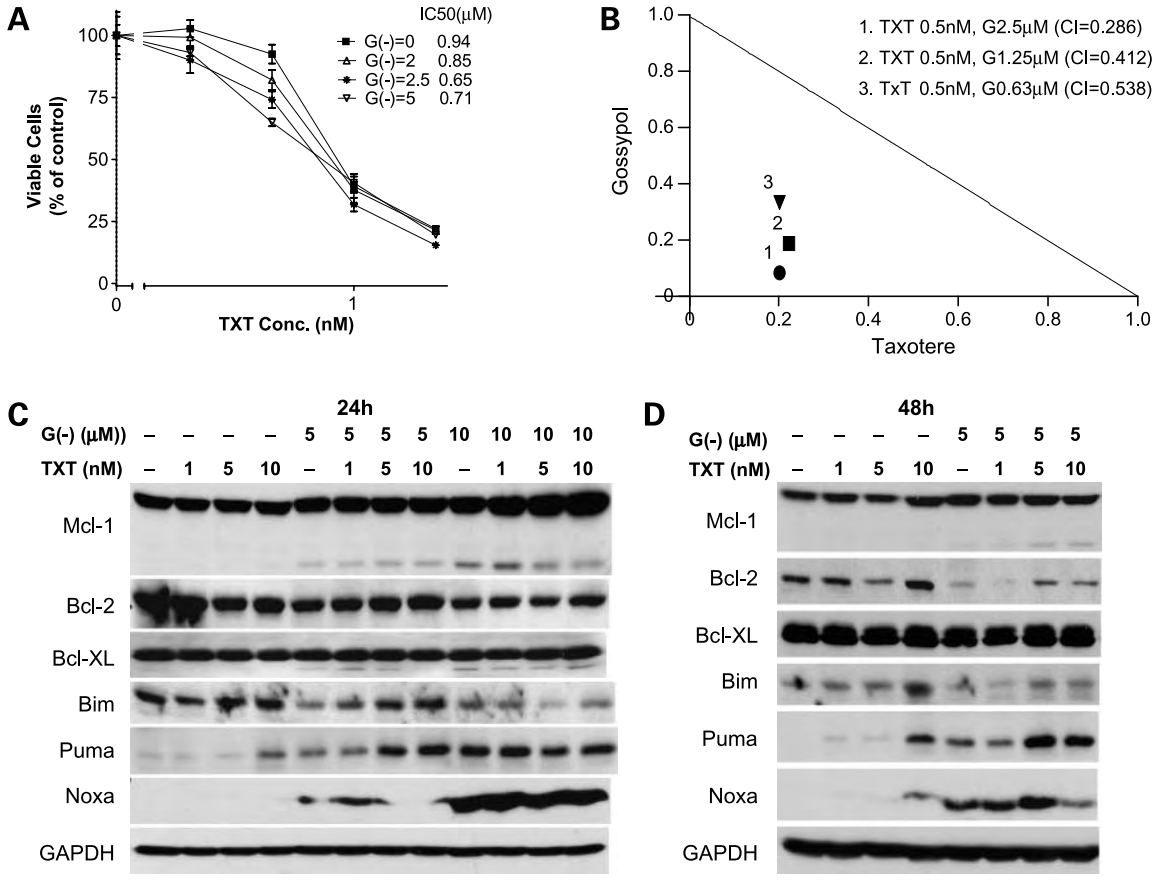

Figure 2. (-)-Gossypol enhances the chemotherapy of docetaxel in human prostate cancer PC-3 cells. **A,** MTT-based cell viability assay of (-)-gossypol docetaxel in PC-3. **B,** IC_{50} isobologram of the combination treatments. In the isobologram, a plot on the diagonal line indicates that the combination is simply additive. A plot to the left under the line indicates that the combination is synergistic, whereas a plot to the right above the line indicates that it is antagonistic. Combination index < 1 is considered synergistic of the combination treatment (20). **C** and **D,** Western blot analysis showed the effect of docetaxel and (-)-gossypol on proteins expression in PC-3 cells. Cells were treatment with docetaxel and (-)-gossypol of the indicated doses for 24 h (**C**) or 48 h (**D**) and then collected for Western blot (60 μg/lane). Data with (-)-gossypol 10 μmol/L treatment for 48 h were not shown because of severe cell death.

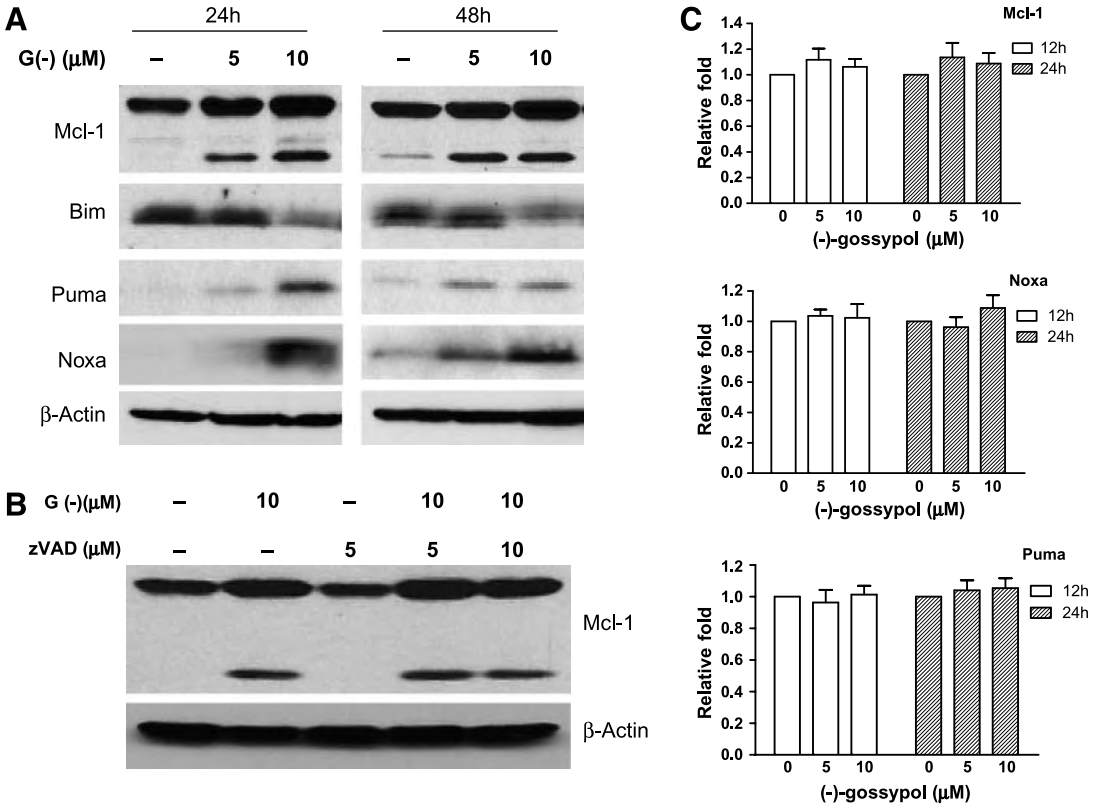

Figure 3. (-)-Gossypol increases Noxa, Puma, and Mcl-1 and decreases Bim at protein levels. **A,** (-)-gossypol dose-dependently induced Mcl-1, Noxa, and Puma increase and Bim decrease. **B,** (-)-gossypol-induced Mcl-1 increase is caspase independent. PC-3 cells were pretreated with zVAD-fmk for 4 h and then incubated with or without (-)-gossypol for another 24 h before collecting for Western blot analysis. **C,** changes of mRNA levels of Mcl-1, Noxa, and Puma. PC-3 cells were treated with (-)-gossypol at the indicated time points and doses. Quantitative real-time PCR with TaqMan Universal PCR Master Mix (Applied Biosystems) were done on the Mastercycler *realplex* 2 system (Eppendorf). Target gene mRNA levels were normalized to actin mRNA according to the following formula: $[2^{\wedge} - (C_T^{target} - C_T^{actin})] \times 100\%$, where C_T is the threshold cycle. Fold increase was calculated by dividing the normalized target gene expression of the treated sample with that of the untreated control.

induction (30, 31). Interestingly, pan-caspase inhibitor zVAD did not block the Mcl-1 increase nor prevented the increase of the shortened form (Fig. 3B), indicating that the (-)-gossypol-induced Mcl-1 increase was caspase independent, and the shortened form might not be the caspase-cleaved Mcl-1 but is likely to be the alternatively spliced proapoptotic Mcl-1.

To evaluate the role of Noxa and Puma in the (-)-gossypol-induced cell response, we employed RNA interference to knock down Noxa and Puma in PC-3 cells before treatment with (-)-gossypol. Figure 4A shows that Noxa and Puma were effectively knocked down (>95%) by respective siRNA in PC-3 cells. Figure 4B shows that knockdown of Noxa or Puma shifted the (-)-gossypol dose-response curve to the right, with the Noxa/Puma double-knockdown cells most resistant to (-)-gossypol ($P < 0.001$, versus control siRNA, two-way ANOVA, $n = 3$). Similar results were observed with colony formation assay (Fig. 4C and D). These data show that Noxa and Puma knockdown rendered PC-3 cells resistant to (-)-gossypol-induced cell death and clonogenic growth, whereas Noxa/Puma double knockdown most effectively attenuated the (-)-gossypol activity. Our results support that Noxa and Puma are involved in (-)-gossypol-mediated growth inhibition and cell death in PC-3 cells.

(-)-Gossypol Dose-Dependently Disrupts Bcl-xL Heterodimerization with Bax and Bad

Using the fluorescence resonance energy transfer assay system described by Dr. Yuan's group (23), we investigated the effect of (-)-gossypol on Bcl-xL heterodimerization with Bax or Bad. (-)-Gossypol dose-dependently inhibited the FRET signal; it inhibited the interaction between Bcl-xL and Bax (Fig. 5A) or Bad (Fig. 5B). (-)-Gossypol (5 μmol/L) blocked 98.5% of interaction between Bcl-xL and Bax and 77% of interaction between Bcl-xL and Bad. The plate-based FRET assay results were also confirmed by FRET analysis under confocal laser scanning microscopy (data not shown). There is a good correlation between (-)-gossypol cellular activity (growth inhibition and apoptosis induction) and the blocking of Bcl-xL-Bax (Pearson's correlation $r = 0.941$) as well as the blocking of Bcl-xL-Bad interaction (Pearson's correlation $r = 0.994$). These data suggest that Bcl-xL might be one of the major molecular targets of (-)-gossypol in cell growth inhibition and

apoptosis induction. These data further support that (-)-gossypol is a potent functional inhibitor of the antiapoptotic protein Bcl-xL.

(-)-Gossypol Overcomes Bcl-xL Protection of FL5.12 Model Cells from Cell Death Induced by IL-3 Withdrawal

FL5.12 cells depend on IL-3 for growth and survival in culture and rapidly undergo apoptosis on withdrawal of the growth factor IL-3 (32). However, when antiapoptotic Bcl-2 or Bcl-xL genes were transfected into FL5.12 cells, they became resistant to apoptosis induction by IL-3 withdrawal (21, 32, 33). Therefore, the FL5.12 is a model system that is frequently used to analyze the antiapoptotic activity of Bcl-2/Bcl-xL. Parental FL5.12 cells transfected with control vector (FL5.12-neo) undergo apoptosis after IL-3 withdrawal, whereas FL5.12 cells overexpressing Bcl-2 or Bcl-xL are protected (21). As shown in Fig. 5C, FL5.12-neo cells rapidly died on IL-3 withdrawal. FL5.12-Bcl-xL cells remained alive after IL-3 deprivation but did not grow as well as the cells in the presence of growth factor IL-3. Our data are consistent with the literature (21, 32, 33) in that Bcl-xL is a potent inhibitor of apoptosis and thus can protect the FL5.12 cells from cell death induced by IL-3 deprivation. On the other hand, because Bcl-xL is not a growth factor on its own, FL5.12-Bcl-xL cells without IL-3 did not grow as fast as those with IL-3 (Fig. 5C). For (-)-gossypol treatment study, the FL5.12 cells were plated in 24-well plates and treated in duplicates with different doses of (-)-gossypol for 2 days, and the live cells were counted by trypan blue exclusion as described (21). As shown in Fig. 5D, the low doses (<6 μmol/L) of (-)-gossypol did not kill FL5.12-neo and FL5.12-Bcl-xL cells in the presence of IL-3; however, in FL5.12-Bcl-xL cells in the absence of IL-3, whose survival is solely dependent on protection from Bcl-xL, the nontoxic dose of (-)-gossypol potently killed the FL5.12-Bcl-xL cells, showing that (-)-gossypol can overcome the Bcl-xL protection of FL5.12 cells on IL-3 withdrawal.

(-)-Gossypol Enhances Prostate Cancer Response to Docetaxel and Inhibits Tumor Growth *In vivo*

To investigate whether (-)-gossypol can sensitize PC-3 cells to docetaxel chemotherapy *in vivo*, we employed a PC-3 xenograft model in athymic nude mice. As shown in Fig. 6A, oral (-)-gossypol given daily at 20 mg/kg dose significantly improved docetaxel efficacy on PC-3 tumors ($P < 0.001$ versus docetaxel alone, ANOVA, $n = 16$). Similar

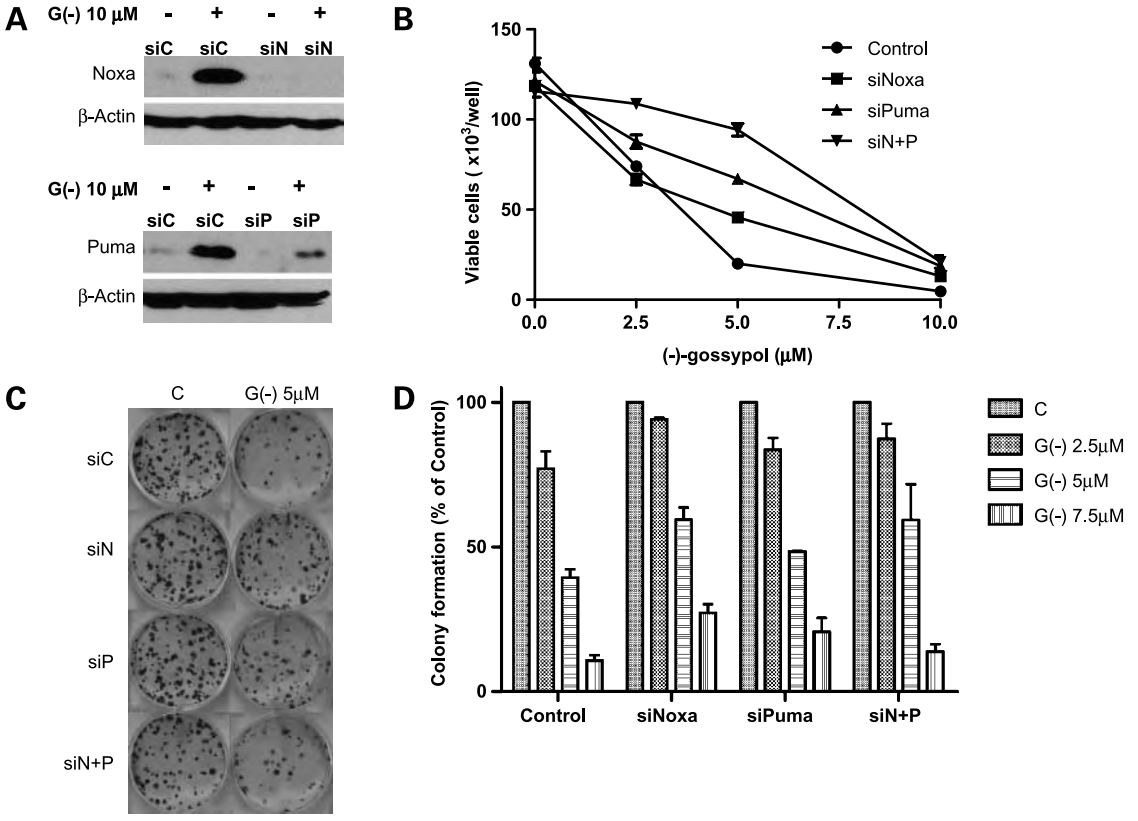

Figure 4. Noxa and Puma knockdown by siRNA attenuate the effects of (-)-gossypol on PC-3 cells. PC-3 cells transfected with Noxa and Puma siRNA for 24 h were used in the following assays. **A,** transfected PC-3 cells were treated with 10 μmol/L (-)-gossypol for an additional 24 h and lysed for Western blot; **B,** transfected PC-3 cells were seeded in 24-well plates and treated in triplicates with (-)-gossypol for 4 d, and the viable cells were counted by trypan blue staining. Mean ± SD of cells per well ($\times 10^3$). **C,** transfected PC-3 cells were plated in six-well plates (300 per well) and treated in triplicates with (-)-gossypol for colony formation. The plates were cultured for 14 d and stained. Representative pictures of the colonies in the plates. **D,** colonies with >50 cells were counted. Mean ± SD ($n = 3$). The assays have been repeated in four independent experiments with similar results.

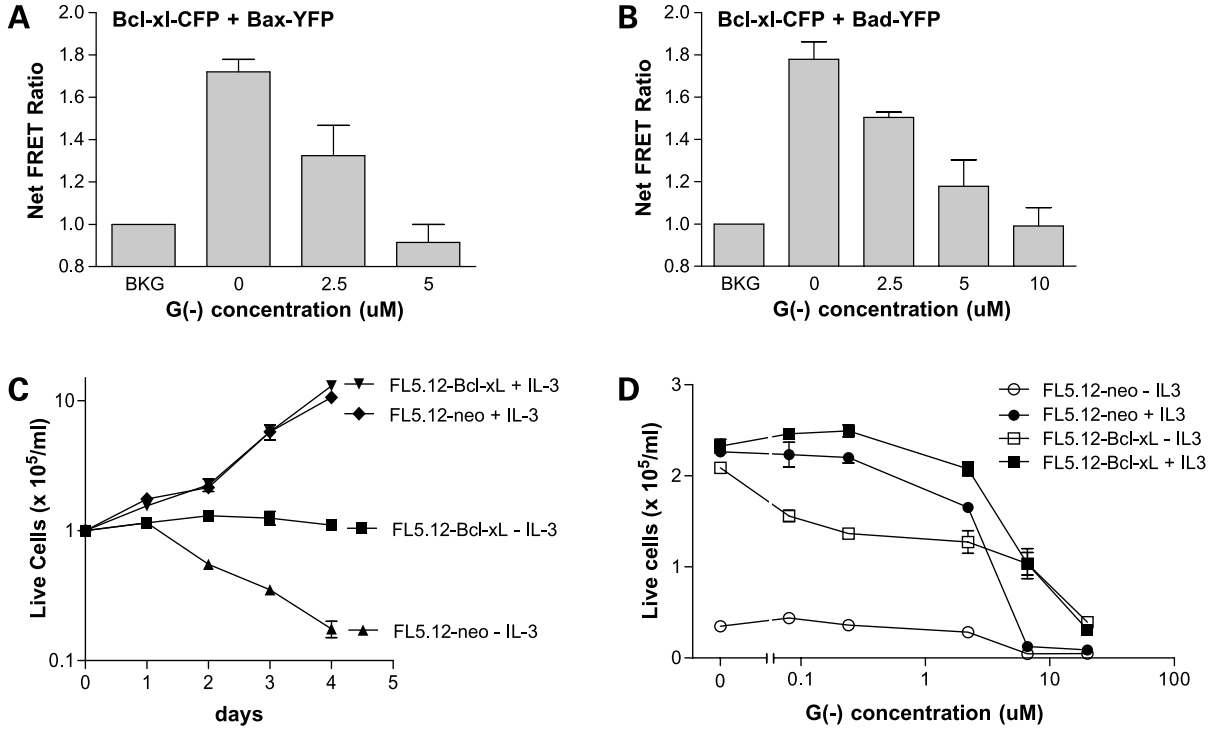

Figure 5. (-)-Gossypol disrupts Bcl-xL heterodimerizaion with Bax and Bad and overcomes Bcl-xL protection of FL5.12 cells. **A** and **B**, FRET analysis of (-)-gossypol-mediated disruption of Bcl-xL-CFP heterodimerization with Bax-YFP (**A**) or Bad-YFP (**B**). DU-145 cells were transiently transfected with Bcl-xL-CFP together with Bax-CFP or Bad-YFP for 24 h and then treated with (-)-gossypol for 15 h. The cells were counted and plated in a 96-well black assay plate and the fluorescence was measured in a Tecan multimode plate reader at excision/emission = 430/485 nm (for CFP), 514/535 nm (for YFP), and 430/535 nm (for FRET). Results are net FRET ratios ($n = 3$) normalized with background (set BKG = 1), which is the fluorescence cross-talk (leak-through) from the cells separately transfected with Bcl-xL-CFP and Bax-YFP or Bad-YFP. **C**, FL5.12/Neo and FL5.12/Bcl-xL cells were cultured in the presence or absence of IL-3. The cell numbers were counted daily by trypan blue exclusion. Bcl-xL expression protected the cells from cell death induced by IL-3 withdrawal. **D**, FL5.12/Neo and FL5.12/Bcl-xL cells were treated with the indicated concentrations of (-)-gossypol in the presence or absence of IL-3 for 48 h, and the viable cells were counted. These experiments were repeated two to four times with consistent results. Representative results.

results were shown when 10 mg/kg (-)-gossypol was administrated (Supplementary Fig. S2A).[5] Tumor growth delay analysis (Fig. 6B) showed that docetaxel combined with (-)-gossypol was more effective in inhibiting tumor growth compared with either treatment alone ($P < 0.05$ versus docetaxel alone; $P < 0.01$ versus (-)-gossypol alone). Supplementary Table S1[5] summarizes the tumor growth inhibition values, calculated from the median tumor size of the treatment group divided by that of the control group on day 32. The combination of docetaxel with (-)-gossypol 10 and 20 mg/kg had tumor growth inhibition values of 37.3% and 29.4%, both of which are <42%, a value considered efficacious according to the National Cancer Institute criteria (34). It is worth noting that (-)-gossypol alone at 10 and 20 mg/kg showed similar but limited effects on PC-3 tumor growth ($P > 0.05$); neither is active as single treatment according to National Cancer Institute criteria, consistent with our earlier study (20). The animal body weight loss was moderate, transient, and tolerable and recovered to normal soon after docetaxel treatment was complete (Supplementary Fig. S2B), indicating that the observed toxicity in the combination therapy was reversible and can be managed.

(-)-Gossypol Increases Docetaxel-Induced Apoptosis of PC-3 Tumors *In vivo*

Because our *in vitro* study showed that (-)-gossypol increased the docetaxel-induced apoptosis, we also sought to determine whether this is still the case *in vivo*. We randomly picked one mouse from each group at the end of docetaxel treatment (week 3) and took the tumor tissues to perform terminal deoxynucleotidyl transferase–mediated dUTP nick end labeling staining for apoptosis. Results are shown in Fig. 6C. (-)-Gossypol plus docetaxel induced significantly more apoptosis than either (-)-gossypol or docetaxel alone. Quantification of terminal deoxynucleotidyl transferase–mediated dUTP nick end labeling–positive cells clearly showed that (-)-gossypol enhanced the apoptotic effect of docetaxel in a dose-dependent manner (Fig. 6D). The effects of combination therapy were also evaluated on the proteins related to the apoptosis signaling pathway. Western blot analysis was done on PC-3 tumor xenografts treated with 3 weeks of (-)-gossypol and docetaxel. (-)-Gossypol- and docetaxel-treated tumors showed poly(ADP-ribose) polymerase cleavage [(-)-gossypol 10 mg/kg] and caspase-3 cleavage [(-)-gossypol 20 mg/kg; Supplementary Fig. S2C].

Discussion

In this study, we have employed (-)-gossypol, a small-molecule inhibitor of Bcl-2/Bcl-xL/Mcl-1, to investigate whether (-)-gossypol potentiate the response of prostate cancer to chemotherapy and whether this potentiation is accompanied with an increase of drug-induced apoptosis. Our *in vitro* and *in vivo* data show that (-)-gossypol inhibits tumor growth and induces apoptosis in human prostate cancer PC-3 cells with high levels of Bcl-2/Bcl-xL proteins. The FRET assay confirmed that (-)-gossypol potently blocks the interactions of Bcl-xL with Bax or Bad in live cells in a dose-dependent manner. In Bcl-xL-transfected model cell lines, (-)-gossypol overcomes the Bcl-xL-mediated protection of FL5.12 cells on IL-3 withdrawal. The data support that (-)-gossypol exerts its antitumor activity, at least in part, through functional inhibition of the antiapoptotic protein Bcl-xL, although other targets might also be involved. More importantly, (-)-gossypol significantly improved the antitumor activity of current chemotherapeutic agent docetaxel in PC-3 cells both *in vitro* and *in vivo* in a nude mice xenograft model. This enhanced response to chemotherapy is correlated with increased induction of apoptosis *in vivo* by the combination therapy.

(-)-Gossypol has recently been reported as a natural BH3 mimetic small-molecule inhibitor of both Bcl-2 and Bcl-xL and induces apoptosis in multiple cancer cell lines with

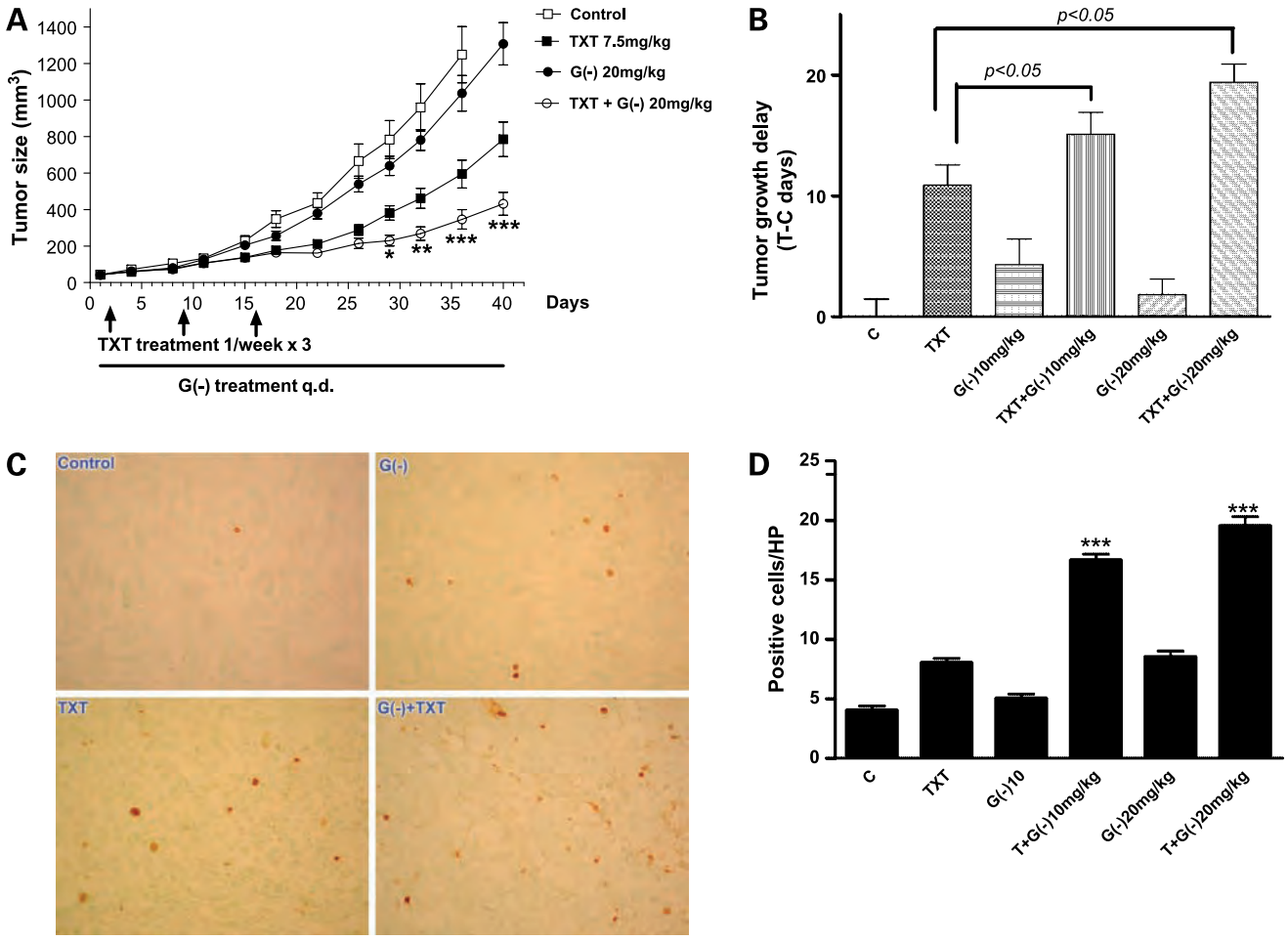

Figure 6. (-)-Gossypol potentiates docetaxel in inhibiting tumor growth and inducing apoptosis in xenograft model of human prostate cancer PC-3. **A,** PC-3 xenograft tumor growth curves. PC-3 cells (5×10^6) were s.c. injected into the flanks on both sides of each mouse. When the tumors reached 50 mm^3, the mice were randomized into 5 to 8 mice per group and treated with 20 mg/kg (-)-gossypol, 7.5 mg/kg docetaxel, or combination of both. (-)-Gossypol was administrated p.o. via oral gavage q.d.; docetaxel was administrated i.v. once weekly for 3 wk. The average tumor sizes were shown (n = 10-16). *, $P < 0.05$; **, $P < 0.01$; ***, $P < 0.001$, compared with docetaxel alone, two-way ANOVA (n = 14-18). Representative results of at least four independent animal experiments. **B,** tumor growth delay (T-C) analysis. *T* is the median time (in days) required for the treatment group tumors to reach 750 mg, and *C* is the median time (in days) for the control group tumors to reach 750 mg (T-C value for control group is zero). **C** and **D,** tumor tissues from each treatment group were taken at the end of the third week and fixed in 10% formalin. The tumor sections were stained for terminal deoxynucleotidyl transferase–mediated dUTP nick end labeling using the ApopTag kit. The apoptotic cells have DNA fragmentation and are stained positive as brown nuclei. **C,** representative pictures: *C,* control; *TXT,* docetaxel; *G(-),* (-)-gossypol; *TXT + G(-),* docetaxel + (-)-gossypol. Original magnification, ×400. **D,** quantification of terminal deoxynucleotidyl transferase–mediated dUTP nick end labeling staining positive cells. Positive cells were counted under ×400 magnification at eight different fields, and the average numbers were calculated and plotted. ***, $P < 0.001$, compared with docetaxel alone, *t* test.

high levels of Bcl-2/Bcl-xL (19, 35). These studies show that (-)-gossypol as a potent inducer of apoptosis in these cancer cells is well tolerated and is clinically safe. Oliver et al. (36) showed that (-)-gossypol acts directly on the mitochondria to overcome Bcl-2- and Bcl-xL-mediated apoptosis resistance. Reports have shown that (-)-gossypol has a significant antitumor activity as a potential novel therapy for the treatment of lymphoma *in vitro* and *in vivo* (29) as well as head and neck cancer cells *in vitro* (37). We have shown previously that (-)-gossypol potently enhanced radiation-induced apoptosis and growth inhibition of human prostate cancer PC-3 cells and improved antitumor activity of X-ray irradiation to PC-3 cells *in vivo*, resulting in tumor regression even in large tumors (20). Interestingly, the (-)-gossypol dose of 1 to 5 μmol/L used in the current study is the dose that can block Bcl-xL-Bax and Bcl-xL-Bad protein-protein interactions in our FRET assay, whereas the same doses of (-)-gossypol potently and specifically overcome the Bcl-xL protection of FL5.12-Bcl-xL cells from cell death induced by IL-3 withdrawal. The same doses of (-)-gossypol also inhibited cell growth of PC-3 and LNCaP cells that have high levels of Bcl-xL in the current study and potently radiosensitized these cells in our earlier publication (20). Taken together, our data support that (-)-gossypol can kill cancer cells, at least in part, through inhibiting the antiapoptotic function of Bcl-xL. Our results show that Bcl-xL is one of the major targets of (-)-gossypol in prostate cancer cell growth inhibition.

The Bcl-2 family of proteins, which includes ≥17 members in mammalian cells, functions as a ''life/death switch'' that integrates diverse intercellular and intracellular cues to determine whether a cell should undergo apoptosis in response to diverse damage signals (38). The switch operates through the interactions between the proteins within three subfamilies of the Bcl-2 protein family. The prosurvival subfamily (Bcl-2, Bcl-xL, Bcl-w, Mcl-1, A1, and also Bcl-B in humans) protects cells exposed to diverse cytotoxic conditions, whereas two other subfamilies, many members of which were identified as Bcl-2-binding proteins, instead promote cell death (38). They are the Bax-like apoptotic subfamily (Bax, Bak, and Bok) and the BH3-only protein subfamily (includes at least eight members: Bik, Bad, Bid, Bim, Bmf, Hrk, Noxa, and Puma; refs. 16, 39). Earlier studies with Noxa- and Puma-knockouts show that Noxa and Puma are critical mediators of the apoptotic responses induced by p53 and cytotoxic drugs. BH3-only proteins Noxa, Puma, and Bim have both overlapping and specialized roles as death initiators in either p53-dependent or p53-independent apoptosis (39). In the current study, (-)-gossypol dose-dependently increased the protein levels of proapoptotic Noxa and Puma independent of p53 (PC-3 is p53 null). This effect on Puma was augmented by combination with docetaxel. Noxa and Puma knockdown by siRNA attenuated the (-)-gossypol-induced cell death and growth inhibition in PC-3 cells, indicating that Noxa and Puma are involved in (-)-gossypol-mediated growth inhibition and cell death in PC-3 cells. Thus, our study provides first proof that (-)-gossypol exerts its antitumor activity not only through inhibition of antiapoptotic protein Bcl-xL (as well as Bcl-2 and Mcl-1) but also through a p53-independent induction of proapoptotic BH3-only proteins Noxa and Puma.

The molecular mechanism(s) underlying the (-)-gossypol-induced, p53-independent increase of Noxa and Puma are not yet clear. Our data show that (-)-gossypol-induced Noxa and Puma increase appears to be post-translational, without significant change of mRNA levels. The interaction of Mcl-1 with Noxa and Puma in the apoptosis process draws increasing attention recently (40). Mcl-1 stability is tightly regulated; BH3-only proteins Noxa and Bim preferentially bind to Mcl-1 and also target it for proteasomal degradation (41). A recent study (40) using a novel BH3 ligand that selectively binds to Mcl-1 showed that apoptosis can proceed without Mcl-1 degradation. This BH3 mimetic ligand, derived from Bim BH3 mutation, preferentially binds to and stabilizes Mcl-1 and promotes cell death only when Bcl-xL is absent or neutralized (40). Blockage of BH3 domain-containing E3 ubiquitin ligase, Mule, which regulates the basal level of Mcl-1 by targeting it for proteasomal degradation, might be involved in this apparent Mcl-1 stabilization (40). This might account for our results that (-)-gossypol dose-dependently increased Mcl-1 protein level. Based on our data and other reports (42, 43), we propose that the BH3 mimetic (-)-gossypol might work in the same way as this unique BH3 ligand: (*a*) binds to and inactivates the antiapoptotic function of Bcl-xL (and/or Bcl-2), (*b*) binds to Mcl-1, blocks and displaces Noxa (and/or Puma), thus blocks Noxa-Mule-mediated Mcl-1 degradation, stabilizes Mcl-1, and increases both full-length and shortened form Mcl-1 (the latter is proapoptotic); and (*c*) the displaced Noxa and Puma accumulate and promote apoptosis. This mode of action by (-)-gossypol lies upstream of Bax/Bak in the mitochondrial apoptosis pathway. Indeed, a recent report with melanoma cells (43) lends support to this action by (-)-gossypol, which showed that (-)-gossypol was effective in killing cancer cells dependent on Mcl-1/Bcl-xL for survival. This effect was enhanced when the proteasome was blocked and accompanied with increase of Noxa (43). We are currently carrying out detailed studies to delineate the mechanism of Mcl-1 increase and Noxa increase induced by (-)-gossypol.

In conclusion, our study shows that (-)-gossypol significantly enhances the antitumor activity of docetaxel in human prostate cancer both *in vitro* and *in vivo* and may represent a promising new adjuvant therapy with a novel molecular mechanism for the treatment of hormone-refractory human prostate cancer with Bcl-2/Bcl-xL/Mcl-1 overexpression. (-)-Gossypol is now in phase II clinical trials for hormone-refractory prostate cancer. Our results provide insight into how (-)-gossypol works with chemotherapy in prostate cancer cells. Our finding contributes to the rational design of coming clinical trials and refines the selection of patients who will benefit the most from Bcl-2 molecular therapy as a promising novel strategy for overcoming chemoresistance of human prostate cancer.

Disclosure of Potential Conflicts of Interest

No potential conflicts of interest were disclosed.

Acknowledgments

We thank Susan Harris for help with the article; Dr. Junyin Yuan (Harvard University) for kindly providing Bcl-xL-CFP, Bax-YFP, and Bad-YFP plasmids for the FRET assay; Dr. Gabriel Nunez (University of Michigan) for kindly providing murine pro-B lymphoid cell line FL5.12 stably transfected with Bcl-xL or control vector; the University of Michigan Comprehensive Cancer Center Histology Core for immunohistology study; the University of Michigan Comprehensive Cancer Center Unit of Laboratory Animal Medicine for help with animal experiments; and the University of Michigan Comprehensive Cancer Center Flow Cytometry Core for flow cytometry analysis.

References

1. Assikis V, Simons JW. Novel therapeutic strategies for androgen-independent prostate cancer: an update. Semin Oncol 2004;31:26 – 32.

2. Oh WK, Kantoff PW. Management of hormone refractory prostate cancer: current standards and future prospects. J Urol 1998;160:1220 – 9.

3. Rago R. Management of hormone-sensitive and hormone-refractory metastatic prostate cancer. Cancer Control 1998;5:513 – 21.

4. Reed JC. Bcl-2 family proteins: strategies for overcoming chemoresistance in cancer. Adv Pharmacol 1997;41:501 – 32.

5. Reed JC, Jurgensmeier JM, Matsuyama S. Bcl-2 family proteins and mitochondria. Biochim Biophys Acta 1998;1366:127 – 37.

6. Korsmeyer SJ. Bcl-2 gene family and the regulation of programmed cell death. Cancer Res 1999;59:1693 – 700s.

7. Makin G, Dive C. Apoptosis and cancer chemotherapy. Trends Cell Biol 2001;11:S22 – 6.

8. Konopleva M, Zhao S, Hu W, et al. The anti-apoptotic genes Bcl-x(l) and Bcl-2 are over-expressed and contribute to chemoresistance of non-proliferating leukaemic $CD34^+$ cells. Br J Haematol 2002;118:521 – 34.

9. Furuya Y, Krajewski S, Epstein JI, Reed JC, Isaacs JT. Expression of Bcl-2 and the progression of human and rodent prostatic cancers. Clin Cancer Res 1996;2:389 – 98.

10. Krajewska M, Krajewski S, Epstein JI, et al. Immunohistochemical analysis of Bcl-2, Bax, Bcl-x, and Mcl-1 expression in prostate cancers. Am J Pathol 1996;148:1567 – 76.

11. Beale PJ, Rogers P, Boxall F, Sharp SY, Kelland LR. Bcl-2 family protein expression and platinum drug resistance in ovarian carcinoma. Br J Cancer 2000;82:436 – 40.

12. Ferlini C, Raspaglio G, Mozzetti S, et al. Bcl-2 down-regulation is a novel mechanism of paclitaxel resistance. Mol Pharmacol 2003;64:51 – 8.

13. Grad JM, Zeng XR, Boise LH. Regulation of Bcl-xl: a little bit of this and a little bit of Stat. Curr Opin Oncol 2000;12:543 – 9.

14. Lebedeva I, Rando R, Ojwang J, Cossum P, Stein CA. Bcl-xl in prostate cancer cells: effects of overexpression and down-regulation on chemosensitivity. Cancer Res 2000;60:6052 – 60.

15. Gleave M, Nelson C, Chi K. Antisense targets to enhance hormone and cytotoxic therapies in advanced prostate cancer. Curr Drug Targets 2003;4:209 – 21.

16. Kim H, Rafiuddin-Shah M, Tu HC, et al. Hierarchical regulation of mitochondrion-dependent apoptosis by Bcl-2 subfamilies. Nat Cell Biol 2006;8:1348 – 58.

17. Willis SN, Chen L, Dewson G, et al. Proapoptotic Bak is sequestered by Mcl-1 and Bcl-xl, but not Bcl-2, until displaced by BH3-only proteins. Genes Dev 2005;19:1294 – 305.

18. Adams KW, Cooper GM. Rapid turnover of Mcl-1 couples translation to cell survival and apoptosis. J Biol Chem 2007;282:6192 – 200.

19. Kitada S, Leone M, Sareth S, Zhai D, Reed JC, Pellecchia M. Discovery, characterization, and structure-activity relationships studies of proapoptotic polyphenols targeting B-cell lymphocyte/leukemia-2 proteins. J Med Chem 2003;46:4259 – 64.

20. Xu L, Yang D, Wang S, et al. (-)-Gossypol enhances response to radiation therapy and results in tumor regression of human prostate cancer. Mol Cancer Ther 2005;4:197 – 205.

21. Simonian PL, Grillot DA, Nunez G. Bcl-2 and Bcl-xl can differentially block chemotherapy-induced cell death. Blood 1997;90:1208 – 16.

22. Biggiogera M, Bottone MG, Pellicciari C. Nuclear ribonucleoprotein-containing structures undergo severe rearrangement during spontaneous thymocyte apoptosis. A morphological study by electron microscopy. Histochem Cell Biol 1997;107:331 – 6.

23. Degterev A, Lugovskoy A, Cardone M, et al. Identification of small-molecule inhibitors of interaction between the BH3 domain and Bcl-xl [comment]. Nat Cell Biol 2001;3:173 – 82.

24. Perez-Galan P, Roue G, Villamor N, Montserrat E, Campo E, Colomer D. The proteasome inhibitor bortezomib induces apoptosis in mantle-cell lymphoma through generation of Ros and Noxa activation independent of p53 status. Blood 2006;107:257 – 64.

25. Castedo M, Coquelle A, Vivet S, et al. Apoptosis regulation in tetraploid cancer cells. EMBO J 2006;25:2584 – 95.

26. Susin SA, Lorenzo HK, Zamzami N, et al. Molecular characterization of mitochondrial apoptosis-inducing factor. Nature 1999;397:441 – 6.

27. Donovan M, Cotter TG. Control of mitochondrial integrity by Bcl-2 family members and caspase-independent cell death. Biochim Biophys Acta 2004;1644:133 – 47.

28. Smaili SS, Hsu YT, Sanders KM, Russell JT, Youle RJ. Bax translocation to mitochondria subsequent to a rapid loss of mitochondrial membrane potential. Cell Death Differ 2001;8:909 – 20.

29. Mohammad RM, Wang S, Aboukameel A, et al. Preclinical studies of a nonpeptidic small-molecule inhibitor of Bcl-2 and Bcl-x(l) [(-)-gossypol] against diffuse large cell lymphoma. Mol Cancer Ther 2005;4:13 – 21.

30. Podar K, Gouill SL, Zhang J, et al. A pivotal role for Mcl-1 in bortezomib-induced apoptosis. Oncogene 2008;27:721 – 31.

31. Gomez-Bougie P, Oliver L, Le Gouill S, Bataille R, Amiot M. Melphalan-induced apoptosis in multiple myeloma cells is associated with a cleavage of Mcl-1 and Bim and a decrease in the Mcl-1/Bim complex. Oncogene 2005;24:8076 – 9.

32. Nunez G, London L, Hockenbery D, Alexander M, McKearn JP, Korsmeyer SJ. Deregulated bcl-2 gene expression selectively prolongs survival of growth factor-deprived hemopoietic cell lines. J Immunol 1990;144:3602 – 10.

33. Boise LH, Gonzalez-Garcia M, Postema CE, et al. Bcl-x, a Bcl-2-related gene that functions as a dominant regulator of apoptotic cell death. Cell 1993;74:597 – 608.

34. Corbett TH. Transplantable syngeneic rodent tumors. Totowa: Humana Press; 2002.

35. Zhang M, Liu H, Guo R, et al. Molecular mechanism of gossypol-induced cell growth inhibition and cell death of HT-29 human colon carcinoma cells. Biochem Pharmacol 2003;66:93 – 103.

36. Oliver CL, Miranda MB, Shangary S, Land S, Wang S, Johnson DE. (-)-Gossypol acts directly on the mitochondria to overcome Bcl-2- and Bcl-x(l)-mediated apoptosis resistance. Mol Cancer Ther 2005;4:23 – 31.

37. Oliver CL, Bauer JA, Wolter KG, et al. *In vitro* effects of the BH3 mimetic, (-)-gossypol, on head and neck squamous cell carcinoma cells. Clin Cancer Res 2004;10:7757 – 63.

38. Adams JM, Cory S. The bcl-2 apoptotic switch in cancer development and therapy. Oncogene 2007;26:1324 – 37.

39. Villunger A, Michalak EM, Coultas L, et al. p53- and drug-induced apoptotic responses mediated by BH3-only proteins Puma and Noxa. Science 2003;302:1036 – 8.

40. Lee EF, Czabotar PE, van Delft MF, et al. A novel BH3 ligand that selectively targets mcl-1 reveals that apoptosis can proceed without Mcl-1 degradation. J Cell Biol 2008;180:341 – 55.

41. Han J, Goldstein LA, Hou W, Rabinowich H. Functional linkage between noxa and bim in mitochondrial apoptotic events. J Biol Chem 2007;282:16223 – 31.

42. Denisov AY, Sprules T, Fraser J, Kozlov G, Gehring K. Heat-induced dimerization of bcl-xl through α-helix swapping. Biochemistry 2007;46:734 – 40.

43. Wolter KG, Verhaegen M, Fernandez Y, et al. Therapeutic window for melanoma treatment provided by selective effects of the proteasome on Bcl-2 proteins. Cell Death Differ 2007;14:1605 – 16.

Am J Transl Res 2009; 1: 4-18
www.ajtr.org/AJTR810001

Review Article

Overcoming cancer therapy resistance by targeting inhibitors of apoptosis proteins and nuclear factor-kappa B

Yao Dai, Theodore S. Lawrence, Liang Xu

Department of Radiation Oncology and Comprehensive Cancer Center, University of Michigan Medical School, Ann Arbor, MI 48109, USA

Received October 18, 2008; accepted October 22, 2008; available online October 30, 2008

Abstract: Chemo- or radioresistance markedly impairs the efficacy of cancer therapy and involves anti-apoptotic signal transduction pathways that prevent cell death. In resistant cancer cells, both inhibitors of apoptosis proteins (IAPs) and nuclear factor-kappa B (NF-κB) play a pivotal role in preventing apoptosis triggered by a variety of stresses, facilitating them as potential targets in cancer treatment. Furthermore, mounting evidences have established the crosstalks between IAPs (eg. XIAP, cIAP-1, cIAP-2) and proteins involved in NF-κB signaling (eg. TRAF2, RIP1, TAB1). Second mitochondria-derived activator of caspases (Smac) is a mitochondrial protein that released into cytoplasm upon apoptotic stimuli. As Smac functions as an endogenous IAP inhibitor, small molecule Smac-mimetics are believed to neutralize IAPs function that results in liberating caspase activity and promoting apoptosis. Moreover, recent studies show that Smac-mimetics may kill cancer cells in a different manner, which involves inducing ubiquitination of cIAPs, regulating NF-κB signaling and facilitating TNFα-triggered, caspase-8-mediated apoptosis in a certain cancer cell types. In other cancer cells that are resistant to TNFα or chemo/radiotherapy, Smac-mimetic IAP-inhibitors can enhance ionizing radiation or tumor necrosis factor-related apoptosis-inducing ligand (TRAIL)-induced apoptosis, indicating the potential role of Smac-mimetics in overcoming acquired therapy-resistance. Such findings provide important impetus for utilizing IAP-inhibitors as novel adjuvant therapy for the TNFα–resistant, NF-κB constitutively active cancers that account for the majority of patients who are refractory to current therapeutic approaches.

Key Words: Chemoresistance, inhibitors of apoptosis proteins, NF-κB, small molecule inhibitors

The aggressive cancer cell phenotype is the result of a variety of genetic and epigenetic alterations leading to deregulation of intracellular signaling pathways, including an impaired ability of the cancer cell to undergo apoptosis [1, 2]. Most of the current anticancer therapies work, at least in part, through inducing apoptosis in cancer cells [3-6]. Lack of appropriate apoptosis due to defects in the normal apoptosis machinery plays a crucial role in the resistance of cancer cells to a wide variety of current anticancer therapies [7, 8]. Chemo- or radioresistance markedly impairs the efficacy of cancer therapy and involves anti-apoptotic signal transduction pathways that prevent cell death [9-11]. For example, primary or acquired resistance of hormone-refractory prostate cancer to current treatment protocols has been associated with apoptosis-resistance of cancer cells and is linked to the failure of therapies [12-14].

Current and future efforts toward designing new therapies to improve survival and quality of life of cancer patients must include strategies that specifically target cancer cell resistance to current chemo/radiotherapies [13, 15]. In this review article, we will summarize the state of our knowledge for the role of both IAPs and NF-κB in relation to cancer therapeutics resistance. Furthermore,

Table 1. The inhibitor of apoptosis proteins family

Gene	Protein
BIRC 1	NAIP
BIRC 2	cIAP-1
BIRC 3	cIAP-2
BIRC 4	XIAP (ILP1)
BIRC 5	Survivin
BIRC 6	Bruce (Apollon)
BIRC 7	ML-IAP (livin, K-IAP)
BIRC 8	ILP2 (TsIAP)

we will discuss the potential role of small molecule candidates that target apoptosis and/or NF-κB signaling pathway on the sensitization of conventional cancer therapy.

The inhibitor of apoptosis proteins are potent negative regulators of apoptosis and related to apoptosis-resistance

Cancer cells will acquire resistance to apoptosis by upregulating multiple pro-survival factors. The inhibitors of apoptosis proteins (IAPs) are a pivotal class of intrinsic cellular inhibitors of apoptosis [16-19]. IAPs widely and potently suppress apoptosis against a large variety of apoptotic stimuli, including chemotherapeutic agents, radiation and immunotherapy in cancer cells [20, 21]. In human, eight IAPs were identified so far (**Table 1**), all can block caspase cascade, but only some of them directly interact with caspases [22]. IAPs are characterized by the presence of one to three domains known as baculoviral IAP repeat (BIR) domains and belong to a larger family of proteins, called the BIR-domain-containing proteins (BIRPs) [16].

Since the IAPs function at the convergence of both mitochondria pathway and death receptor pathway, they are described as an apoptosis "brake" and IAP antagonists function to release the "brake" [14, 23]. Most components of the major cell death regulatory pathways have been implicated in radiation-induced cell death [24]. Some of these apoptosis pathway proteins have overlapping functions and compensatory pathways, and these apoptosis pathways have extensive cross-talks [24]. Inside a live cell upon irradiation, multiple apoptosis pathway proteins are involved in the shifting of the balance of life and death signals. In the context of IAP-inhibitor treatment and most conventional therapy, the relative levels of individual apoptosis pathway proteins and their roles in the process of irradiation-induced cell death dictate the outcome of the cell's response to therapy. Therefore, investigation of the potential role of apoptosis pathway proteins in IAP-inhibitor-mediated sensitization will provide critical information as to how the IAP-inhibitors work in the context of radiation, and what types of cells may respond better to the therapy. The latter has clear clinical relevance in that the information will be useful to predict or select the patients who will benefit the most from the molecular therapy targeting IAPs [14, 23].

Although these BIRP proteins were all initially called IAP proteins, it is apparent that they are divided into two distinct groups based upon their binding properties to caspases and inhibition of caspase activity. The first group of mammalian BIRPs includes XIAP (BIRC4), cIAP-1 (BIRC2), cIAP-2 (BIRC3), ML-IAP (BIRC7), NAIP (BIRC1) and ILP2 (BIRC8) (**Table 1**). These IAP proteins potently bind to and inhibit caspase-3, -7 and -9 and function as potent apoptosis inhibitors (**Figure 1**). The second group of BIRPs includes the mammalian proteins Survivin (BIRC5) and Bruce (BIRC6) as well as BIR-containing proteins in yeasts and C. elegans [16] (**Table 1**). In contrast to the first group of BIRPs, these Survivin-like BIRPs don't bind to caspases. In addition to their potent anti-apoptotic activity, these Survivin-like BIRPs also regulate cytokinesis and mitotic spindle formation [25, 26].

X-linked IAP protein (XIAP) is the first well-characterized IAP family member due to its potent anti-apoptosis activity [17, 19, 27]. XIAP protein was found to be expressed in most of the NCI 60 human cancer cell lines [28]. Analysis of tumor samples in 78 previously untreated patients showed that those with lower levels of XIAP had significantly longer survival [28]. Two regions in XIAP confer different specificity in the inhibition of caspase-3, -7, and -9. The third BIR domain (BIR3) of XIAP selectively targets caspase-9, whereas the linker region between BIR1 and BIR2 of XIAP inhibits both caspase-3 and caspase-7, the effector caspases that triggers downstream apoptosis [23, 29] (**Figure 1**).

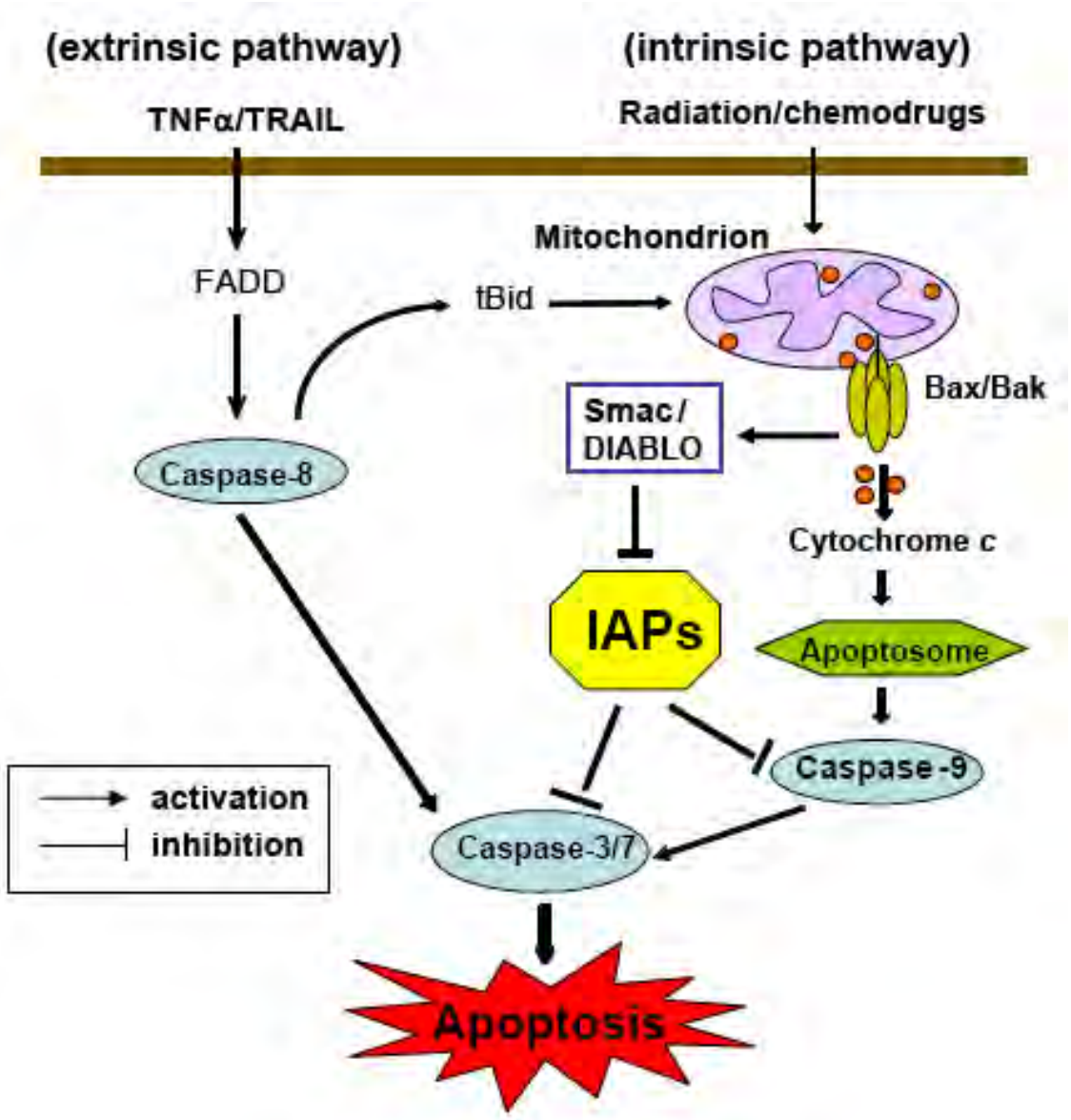

Figure 1: Apoptosis pathways in mammalian cells. Apoptosis activation by the extrinsic pathway involves the binding of extracellular death ligands (such as TNF ligand/TRAIL) to death receptors, provoking the recruitment of adaptor proteins, such as the Fas-associated death domain protein (FADD) and recruiting caspase-8. Active caspase-8 then activates effector caspase-3 and/or -7. In some situations, extrinsic death signals can crosstalk with the intrinsic pathway through caspase-8-mediated proteolysis of BID (BH3-interacting domain death agonist). Truncated BID (tBID) can promote mitochondrial cytochrome c release and assembly of the apoptosome. In the intrinsic pathway, stresses such as radiation or chemotherapeutic agents target mitochondria and induce efflux of intermembrane space proteins, such as cytochrome c and Smac/DIABLO, into the cytosol, by the formation of BAK–BAX oligomers on mitochondrial outer membranes. On release from mitochondria, cytochrome c can join the apoptosome assembly. Active caspase-9 then propagates a cascade of further caspase activation events. The inhibitors of apoptosis proteins (IAPs) is an important class of intrinsic cellular apoptosis inhibitors that function as potent endogenous apoptosis inhibitors by directly binding to and effectively inhibiting both initiator caspase-9 and effector caspases -3/-7. Smac can neutralize IAP inhibition of caspases thus functions as an endogenous IAP-antagonist. Functional blockade of IAPs by Smac results in facilitating caspase activation and apoptosis.

While XIAP prevents the activation of all three caspases, it was shown that the interaction of XIAP with caspase-9 is the most critical for its inhibition of apoptosis [16].

In contrast to XIAP, cIAP-1 and cIAP-2 are weak caspase inhibitors *in vitro* [30]. Although the role of cIAP-1 and -2 in apoptosis is less defined, their function on the cellular responses other than apoptosis are widely reported. Over ten years before, several studies have proposed that both cIAP-1 and cIAP-2 were associated with the TNF receptor 1 signaling complex [31-33]. Moreover, the cIAP-1 and -2 do not directly contact TNF-receptor 2, but rather physiologically interact with TNF-receptor associated factors (TRAFs) [32], and regulate their function by mutually ubiquitination [34, 35]. Through binding to TRAF2, cIAPs are recruited to TNFR signaling complexes where they regulate the activation of caspase-8 [32, 36]. Also, cIAP-1 and cIAP-2 directly ubiquitinate RIP1 and induce constitutive RIP1 ubiquitination in cancer cells and demonstrate that constitutively ubiquitinated RIP1 associates with the prosurvival kinase TAK1 [37]. Collectively, these studies elucidate the potential role of cIAPs on regulating TNFα-induced both apoptosis and NF-κB signaling.

Second mitochondria-derived activator of Caspases (Smac) was identified as a pro-apoptotic factor released from mitochondria into the cytosol triggered by multiple apoptosis stimuli [38-41]. Upon stimulation, the released Smac physically interacts with XIAP through the N-terminal four conserved amino acid residues (AVPI) that bind to the baculoviral IAP repeat 3 (BIR3) domain of XIAP, and eliminate the inhibitory effect of XIAP on caspase activation [42-44]. Therefore, Smac functions as an endogenous IAP-antagonist. Due to the potent pro-apoptotic role of Smac, synthetic small molecule Smac-mimicking compounds (Smac-mimetics) are being developed to sensitize apoptosis-resistant cancer cells to various apoptotic stimuli [45, 46]. Smac-mimetic IAP-antagonists induce TNFα-dependent apoptosis in several transformed cell lines [47-49]. Other reports show that small molecule Smac-mimetics successfully sensitize TRAIL-induced apoptosis by blocking functions of IAPs in multiple cancer cells [38, 50-52]. Also, Smac-mimetic tetrapeptide pSmac-8c significantly sensitized androgen-independent prostate cancer cells to chemotherapeutic agents [53, 54]. These studies manifest that mimicking Smac may represent a promising strategy for restoring defective apoptosis signaling in human cancer therapy. Furthermore, it has recently been reported that Smac can potentiate apoptosis by simultaneously antagonizing caspase-IAP interactions and repressing IAP ubiquitin ligase activities [55]. Yoon, et al [56] identified a Smac-binding protein, NADE. The interaction between Smac and NADE regulates apoptosis through the inhibition of Smac ubiquitination [56]. Dr. Duckett's group reported that some cytoprotective IAPs can inhibit apoptosis through the neutralization of IAP antagonists, such as Smac, rather than by directly inhibiting caspases [27]. These recent studies suggest that endogenous Smac protein plays more complicated roles than expected in apoptosis.
In a subset of highly sensitive tumor cell lines, activity of Smac mimetic compounds is dependent on TNFα signaling. Mechanistic studies indicate that in the system they tested, XIAP is a positive modulator of TNFα induction whereas cIAP-1 negatively regulates TNFα-mediated apoptosis, indicating the opposite effect of XIAP versus cIAP-1 on modulation TNFα signaling [57]. Also, Smac-mimic IAP-antagonists sensitize TRAIL-induced apoptosis by blocking XIAP function in multiple tumor models, including breast cancer [50], multiple myeloma [52], glioblastoma [38], and ovarian cancer [51].

Inhibitor of apoptosis proteins are attractive molecular targets for designing novel therapy for human cancers

XIAP is so far the most potent inhibitor of apoptosis among all the IAP proteins [17]. XIAP effectively inhibits both intrinsic and extrinsic apoptosis pathways by binding and inhibiting the initiator caspase-9 and effector caspases (caspase-3 and -7), whose activity is crucial for the execution of apoptosis [17, 58]. Because effector caspase activity is both necessary and sufficient for irrevocable programmed cell death, XIAP functions as a gatekeeper to this final stage of the process [38]. XIAP is overexpressed in many cancer cell lines and tumor tissues but not in normal cells, and a high level of XIAP results in apoptosis-resistance of cancer cells to a wide variety of therapeutic agents [59]. The multiple

biological activities of XIAP, its unique translational and post-translational control and the centrality of the caspase cascade make XIAP an exceptionally promising molecular target for modulating apoptosis [14, 19, 60]. For example, overexpression of XIAP increases resistance to tumor necrosis factor-related apoptosis-inducing ligand (TRAIL)-induced apoptosis, while downregulation of XIAP restores cell response to TRAIL [61-63].

Since IAPs block apoptosis at the down-stream effector phase, a point where multiple apoptosis signaling pathways converge, strategies targeting IAP may prove to be highly effective for overcoming apoptosis-resistance in human cancers that overexpress IAPs. The link between therapy resistance and IAPs is supported by recent studies in which the suppression of XIAP levels by RNA interference or antisense indeed sensitized XIAP-overexpressing cancer cells to death receptor-induced apoptosis as well as radiation [64, 65]. Combination of irradiation and inhibition of XIAP through the antisense approach resulted in improved tumor control by radiotherapy *in vivo* [66], advocating a distinct role for XIAP in radiation resistant phenotype of human cancers, and providing a proof-of-concept that IAPs may be a novel and promising target for chemo/ radiosensitization of human cancers. Loss of XIAP by RNAi also sensitized cancer cells to a certain chemotherapeutic agents and TRAIL, and the increased sensitivity of the XIAP shRNA cells was correlated with enhanced Caspase activation [67]. We have found that embelin, the first non-peptidic natural XIAP inhibitor identified by us, induces apoptosis in prostate cancer cells [68]. Embelin sensitized TRAIL-induced apoptosis in pancreatic cancer cells [69]. These findings provide a strong rationale that downmodulation of overexpressed XIAP will achieve sensitization on current therapeutic modality.

Through computational structure-based 3D-database search and rational design, a series of small molecule inhibitors of IAPs have been discovered and synthesized, which show potent therapeutic activity to overcome apoptosis-resistance *in vitro* in cancer cells overexpressing IAPs while minimize side-effect on normal cells with relative low level of IAPs [38, 51]. Based on the high-resolution experimental 3D structure of Smac in complex with the XIAP BIR3 domain, Wang and his colleagues have designed and synthesized a group of potent non-peptidic compounds that mimic the tetra-peptide at the N-terminal of natural Smac [53, 54]. These cell-permeable compounds show at least 20-fold more potential than the natural Smac peptide in binding to the XIAP BIR3 domain in a cell-free system [53, 54, 70]. It has been shown that SH130, one of the most potential compounds, enhances ionizing radiation-induced apoptosis *in vitro* and combination therapy achieves significant tumor regression in hormone-refractory prostate cancer models [71]. Also, SH122, another potential compound, promotes TRAIL-mediated cell death in several human prostate cancer cell lines (Dai et al., manuscript submitted). These findings suggest that Smac-mimetic IAP-antagonist can sensitize cell-killing effect by either radiation or death-receptor therapy.

However, little is known about the role of endogenous Smac in cells treated with Smac-mimetic IAP-inhibitors and irradiation. In multiple human cancer models, full-length Smac enhanced gamma-irradiation-induced apoptosis by loss of mitochondrial membrane potential, cytochrome c release, and activation of a serial of caspases [72]. Takasawa et al. shows that the sustained release of Smac/DIABLO from mitochondria is an important event for the onset of apoptosis in keratinocytes exposed to UVB irradiation [40]. In hormone refractory prostate cancer, small molecule IAP inhibitors exhibit a promising therapeutic potential to overcome resistance of prostate cancer cells to radiation-induced growth inhibition, both *in vitro* and *in vivo* in xenograft tumor models, suggesting that targeting IAPs may be a promising approach for radiosensitization of human prostate cancer with high levels of IAPs [71], and provides important impetus for utilizing IAP-inhibitors as an adjuvant therapy for the TNFα–resistant cancers that account for the majority of patients who are refractory to radiation/chemotherapy.

NF-κB is a pro-survival factor that blocks apoptosis and promote therapeutic resistance

The transcription factor NF-κB pathway plays important roles in the control of cell proliferation, apoptosis, inflammation, cell signaling transduction, and other physiological processes [73, 74]. Because the disorder of

these physiological processes has been linked with the onset of cancers, NF-κB has been described as a major culprit in cancer [74]. Current evidences have also shown that NF-κB participates in the processes of angiogenesis, invasion, and metastasis [73, 75, 76]. Moreover, NF-κB is critically involved in the processes of development and progression of cancers, raising its importance in cancer research [77]. NF-κB is constitutively activated in most of human cancers, suggesting that the activation of NF-κB is involved in the process of carcinogenesis. Therefore, targeting NF-κB is attracting more attention as a novel preventive and therapeutic strategy against human cancers.

Besides death receptors, genotoxic stress also activates NF-κB signaling pathway that attenuates apoptotic responses. Blocking NF-κB pathway can sensitize cancer cells to chemotherapeutic agents and radiation [78-82]. It has been shown that NF-κB is activated by ionizing radiation (IR)-induced double-strand breaks (DSB) [81-84] (**Figure 2**). IR-induced DSB directly activates ATM and PIDD (p53-inducible death domain –containing protein), which further recruit NEMO, a member of IKKs signalsome, by serial of posttranslational modification [85, 86]. Modified NEMO participates to the formation of IKK complex, and thus activates downstream NF-κB pathway through

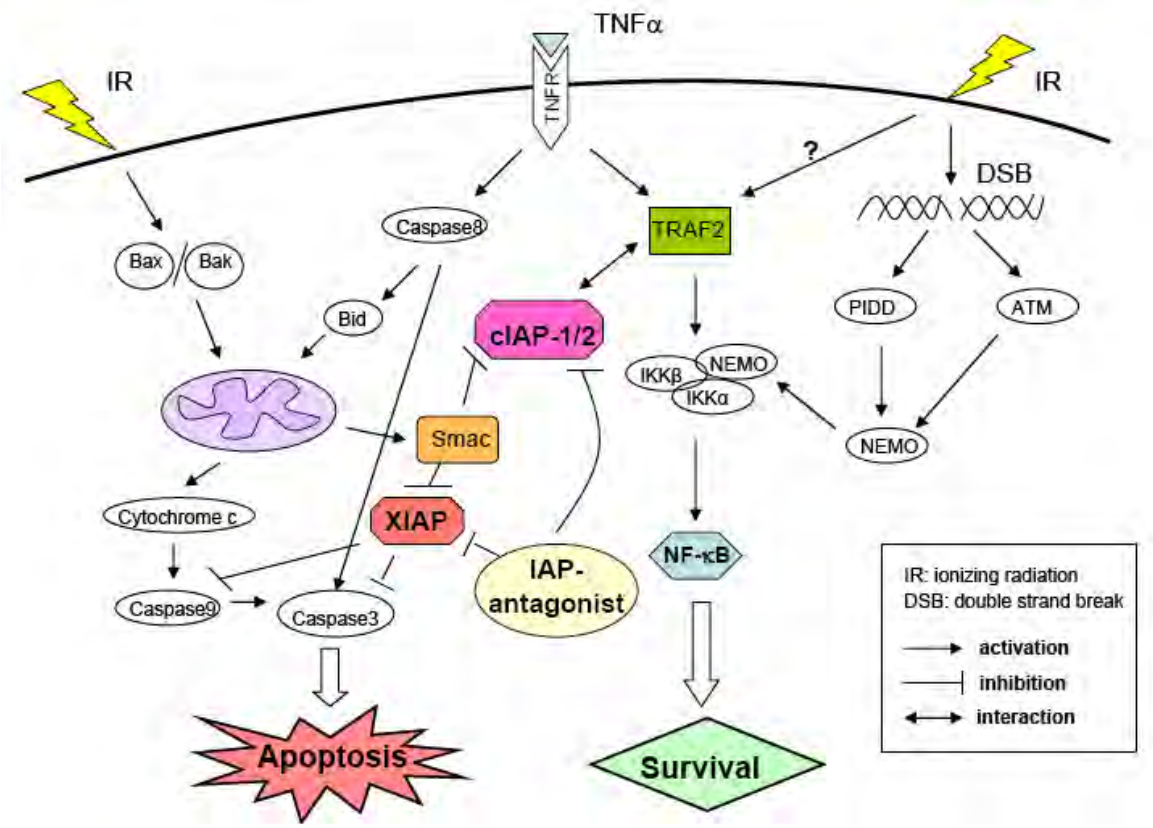

Figure 2: Crosstalk between ionizing radiation-induced apoptosis and NF-κB pathway. IR activates both apoptosis and NF-κB signaling pathway. IR triggers instrinsic apoptosis pathway as described in Figure 1. Simultaneously, NF-κB pathway is activated by IR-induced DNA damage. IR induced double-strand breaks (DSB) directly activates initiator kinase ATM and PIDD, which further recruit NEMO, also known as IKKγ, by multiple steps of posttranslational modification. Modified NEMO joins formation of IKKs signalosome and further activates classical NF-κB pathway. Upon apoptotic stimuli (IR or TNFα), natural Smac can bind to both XIAP and cIAPs, and predominantly neutralize the suppression effect of XIAP on caspases. It has been shown that cIAP-1 physically binds to TRAF2 and regulates its function through ubiquitination in TNFα signaling. Smac-mimetics that function as IAP-antagonists, not only promote caspase activation by neutralizing IAPs, but also interferes the stability and interaction between cIAP-1/2 and TRAF2, thus modulate the balance between apoptosis and NF-κB signaling pathway.

degradation of IκBα and liberate NF-κB heterodimer from cytosol into nucleus [87, 88]. On the other side, IR can directly trigger intrinsic apoptosis pathway through activation of pro-apoptotic Bcl-2 family members Bax and Bak [89, 90], and activates downstream caspase cascade and apoptosis (**Figure 2**).

It has been established that NF-κB is the major survival factor in preventing apoptosis, and inhibition of this transcription factor may improve the efficacy of apoptosis-inducing cancer therapies [74, 91, 92]. Due to its constitutive or treatment-induced activity, NF-κB functions mainly as an inhibitor of apoptosis and is prerequisite for cell survival. NF-κB-mediated protection of lymphoid cells from antigen receptor- and death receptor-induced apoptosis plays an instrumental role in activation of the immune response [93]. In addition, NF-κB may also protect cells from cellular stresses, such as DNA damage, which activate the mitochondrial-dependent "intrinsic" pathway [93-96]. Suppression of NF-κB by genetic or chemical inhibitors induces the apoptosis and/or restores the apoptotic response after treatment with chemotherapeutic agents or radiation in various tumor cells, thus overcoming NF-κB-mediated chemo-/radioresistance [95, 97, 98]. Moreover, the mechanisms of action of several more ancient drugs have been re-evaluated and some of them were discovered to act at least partially through NF-κB inhibition. However, the role of NF-κB in the control of apoptosis is not unambiguous and this factor is also, in some experimental conditions, required for the induction of apoptosis either of mutated cells or in response to anti-cancer agents [98-101]. Therefore, a precise knowledge of the signaling pathways controlling NF-κB as well as of the NF-κB target genes is essential in order to define who will benefit the most from the anti-NF-κB therapies. More preclinical studies are needed to determine a tolerable and efficacious dose and schedule for NF-κB inhibitors [73, 102-104]. Other NF-κB inhibitors might also have a greater effect on sensitizing anticancer agents. It is important to clarify what type of NF-κB inhibitors is most effective and least toxic.

Molecular targeting of NF-κB pathway in sensitization of conventional therapies

Many chemotherapeutic agents trigger the cell-death process through activation of the tumor-suppressor protein p53 [105]. However, NF-κB is also activated in response to treatment that attenuates p53-medieated cell death [106] with chemotherapy and radiation therapy. The NF-κB pathway thus impinges on many aspects of cell survival. Recent studies indicate that the effects of conventional cancer therapeutics could be enhanced by natural and synthetic NF-κB inhibitors, suggesting that down-regulation of NF-κB could sensitize cancer cells to conventional therapeutics [74, 103]. For example, genistein, one of three main isoflavones found in soybeans, inactivates NF-κB and leads to increased growth inhibition and apoptosis induced by various chemotherapeutic agents and promote drug-induced cell-killing effect in many types of cancers [107, 108]. Indole-3-carbinol that is produced from cruciferous vegetables, significantly inhibited NF-κB DNA binding activity in prostate and breast cancer cells, corresponding with the inhibition of cell proliferation and the induction of apoptosis [109, 110].

As it is well-established that in classical NF-κB pathway, proteasomes are responsible for IκBα degradation, which facilitates NF-κB nuclear translocation and activates multiple target gene expression [111], modulation of proteasomal function with specific inhibitors has been demonstrated as a promising strategy for the treatment of human cancers, presumably by suppression NF-κB [112, 113]. In preclinical cancer models, proteasome inhibitors alone induce apoptosis [113-115], as well as overcome radioresistance of tumor cells and enhance radiation–mediated response, typically apoptosis [114]. Bortezomib (Velcade; PS-341), the first proteasome inhibitor to be used in clinical applications, has demonstrated impressive antitumor activity, both as a single agent and in combination with conventional therapies [116-118]. More significantly, in preclinical studies, bortezomib in combination with radiation therapy has been shown to achieve potential therapeutic benefits in various cancers [119, 120]. Besides bortezomib, many other proteasome inhibitory candidates are under investigation in preclinical models, either alone or in combination with conventional therapies [121, 122]. We have found that Celastrol, a natural proteasome

inhibitor, enhances therapeutic efficacy of ionizing radiation both *in vitro* and *in vivo*, typically by increasing apoptosis and decreasing both primary and acquired NF-κB activity (Dai et al., manuscript in revision). These studies provide substantial evidence that proteasome inhibitors can potentiate response of cancer cells to chemotherapeutic agents or radiation.

Crosstalks between apoptosis and NF-κB signaling by IAP-antagonist

As NF-κB has been proved to play a pivotal role in mediating cell survival, blockade of NF-κB activation can shift the tumor survival/death balance towards apoptosis, suggesting that targeting IAPs and/or NF-κB may become a potential approach to overcoming resistance of human cancer.

The cytokine TNFα elicits a wide range of biological responses, including inflammation, cell proliferation, differentiation, and apoptosis. Although the molecular mechanisms of TNF signaling have been largely elucidated, the principle that regulates the balance of life and death is still unknown. Several reviews have focused on the crosstalk that exists between proteins of the TNF receptor (TNF-R) which are involved in the initiation of NF-κB activation or apoptosis [106, 123, 124]. At least three different mechanisms of regulation can be distinguished: (i) NF-κB-mediated recruitment of TNF-R complex [125]; (ii) NF-κB-independent protection against apoptosis by the TRAF2-mediated recruitment of antiapoptotic proteins [126]; (iii) dual activation of apoptosis and NF-κB by a single molecule, such as TNFα, TRAIL and radiation [74, 98]. Overall, the multiple facets of

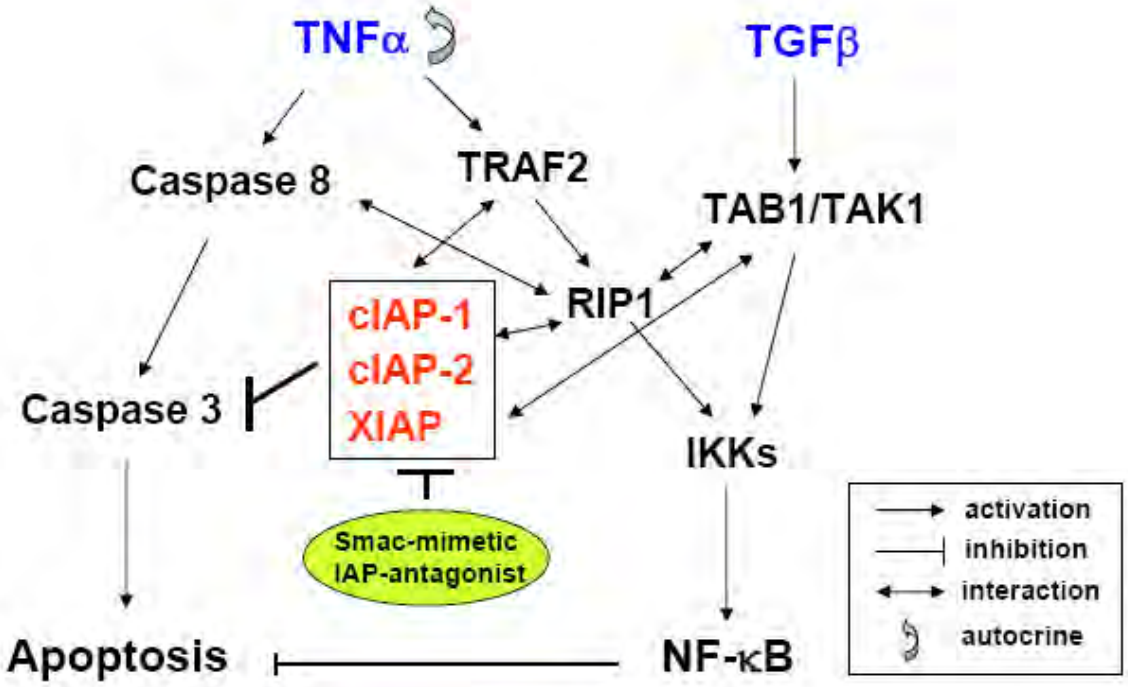

Figure 3: Crosstalk between apoptosis and NF-κB signaling by IAP-antagonist. TNFα induces both apoptosis and NF-κB activation in cancer cells. TNFα induces extrinsic apoptosis via activation of caspase cascade that involves initiator Caspase-8 and effector Caspase-3. IAPs (XIAP, cIAP-1 and cIAP-2) are anti-apoptotic proteins that block caspase- mediated apoptosis. Paradoxically, TNFα still activates NF-κB and promotes cell survival that counteracts with apoptosis. The classical NF-κB pathway that is mediated by IKKs signalosome can be triggered either by TNFα via TRAF2 and RIP1, or alternatively, by TGFβ via TAB1 and TAK1. Multiple studies have established crosstalk between IAPs and proteins that mediate NF-κB signaling pathway (see text). Smac mimetics that function as IAP antagonists can modulate the interaction between IAP proteins and NF-κB signaling proteins, which leads to TNFα-triggered apoptosis primarily via an autocrine manner (see text). TNFα, tumor necrosis factor alpha; TGFβ, transforming growth factor beta; TRAF2, TNF receptor-associated factor 2; RIP1, receptor interacting protein 1; TAK1, TGFβ activated kinase 1; TAB1, TAK1 bind protein 1; IKK, IκBα kinase.

crosstalk have been established between the apoptosis and NF-κB signaling pathways. A direct evidence is that cIAP-1 physically binds to TRAF2 through its BIR1 domain and regulates its biological function through ubiquitination [32, 127-130], suggesting a potential role of cIAP-1 on linking apoptosis and NF-κB pathways (**Figure 2**). Interestingly, a recent study shows that TRAF2-knockdown by siRNA indeed radiosensitizes cancer cells via reduced NF-κB activation, suggesting that TRAF2 is an attractive drug target for anticancer therapy and radiosensitization [131]. Function as an adaptor protein in NF-κB signaling, TRAF2 may thus play a potential role in protecting radiation-induced cell death, and establish the crosstalk between NF-κB and DNA damage-induced apoptosis (**Figure 2**).

Studies in recent two years tend to elucidate the potential mechanism in TNFα signaling by Smac-mimetics in cancer cells. It has been demonstrated that Smac-mimetics stimulate autoubiquitination of cIAPs, resulting in their proteasomal degradation [30, 48] (**Figure 3**). This in turn leads to NIK stabilization and facilitates RIP1 recruitment [49, 132] (**Figure 3**). Moreover, cIAP-1 and cIAP-2 promote cancer cell survival by functioning as E3 ubiquitin ligases that maintain constitutive ubiquitination of the RIP1 adaptor protein, suggesting that constitutively ubiquitinated RIP1 associates with the prosurvival kinase TAK1 [37]. Collective reports demonstrate that either cIAP-1 or 2 is required for proper RIP1 polyubiquitination and NF-κB activation upon TNFα treatment [37, 132] (**Figure 3**). This results in the activation of the noncanonical and canonical NF-κB pathways, causing autocrine TNFα production in a substantial number of tumor cells. Besides cIAPs, a recent study proposes that BIR1 domain of XIAP, which has no previously ascribed function, directly interacts with TAB1 to induce NF-κB activation [133] (**Figure 3**). Smac, the antagonist for caspase inhibition by XIAP, also inhibits the XIAP/TAB1 interaction. Disruption of BIR1 dimerization abolishes XIAP-mediated NF-κB activation, implicating a proximity-induced mechanism for TAK1 activation [133]. Taken together, mounting experimental evidence indicate that IAPs function as "bridging" molecules that mediate cross-talk between the apoptosis pathway and NF-κB pathway.

As multiple recent studies suggest the role of IAPs on the crosstalks between apoptosis and NF-κB pathway [37, 47-49, 57, 132-134] (**Figure 3**), it is reasonable to speculate that an IAP inhibitor may also function as a modulator in regulating such crosstalk. Indeed, several Smac-mimetic IAP-inhibitors can induce TNFα-dependent apoptosis in several transformed cell lines, via cIAP-1 down-regulation and NF-κB activation [47-49]. Blocking NF-κB activation reduced TNF production and protected cells from Smac-mimetics-induced cell death (**Figure 2**). Ahn et al. suggests that embelin sequentially inhibits NF-κB activation induced by TNFα at the IκBα kinase (IKK), IκBα degradation, and RelA nuclear translocation levels in several cancer cell lines [135]. Other studies show that Smac mimetics lead to sensitivity to TNFα-induced cell death, likely through the degradation of cIAPs and by favoring the formation of a RIP1-dependent caspase-8-activating complex [136]. Highlighting the potential of Smac mimetics for clinical application will validate that cancer cells that are sensitive to Smac-mimetic treatment *in vitro* are also responsive to the same treatment in an *in vivo* mouse model. AEG40730, a Smac mimetic dimer compound, binds to cIAP-1 and cIAP-2, facilitates their autoubiquitination and proteasomal degradation, and causes a dramatic reduction in RIP1 ubiquitination [37]. When deubiquitinated by AEG40730 treatment, RIP1 binds caspase-8 and induces apoptosis in cancer cells [37]. In addition, in Smac-mimetic sensitive cell lines, apoptosis caused by Smac-mimetics is blocked by the caspase-8 inhibitor crmA and that IAP antagonists activate NF-κB signaling via inhibition of cIAP-1 [48]. In those transformed tumor lines, IAP antagonist induced NF-κB-stimulated production of TNFα that killed cells in an autocrine fashion. Inhibition of NF-κB reduced TNFα production, and blocking NF-κB activation or TNFα allowed tumor cells to survive Smac-mimetic-induced apoptosis [48]. Moreover, in a subset of highly sensitive tumor cell lines, XIAP is a positive modulator of TNFα production whereas cIAP-1 negatively regulates TNFα-mediated apoptosis [57]. It is interesting that Smac mimetics induced degradation of cIAPs in certain types of cancer cell lines, suggesting that additional switch points control the sensitivity to Smac mimetics [30].

In a vast amount of solid tumors that are

resistant to therapeutics, for example, most of androgen-independent human prostate cancers exert highly constitutive NF-κB activity [75, 137] that may result in resistance to TNFα. How these majority resistant cancer cells respond to IAP-inhibitors remains to be investigated. In our recent publication [71], we found that those androgen-independent prostate cancer cells are highly resistant to Smac-mimetics, which has a IAP-binding affinity comparable to that of the compounds used in other reports [47-49]. Surprisingly, although Smac-mimetics alone hardly show any cell-killing effect both *in vitro* and *in vivo*, they potently sensitize those TNFα–resistant cells to radiation-induced growth inhibition and apoptosis, which might involve blocking radiation-induced NF-κB activation [71]. Moreover, such Smac-mimetic compound treatment does not induce cIAP-1 degradation, TNFα upregulation and NF-κB activation when used alone in those resistant cells [71]. This mode of action of Smac-mimetic IAP-inhibitor is distinct from that in TNFα–sensitive cells reported recently [47-49] . Similarly, another study indicates that blockade of IAPs by a small molecule Smac-mimetic compound promotes TRAIL-induced apoptosis in TRAIL-resistant prostate cancer cells, via modulating both the apoptosis pathway and NF-κB pathway (Dai et al, manuscript submitted). This discrepancy of the mechanisms of Smac-mimetic IAP-inhibitors in chemo/radiosensitization has significant clinical implications and provides important impetus for utilizing IAP-inhibitors as an adjuvant therapy for the TNFα–resistant, NF-κB constitutively active cancers that account for the majority of patients who are refractory to current therapeutic approaches.

Conclusion and perspective

Conventional chemo/radiotherapies the most commonly used current therapies for cancer patients, however primary or acquired resistance remains to be a major challenge in clinic and is emerging as a significant impediment to effective cancer treatment. Although both IAPs and NF-κB pathways have been subjected to intense preclinical and clinical studies, the detailed clinically relevant correlation between these two classes of proteins still remains unclear. Answers to such question will provide a clear rationale for combining Smac-mimetic IAP-antagonists with conventional therapy that will achieve a significantly improved therapeutic outcome.

Mounting evidences have established the potential crosstalks between IAPs (eg. XIAP, cIAP-1, cIAP-2) and the proteins that are involved in NF-κB signaling (eg. TRAF2, RIP1, TAB1). As Smac functions as an endogenous IAP inhibitor, small molecule Smac-mimetics are believed to neutralize IAPs function that promotes apoptosis. However, Smac-mimetics may kill cancer cells in a different manner, which involves inducing ubiquitination of cIAPs, regulating NF-κB signaling and facilitating TNFα-triggered, caspase-8-mediated apoptosis in a certain cancer cell types. In other cancer cells that are resistant to TNFα or chemo/radiotherapy, exhibit a promising therapeutic potential to overcome resistance of cancer cells to radiation therapy, at least in part, by suppressing NF-κB activation. For example, in hormone-refractory prostate cancer, molecular modulation of IAPs and/or NF-κB has been proven to be a novel adjuvant approach to enhance the efficacy of radiation therapy [14, 15, 71, 73, 75, 138]. Therefore, IAP antagonists may be developed as a personalized medicine in IAP-targeting molecular therapy and establish promising novel strategy to overcome the resistance to current therapies, with the ultimate goal of improving the survival of cancer patients who will benefit the most from the individualized therapy modality. This strategy may also benefit patients of other malignancies with high levels of IAPs and high constitutive NF-κB activity in a clinical setting.

In the clinic, continued treatment with potent IAP-inhibitors throughout the cycles of chemo/radiotherapy may help to further reduce or eliminate the "minimal residual disease", thus may reduce the risk of tumor local recurrence as well as metastasis. A rationale patient screen based on individual genetic background will help to optimize the personalized therapeutic advantage. Therefore, the combination of IAP-targeting molecular therapy and conventional chemo/ radiotherapy may become a promising novel strategy to enhance the efficacy of current cancer treatments and ultimately improve the survival of cancer patients.

Acknowledgements

This study was supported in part by grants from Department of Defense Prostate Cancer Research Program W81XWH-06-1-0010 (to L. X.), NIH R01 CA121830-01 and R21 CA128220-01 (to L. X.).

Please address all correspondence to: Liang Xu, M.D., Ph.D., Department of Radiation Oncology, Division of Cancer Biology, University of Michigan, 4424E Med Sci I, 1301 Catherine St., Ann Arbor, MI 48109-5637, USA. Tel: 734-615-7017, Fax: 734-615-3422, E-mail: liangxu@umich.edu

References

[1] Ponder BA. Cancer genetics. Nature 2001; 411: 336-41.
[2] Kumar MV, Shirley R, Ma Y, Lewis RW. Role of genomics-based strategies in overcoming chemotherapeutic resistance. Curr Pharm Biotechnol 2004; 5: 471-80.
[3] Hall EJ. Radiobiology for the Radiologist. Fourth edition, Philadelphia: J.B.Lippincott Company, 1994.
[4] Makin G, Dive C. Apoptosis and cancer chemotherapy. Trends Cell Biol 2001; 11: S22-6.
[5] Ikuta K, Takemura K, Kihara M, Naito S, Lee E, Shimizu E, Yamauchi A. Defects in apoptotic signal transduction in cisplatin-resistant non-small cell lung cancer cells. Oncol Rep 2005; 13: 1229-34.
[6] Li J, Feng Q, Kim JM, Schneiderman D, Liston P, Li M, Vanderhyden B, Faught W, Fung MF, Senterman M, Korneluk RG, Tsang BK. Human ovarian cancer and cisplatin resistance: possible role of inhibitor of apoptosis proteins. Endocrinology 2001; 142: 370-80.
[7] Reed JC. Apoptosis-targeted therapies for cancer. Cancer Cell 2003; 3: 17-22.
[8] Reed JC. Apoptosis-based therapies. Nat Rev Drug Discov 2002; 1: 111-21.
[9] Lawrence TS, Davis MA, Hough A, Rehemtulla A. The Role of Apoptosis in 2',2'-Difluoro-2'-deoxycytidine (Gemcitabine)-mediated Radiosensitization. Clin Cancer Res 2001; 7: 314-9.
[10] Algan O, Stobbe CC, Helt AM, Hanks GE, Chapman JD. Radiation inactivation of human prostate cancer cells: the role of apoptosis. Radiat Res 1996; 146: 267-75.
[11] Brown JM, Attardi LD. The role of apoptosis in cancer development and treatment response. Nat Rev Cancer 2005; 5: 231-7.
[12] Xu L, Frederik P, Pirollo KF, Tang WH, Rait A, Xiang LM, Huang W, Cruz I, Yin Y, Chang EH. Self-assembly of a virus-mimicking nanostructure system for efficient tumor-targeted gene delivery. Hum Gene Ther 2002; 13: 469-81.
[13] DiPaola RS, Patel J, Rafi MM. Targeting apoptosis in prostate cancer. Hematol Oncol Clin North Am 2001; 15: 509-24.
[14] Devi GR. XIAP as target for therapeutic apoptosis in prostate cancer. Drug News Perspect 2004; 17: 127-34.
[15] Watson RW, Fitzpatrick JM. Targeting apoptosis in prostate cancer: focus on caspases and inhibitors of apoptosis proteins. BJU Int 2005; 96 Suppl 2: 30-4.
[16] Schimmer AD. Inhibitor of Apoptosis Proteins: Translating Basic Knowledge into Clinical Practice. Cancer Res 2004; 64: 7183-90.
[17] Deveraux QL, Takahashi R, Salvesen GS, Reed JC. X-linked IAP is a direct inhibitor of cell-death proteases. Nature 1997; 388: 300-4.
[18] Deveraux QL, Stennicke HR, Salvesen GS, Reed JC. Endogenous inhibitors of caspases. J Clin Immunol 1999; 19: 388-98.
[19] Srinivasula SM, Ashwell JD. IAPs: what's in a name? Mol Cell 2008; 30: 123-35.
[20] Salvesen GS, Duckett CS. IAP proteins: blocking the road to death's door. Nat Rev Mol Cell Biol 2002; 3: 401-10.
[21] Hunter AM, LaCasse EC, Korneluk RG. The inhibitors of apoptosis (IAPs) as cancer targets. Apoptosis 2007; 12: 1543-68.
[22] Zangemeister-Wittke U, Simon HU. An IAP in action: the multiple roles of survivin in differentiation, immunity and malignancy. Cell Cycle 2004; 3: 1121-3.
[23] Holcik M, Gibson H, Korneluk RG. XIAP: apoptotic brake and promising therapeutic target. Apoptosis 2001; 6: 253-61.
[24] Zhou L, Yuan R, Serggio L. Molecular mechanisms of irradiation-induced apoptosis. Front Biosci 2003; 8: d9-19.
[25] Yang D, Welm A, Bishop JM. Cell division and cell survival in the absence of survivin. Proc Natl Acad Sci U S A 2004; 101: 15100-5.
[26] Pennati M, Folini M, Zaffaroni N. Targeting survivin in cancer therapy. Expert Opin Ther Targets 2008; 12: 463-76.
[27] Wilkinson JC, Cepero E, Boise LH, Duckett CS. Upstream regulatory role for XIAP in receptor-mediated apoptosis. Mol Cell Biol 2004; 24: 7003-14.
[28] Tamm I, Trepel M, Cardó-Vila M, Sun Y, Welsh K, Cabezas E, Swatterthwait A, Arap W, Reed JC, Pasqualini R. Peptides targeting caspase inhibitors. J Biol Chem 2003; 278: 14401-5.
[29] Takahashi R, Deveraux Q, Tamm I, Welsh K, Assa-Munt N, Salvesen GS, Reed JC. A single BIR domain of XIAP sufficient for inhibiting caspases. Journal of Biological Chemistry 1998; 273: 7787-90.
[30] Wu H, Tschopp J, Lin SC. Smac mimetics and TNFalpha: a dangerous liaison? Cell 2007; 131: 655-8.
[31] Uren AG, Pakusch M, Hawkins CJ, Puls KL, Vaux DL. Cloning and expression of apoptosis inhibitory protein homologs that function to inhibit apoptosis and/or bind tumor necrosis factor receptor-associated factors. Proc Natl

Acad Sci U S A 1996; 93: 4974-8.
[32] Rothe M, Pan MG, Henzel WJ, Ayres TM, Goeddel DV. The TNFR2-TRAF signaling complex contains two novel proteins related to baculoviral inhibitor of apoptosis proteins. Cell 1995; 83: 1243-52.
[33] Hawkins CJ, Ekert PG, Uren AG, Holmgreen SP, Vaux DL. Anti-apoptotic potential of insect cellular and viral IAPs in mammalian cells. Cell Death Differ 1998; 5: 569-76.
[34] Li X, Yang Y, Ashwell JD. TNF-RII and c-IAP1 mediate ubiquitination and degradation of TRAF2. Nature 2002; 416: 345-7.
[35] Samuel T WK, Lober T, Togo SH, Zapata JM, Reed JC. . Distinct BIR domains of cIAP1 mediate binding to and ubiquitination of tumor necrosis factor receptor-associated factor 2 and second mitochondrial activator of caspases. J Biol Chem 2006; 281: 1080-90.
[36] Wang CY, Mayo MW, Korneluk RG, Goeddel DV, Baldwin AS, Jr. NF-kappaB antiapoptosis: induction of TRAF1 and TRAF2 and c-IAP1 and c-IAP2 to suppress caspase-8 activation. Science 1998; 281: 1680-3.
[37] Bertrand MJ, Milutinovic S, Dickson KM, et al. cIAP1 and cIAP2 facilitate cancer cell survival by functioning as E3 ligases that promote RIP1 ubiquitination. Mol Cell 2008; 30: 689-700.
[38] Li L, Thomas RM, Suzuki H, De Brabander JK, Wang X, Harran PG. A small molecule Smac mimic potentiates TRAIL- and TNFalpha-mediated cell death. Science 2004; 305: 1471-4.
[39] Irmler M, Steiner V, Ruegg C, Wajant H, Tschopp J. Caspase-induced inactivation of the anti-apoptotic TRAF1 during Fas ligand-mediated apoptosis. FEBS Lett 2000; 468: 129-33.
[40] Takasawa R, Tanuma S. Sustained release of Smac/DIABLO from mitochondria commits to undergo UVB-induced apoptosis. Apoptosis 2003; 8: 291-9.
[41] Shankar S, Siddiqui I, Srivastava RK. Molecular mechanisms of resveratrol (3,4,5-trihydroxy-trans-stilbene) and its interaction with TNF-related apoptosis inducing ligand (TRAIL) in androgen-insensitive prostate cancer cells. Mol Cell Biochem 2007; 304: 273-85.
[42] Holcik M, Gibson H, Korneluk RG. XIAP: apoptotic brake and promising therapeutic target. Apoptosis 2001; 6: 253-61.
[43] Wu G, Chai J, Suber TL, Wu JW, Du C, Wang X, Shi Y. Structural basis of IAP recognition by Smac/DIABLO. Nature 2000; 408: 1008-12.
[44] Liu Z, Sun C, Olejniczak ET, Meadows RP, Betz SF, Oost T, Herrmann J, Wu JC, Fesik SW. Structural basis for binding of Smac/DIABLO to the XIAP BIR3 domain. Nature 2000; 408: 1004-8.
[45] Bucur O, Ray S, Bucur MC, Almasan A. APO2 ligand/tumor necrosis factor-related apoptosis-inducing ligand in prostate cancer therapy. Front Biosci 2006; 11: 1549-68.
[46] Srinivasula SM, Ashwell JD. IAPs: What's in a Name? Mol Cell 2008; 30: 123-35.
[47] Varfolomeev E, Blankenship JW, Wayson SM, Fedorova AV, Kayagaki N, Garg P, Zobel K, Dynek JN, Elliott LO, Wallweber HJ, Flygare JA, Fairbrother WJ, Deshayes K, Dixit VM, Vucic D. IAP antagonists induce autoubiquitination of c-IAPs, NF-kappaB activation, and TNFalpha-dependent apoptosis. Cell 2007; 131: 669-81.
[48] Vince JE, Wong WW, Khan N, Feltham R, Chau D, Ahmed AU, Benetatos CA, Chunduru SK, Condon SM, McKinlay M, Brink R, Leverkus M, Tergaonkar V, Schneider P, Callus BA, Koentgen F, Vaux DL, Silke J. IAP antagonists target cIAP1 to induce TNFalpha-dependent apoptosis. Cell 2007; 131: 682-93.
[49] Petersen SL, Wang L, Yalcin-Chin A, Li L, Peyton M, Minna J, Harran P, Wang X. Autocrine TNFalpha signaling renders human cancer cells susceptible to Smac-mimetic-induced apoptosis. Cancer Cell 2007; 12: 445-56.
[50] Bockbrader KM, Tan M, Sun Y. A small molecule Smac-mimic compound induces apoptosis and sensitizes TRAIL- and etoposide-induced apoptosis in breast cancer cells. Oncogene 2005; 24: 7381-8.
[51] Petrucci E, Pasquini L, Petronelli A, Saulle E, Mariani G, Riccioni R, Biffoni M, Ferretti G, Benedetti-Panici P, Cognetti F, Scambia G, Humphreys R, Peschle C, Testa U. A small molecule Smac mimic potentiates TRAIL-mediated cell death of ovarian cancer cells. Gynecol Oncol 2007; 105: 481-92.
[52] Chauhan D, Neri P, Velankar M, Podar K, Hideshima T, Fulciniti M, Tassone P, Raje N, Mitsiades C, Mitsiades N, Richardson P, Zawel L, Tran M, Munshi N, Anderson KC. Targeting mitochondrial factor Smac/DIABLO as therapy for multiple myeloma (MM). Blood 2007; 109: 1220-7.
[53] Sun H, Nikolovska-Coleska Z, Yang CY, Xu L, Tomita Y, Krajewski K, Roller PP, Wang S. Structure-based design, synthesis, and evaluation of conformationally constrained mimetics of the second mitochondria-derived activator of caspase that target the X-linked inhibitor of apoptosis protein/caspase-9 interaction site. J Med Chem 2004; 47: 4147-50.
[54] Sun H, Nikolovska-Coleska Z, Yang CY, Xu L, Liu M, Tomita Y, Pan H, Yoshioka Y, Krajewski K, Roller PP, Wang S. Structure-based design of potent, conformationally constrained Smac mimetics. J Am Chem Soc 2004; 126: 16686-7.
[55] Creagh EM, Murphy BM, Duriez PJ, Duckett CS, Martin SJ. Smac/Diablo antagonizes ubiquitin ligase activity of inhibitor of apoptosis proteins. J Biol Chem 2004; 279: 26906-14.
[56] Yoon K, Jang HD, Lee SY. Direct interaction of Smac with NADE promotes TRAIL-induced apoptosis. Biochem Biophys Res Commun 2004; 319: 649-54.

[57] Gaither A, Porter D, Yao Y, Borawski J, Yang G, Donovan J, Sage D, Slisz J, Tran M, Straub C, Ramsey T, Iourgenko V, Huang A, Chen Y, Schlegel R, Labow M, Fawell S, Sellers WR, Zawel L. A Smac mimetic rescue screen reveals roles for inhibitor of apoptosis proteins in tumor necrosis factor-alpha signaling. Cancer Res 2007; 67: 11493-8.

[58] Srinivasula SM, Hegde R, Saleh A, Datta P, Shiozaki E, Chai J, Lee RA, Robbins PD, Fernandes-Alnemri T, Shi Y, Alnemri ES. A conserved XIAP-interaction motif in caspase-9 and Smac/DIABLO regulates caspase activity and apoptosis.[comment][erratum appears in Nature 2001 Jun 28;411(6841):1081]. Nature 2001; 410: 112-6.

[59] Huang Q, Deveraux QL, Maeda S, Stennicke HR, Hammock BD, Reed JC. Cloning and characterization of an inhibitor of apoptosis protein (IAP) from Bombyx mori. Biochim Biophys Acta 2001; 1499: 191-8.

[60] Vucic D. Targeting IAP (inhibitor of apoptosis) proteins for therapeutic intervention in tumors. Curr Cancer Drug Targets 2008; 8: 110-7.

[61] Chawla-Sarkar M, Bae SI, Reu FJ, Jacobs BS, Lindner DJ, Borden EC. Downregulation of Bcl-2, FLIP or IAPs (XIAP and survivin) by siRNAs sensitizes resistant melanoma cells to Apo2L/TRAIL-induced apoptosis. Cell Death Differ 2004; 11: 915-23.

[62] Zhang L, Fang B. Mechanisms of resistance to TRAIL-induced apoptosis in cancer. Cancer Gene Ther 2005; 12: 228-37.

[63] Johnson RW, A.J. F, M.J. S. The TRAIL apoptotic pathway in cancer onset, progression and therapy. Nat Rev Cancer 2008; 8: 782-98.

[64] Ohnishi K, Scuric Z, Schiestl RH, Okamoto N, Takahashi A, Ohnishi T. siRNA targeting NBS1 or XIAP increases radiation sensitivity of human cancer cells independent of TP53 status. Radiat Res 2006; 166: 454-62.

[65] Yamaguchi Y, Shiraki K, Fuke H, Inoue T, Miyashita K, Yamanaka Y, Saitou Y, Sugimoto K, Nakano T. Targeting of X-linked inhibitor of apoptosis protein or survivin by short interfering RNAs sensitize hepatoma cells to TNF-related apoptosis-inducing ligand- and chemotherapeutic agent-induced cell death. Oncol Rep 2005; 14: 1311-6.

[66] Cao C, Mu Y, Hallahan DE, Lu B. XIAP and survivin as therapeutic targets for radiation sensitization in preclinical models of lung cancer. Oncogene 2004; 23: 7047-52.

[67] McManus DC, Lefebvre CA, Cherton-Horvat G, et al. Loss of XIAP protein expression by RNAi and antisense approaches sensitizes cancer cells to functionally diverse chemotherapeutics. Oncogene 2004; 23: 8105-17.

[68] Nikolovska-Coleska Z, Xu L, Hu Z, Tomita Y, Li P, Roller PP, Wang R, Fang X, Guo R, Zhang M, Lippman ME, Yang D, Wang S. Discovery of embelin as a cell-permeable, small-molecular weight inhibitor of XIAP through structure-based computational screening of a traditional herbal medicine three-dimensional structure database. J Med Chem 2004; 47: 2430-40.

[69] Naumann U, Bähr O, Wolburg H, Altenberend S, Wick W, Liston P, Ashkenazi A, Weller M. Adenoviral expression of XIAP antisense RNA induces apoptosis in glioma cells and suppresses the growth of xenografts in nude mice. Gene Ther 2007; 14: 147-61.

[70] Sun H, Nikolovska-Coleska Z, Lu J, Qiu S, Yang CY, Gao W, Meagher J, Stuckey J, Wang S. Design, synthesis, and evaluation of a potent, cell-permeable, conformationally constrained second mitochondria derived activator of caspase (Smac) mimetic. J Med Chem 2006; 49: 7916-20.

[71] Dai Y, Liu ML, Tang WH. et al. Molecularly Targeted Radiosensitization of Human Prostate Cancer by Modulating Inhibitor of Apoptosis. Clin Cancer Res (in press) 2008.

[72] Giagkousiklidis S, Vogler M, Westhoff MA, Kasperczyk H, Debatin KM, Fulda S. Sensitization for gamma-irradiation-induced apoptosis by second mitochondria-derived activator of caspase. Cancer Res 2005; 65: 10502-13.

[73] Naugler WE, Karin M. NF-kappaB and cancer-identifying targets and mechanisms. Curr Opin Genet Dev 2008; 18: 19-26.

[74] Sarkar FH, Li Y. NF-kappaB: a potential target for cancer chemoprevention and therapy. Front Biosci 2008; 13: 2950-9.

[75] Suh J, Rabson AB. NF-kappaB activation in human prostate cancer: important mediator or epiphenomenon? J Cell Biochem 2004; 91: 100-17.

[76] Bharti AC, Aggarwal BB. Nuclear factor-kappa B and cancer: its role in prevention and therapy. Biochem Pharmacol 2002; 64: 883-8.

[77] Karin M. Nuclear factor-kappaB in cancer development and progression. Nature 2006; 441: 431-6.

[78] Magne N TR, Bottero V, Didelot C, Houtte PV, Gerard JP, Peyron JF. . NF-kappaB modulation and ionizing radiation: mechanisms and future directions for cancer treatment. Cancer Lett 2006; 231: 158-68.

[79] Voboril R, Weberova-Voborilova J. Constitutive NF-kappaB activity in colorectal cancer cells: impact on radiation-induced NF-kappaB activity, radiosensitivity, and apoptosis. Neoplasma 2006; 53: 518-23.

[80] Rho HS, Kim SH, Lee CE. Mechanism of NF-kappaB activation induced by gamma-irradiation in B lymphoma cells: role of Ras. J Toxicol Environ Health A 2005; 68: 2019-31.

[81] Kim BY, Kim KA, Kwon O, Kim SO, Kim MS, Kim BS, Oh WK, Kim GD, Jung M, Ahn JS. NF-kappaB inhibition radiosensitizes Ki-Ras-transformed cells to ionizing radiation. Carcinogenesis 2005; 26: 1395-403.

[82] Habraken Y, Piette J. NF-kappaB activation by

double-strand breaks. Biochem Pharmacol 2006; 72: 1132-41.
[83] Kim KM, Zhang Y, Kim BY, Jeong SJ, Lee SA, Kim GD, Dritschilo A, Jung M. The p65 subunit of nuclear factor-kappaB is a molecular target for radiation sensitization of human squamous carcinoma cells. Mol Cancer Ther 2004; 3: 693-8.
[84] Russo SM, Tepper JE, Baldwin AS Jr, Liu R, Adams J, Elliott P, Cusack JC Jr. Enhancement of radiosensitivity by proteasome inhibition: implications for a role of NF-kappaB. Int J Radiat Oncol Biol Phys 2001; 50: 183-93.
[85] Janssens S, Tinel A, Lippens S, Tschopp J. PIDD mediates NF-kappaB activation in response to DNA damage. Cell 2005; 123: 1079-92.
[86] Ahmed KM, Li JJ. ATM-NF-kappaB connection as a target for tumor radiosensitization. Curr Cancer Drug Targets 2007; 7: 335-42.
[87] Wuerzberger-Davis SM, Nakamura Y, Seufzer BJ, Miyamoto S. NF-kappaB activation by combinations of NEMO SUMOylation and ATM activation stresses in the absence of DNA damage. Oncogene 2007; 26: 641-51.
[88] Wu ZH, Shi Y, Tibbetts RS, Miyamoto S. Molecular linkage between the kinase ATM and NF-kappaB signaling in response to genotoxic stimuli. Science 2006; 311: 1141-6.
[89] Wei MC, Zong WX, Cheng EH, Lindsten T, Panoutsakopoulou V, Ross AJ, Roth KA, MacGregor GR, Thompson CB, Korsmeyer SJ. Proapoptotic BAX and BAK: a requisite gateway to mitochondrial dysfunction and death.[see comment]. Science 2001; 292: 727-30.
[90] Willis SN, Chen L, Dewson G, Wei A, Naik E, Fletcher JI, Adams JM, Huang DC. Proapoptotic Bak is sequestered by Mcl-1 and Bcl-xL, but not Bcl-2, until displaced by BH3-only proteins. Genes Dev 2005; 19: 1294-305.
[91] Beg AA, Baltimore D. An essential role for NF-kappaB in preventing TNF-alpha-induced cell death. Science 1996; 274: 782-4.
[92] Kucharczak J, Simmons MJ, Fan Y, Gelinas C. To be, or not to be: NF-kappaB is the answer--role of Rel/NF-kappaB in the regulation of apoptosis. Oncogene 2003; 22: 8961-82.
[93] Ravi R, Bedi A. NF-kappaB in cancer--a friend turned foe. Drug Resist Updat 2004; 7: 53-67.
[94] Wang CY, Mayo MW, Baldwin AS, Jr. TNF- and cancer therapy-induced apoptosis: potentiation by inhibition of NF-kappaB. Science 1996; 274: 784-7.
[95] Wang CY, Cusack JC, Jr., Liu R, Baldwin AS, Jr. Control of inducible chemoresistance: enhanced anti-tumor therapy through increased apoptosis by inhibition of NF-kappaB. Nat Med 1999; 5: 412-7.
[96] Wang CY, Guttridge DC, Mayo MW, Baldwin AS, Jr. NF-kappaB induces expression of the Bcl-2 homologue A1/Bfl-1 to preferentially suppress chemotherapy-induced apoptosis. Mol Cell Biol 1999; 19: 5923-9.
[97] Bentires-Alj M, Barbu V, Fillet M, et al. NF-kappaB transcription factor induces drug resistance through MDR1 expression in cancer cells. Oncogene 2003; 22: 90-7.
[98] Olivier S, Robe P, Bours V. Can NF-kappaB be a target for novel and efficient anti-cancer agents? Biochem Pharmacol 2006; 72: 1054-68.
[99] Campbell KJ, Rocha S, Perkins ND. Active repression of antiapoptotic gene expression by RelA(p65) NF-kappa B. Mol Cell 2004; 13: 853-65.
[100] Dajee M, Lazarov M, Zhang JY, Cai T, Green CL, Russell AJ, Marinkovich MP, Tao S, Lin Q, Kubo Y, Khavari PA. NF-kappaB blockade and oncogenic Ras trigger invasive human epidermal neoplasia. Nature 2003; 421: 639-43.
[101] Ho WC, Dickson KM, Barker PA. Nuclear factor-kappaB induced by doxorubicin is deficient in phosphorylation and acetylation and represses nuclear factor-kappaB-dependent transcription in cancer cells. Cancer Res 2005; 65: 4273-81.
[102] Tabruyn SP, Griffioen AW. NF-kappa B: a new player in angiostatic therapy. Angiogenesis 2008; 11: 101-6.
[103] Nakanishi C, Toi M. Nuclear factor-kappaB inhibitors as sensitizers to anticancer drugs. Nat Rev Cancer 2005; 5: 297-309.
[104] Montagut C, Rovira A, Albanell J. The proteasome: a novel target for anticancer therapy. Clin Transl Oncol 2006; 8: 313-7.
[105] Chen L, Yin H, Farooqi B, Sebti S, Hamilton AD, Chen J. p53 {alpha}-Helix mimetics antagonize p53/MDM2 interaction and activate p53. Mol Cancer Ther 2005; 4: 1019-25.
[106] Tergaonkar V, Perkins ND. p53 and NF-kappaB crosstalk: IKKalpha tips the balance. Mol Cell 2007; 26: 158-9.
[107] Banerjee S, Zhang Y, Ali S, Bhuiyan M, Wang Z, Chiao PJ, Philip PA, Abbruzzese J, Sarkar FH. Molecular evidence for increased antitumor activity of gemcitabine by genistein *in vitro* and *in vivo* using an orthotopic model of pancreatic cancer. Cancer Res 2005; 65: 9064-72.
[108] Li Y, Ahmed F, Ali S, Philip PA, Kucuk O, Sarkar FH. Inactivation of nuclear factor kappaB by soy isoflavone genistein contributes to increased apoptosis induced by chemotherapeutic agents in human cancer cells. Cancer Res 2005; 65: 6934-42.
[109] Li Y, Chinni SR, Sarkar FH. Selective growth regulatory and pro-apoptotic effects of DIM is mediated by AKT and NF-kappaB pathways in prostate cancer cells. Front Biosci 2005; 10: 236-43.
[110] Chinni SR, Li Y, Upadhyay S, Koppolu PK, Sarkar FH. Indole-3-carbinol (I3C) induced cell growth inhibition, G1 cell cycle arrest and apoptosis in prostate cancer cells. Oncogene 2001; 20: 2927-36.
[111] Chen LF, Greene WC. Shaping the nuclear action of NF-kappaB. Nat Rev Mol Cell Biol

2004; 5: 392-401.
[112]Nalepa G, Rolfe M, Harper JW. Drug discovery in the ubiquitin-proteasome system. Nat Rev Drug Discov 2006; 5: 596-613.
[113]Zavrski I, Kleeberg L, Kaiser M, Fleissner C, Heider U, Sterz J, Jakob C, Sezer O. Proteasome as an emerging therapeutic target in cancer. Curr Pharm Des 2007; 13: 471-85.
[114]Voorhees PM, Dees EC, O'Neil B, Orlowski RZ. The proteasome as a target for cancer therapy. Clin Cancer Res 2003; 9: 6316-25.
[115]Moran E, Nencioni A. The role of proteasome in malignant diseases. J Buon 2007; 12 Suppl 1: S95-9.
[116]Nencioni A, Grunebach F, Patrone F, Ballestrero A, Brossart P. Proteasome inhibitors: antitumor effects and beyond. Leukemia 2007; 21: 30-6.
[117]Montagut C, Rovira A, Mellado B, Gascon P, Ross JS, Albanell J. Preclinical and clinical development of the proteasome inhibitor bortezomib in cancer treatment. Drugs Today (Barc) 2005; 41: 299-315.
[118]Milano A, Iaffaioli RV, Caponigro F. The proteasome: a worthwhile target for the treatment of solid tumours? Eur J Cancer 2007; 43: 1125-33.
[119]Zhang Y, Saylor M, Wen S, Silva MD, Rolfe M, Bolen J, Muir C, Reimer C, Chandra S. Longitudinally quantitative 2-deoxy-2-[18F]fluoro-D-glucose micro positron emission tomography imaging for efficacy of new anticancer drugs: a case study with bortezomib in prostate cancer murine model. Mol Imaging Biol 2006; 8: 300-8.
[120]Papandreou CN, Logothetis CJ. Bortezomib as a potential treatment for prostate cancer. Cancer Res 2004; 64: 5036-43.
[121]Sorolla A, Yeramian A, Dolcet X, Pérez de Santos AM, Llobet D, Schoenenberger JA, Casanova JM, Soria X, Egido R, Llombart A, Vilella R, Matias-Guiu X, Marti RM. Effect of proteasome inhibitors on proliferation and apoptosis of human cutaneous melanoma-derived cell lines. Br J Dermatol 2008; 158: 496-504.
[122]Grimes KR, Daosukho C, Zhao Y, Meigooni A, St Clair W. Proteasome inhibition improves fractionated radiation treatment against non-small cell lung cancer: an antioxidant connection. Int J Oncol 2005; 27: 1047-52.
[123]Wajant H, Pfizenmaier K, Scheurich P. Tumor necrosis factor signaling. Cell Death Differ 2003; 10: 45-65.
[124]Heyninck K, Beyaert R. Crosstalk between NF-kappaB-activating and apoptosis-inducing proteins of the TNF-receptor complex. Mol Cell Biol Res Commun 2001; 4: 259-65.
[125]Sheikh MS, Huang Y. Death receptor activation complexes: it takes two to activate TNF receptor 1. Cell Cycle 2003; 2: 550-2.
[126]Karin M, Lin A. NF-kappaB at the crossroads of life and death. Nat Immunol 2002; 3: 221-7.
[127]Wu CJ, Conze DB, Li X, Ying SX, Hanover JA, Ashwell JD. TNF-alpha induced c-IAP1/TRAF2 complex translocation to a Ubc6-containing compartment and TRAF2 ubiquitination. EMBO J 2005; 24: 1886-98.
[128]Li X, Yang Y, Ashwell JD. TNF-RII and c-IAP1 mediate ubiquitination and degradation of TRAF2. Nature 2002; 416: 345-7.
[129]Xia ZP, Chen ZJ. TRAF2: a double-edged sword? Sci STKE 2005; 272: pe7.
[130]Chen ZJ. Ubiquitin signalling in the NF-kappaB pathway. Nat Cell Biol 2005; 7: 758-65.
[131]Zheng M, Morgan-Lappe SE, Yang J, Bockbrader KM, Pamarthy D, Thomas D, Fesik SW, Sun Y. Growth inhibition and radiosensitization of glioblastoma and lung cancer cells by small interfering RNA silencing of tumor necrosis factor receptor-associated factor 2. Cancer Res 2008; 68: 7570-8.
[132]Varfolomeev E, Goncharov T, Fedorova AV, Dynek JN, Zobel K, Deshayes K, Fairbrother WJ, Vucic D. c-IAP1 and c-IAP2 Are Critical Mediators of Tumor Necrosis Factor {alpha} (TNF{alpha})-induced NF-{kappa}B Activation. J Biol Chem 2008; 283: 24295-9.
[133]Lu M, Lin SC, Huang Y, Kang YJ, Rich R, Lo YC, Myszka D, Han J, Wu H. XIAP induces NF-kappaB activation via the BIR1/TAB1 interaction and BIR1 dimerization. Mol Cell 2007; 26: 689-702.
[134]Mahoney DJ, Cheung HH, Mrad RL, Plenchette S, Simard C, Enwere E, Arora V, Mak TW, Lacasse EC, Waring J, Korneluk RG. Both cIAP1 and cIAP2 regulate TNFalpha-mediated NF-kappaB activation. Proc Natl Acad Sci U S A 2008; 105: 11778-83.
[135]Ahn KS, Sethi G, Aggarwal BB. Embelin, an inhibitor of X chromosome-linked inhibitor-of-apoptosis protein, blocks nuclear factor-kappaB (NF-kappaB) signaling pathway leading to suppression of NF-kappaB-regulated antiapoptotic and metastatic gene products. Mol Pharmacol 2007; 71: 209-19.
[136]Wang L, Du F, Wang X. TNF-alpha induces two distinct caspase-8 activation pathways. Cell 2008; 133: 693-703.
[137]Lee EC, Tenniswood M. Programmed cell death and survival pathways in prostate cancer cells. Arch Androl 2004; 50: 27-32.
[138]Chi KN, Gleave ME. Antisense approaches in prostate cancer. Expert Opin Biol Ther 2004; 4: 927-36.

A Smac-mimetic sensitizes prostate cancer cells to TRAIL-induced apoptosis via modulating both IAPs and NF-kappa B

Yao Dai[1*], Meilan Liu[2*], Wenhua Tang[1], Kenneth J Pienta[3,4], Theodore S Lawrence[1,4], and Liang Xu[1,4 #]

Departments of Radiation Oncology[1], Internal Medicine[2] and Urology[3], Comprehensive Cancer Center[4]

University of Michigan, Ann Arbor, MI 48109, USA

*Contributed equally to this study

Running Title: Smac-mimetic promotes TRAIL sensitivity

Key Words: TRAIL; Smac-mimetic; NF-κB; IAPs; prostate cancer

#Correspondence:

Liang Xu, M.D., Ph.D.
Department of Radiation Oncology
Division of Cancer Biology
University of Michigan
4424E Med Sci I
1301 Catherine Street
Ann Arbor, MI 48109-5637
Tel: 734-615-7017
Fax: 734-615-3422
E-mail: liangxu@umich.edu

Abstract

Background: Although tumor necrosis factor-related apoptosis-inducing ligand (TRAIL) is a promising agent for human cancer therapy, prostate cancer still remains resistant to TRAIL. Both X-linked inhibitor of apoptosis (XIAP) and nuclear factor-kappa B function as key negative regulators of TRAIL signaling. In this study, we evaluated the effect of SH122, a small molecule second mitochondria-derived activator of caspases (Smac) mimetic, on TRAIL-induced apoptosis in prostate cancer cells.

Methods: Binding potential of Smac-mimetics on XIAP or cIAP-1 was examined by pull-down assay. Cytotoxicity of TRAIL and/or Smac-mimetics was determined by a standard cell growth assay. Silencing XIAP or cIAP-1 was achieved by transient transfection of short hairpin RNA. Apoptosis was detected by Annexin V-PI staining followed by flow cytometry, and Western Blot analysis of caspases, PARP and Bid. NF-kappa B activation was determined by subcellular fractionation and real time RT-PCR.

Results: SH122, but not its inactive analog, effectively bind to XIAP and cIAP-1. SH122 significantly sensitized prostate cancer cells to TRAIL-mediated cell death. Moreover, SH122 enhanced TRAIL-induced apoptosis via both death receptor and mitochondrial pathway. Knockdown of both XIAP and cIAP-1 sensitized cell response to TRAIL, however, XIAP-knockdown attenuated sensitivity of SH122 on TRAIL-induced cytotoxicity, confirming that XIAP is an important target for IAP-inhibitor-mediated TRAIL sensitization. SH122 also suppressed TRAIL-induced NF-kappa B activation by preventing cytosolic IkappaBalpha degradation and RelA nuclear translocation, as well as suppressing NF-kappa B target gene expression.

Conclusion: These results demonstrate that functioning as a potential Smac-mimetic, SH122 sensitizes human prostate cancer cells to TRAIL-induced apoptosis via blocking both IAPs and NF-kappa B. Modulating IAPs may represent a promising approach to overcoming TRAIL-resistance in human prostate cancer with constitutively active NF-kappa B signaling.

Background

Primary or acquired resistance of prostate cancer to current treatment protocols has been associated with apoptosis-resistance in cancer cells, leading to therapy failure [1, 2]. Tumor necrosis factor-related apoptosis-inducing ligand (TRAIL) is a member of the TNF family that is in clinical trials for the treatment of prostate cancer, either alone or in combination with other treatments [3]. TRAIL is demonstrated to selectively induce apoptosis in prostate cancer cells other than normal prostate epithelial cells [4]. The relative resistance of normal cells to TRAIL has been explained by the lower expression levels of functional death receptors relative to cancer cells [5, 6]. Hence, TRAIL exerts a selective antitumor activity without eliciting systemic toxicity in multiple preclinical models, and is considered to be a prime candidate for prostate cancer therapy [3].

Mechanistically, TRAIL triggers apoptosis via binding to its functional death receptors DR4 and DR5, and activating both death receptor (extrinsic) and mitochondria (intrinsic) apoptosis pathways [7]. Ligation of DR4/DR5 by TRAIL results in caspase-8 activation and directly cleaves downstream effector caspases [8]. Signals originating from death receptors can be linked to mitochondria via Bid, which causes mitochondrial cytochrome c release and caspase-9 activation. The mitochondria pathway is engaged by the release of multiple pro-apoptotic factors from mitochondria into the cytosol, such as cytochrome c, Smac and apoptosis inducing factor (AIF). These apoptogenic factors execute cells to apoptosis in either a caspase-dependent or independent manner [9].

Despite the fact that TRAIL selectively induces apoptosis in cancer cells, TRAIL-resistance still challenges its clinical application as a therapeutic agent in a substantial number of cancers, including prostate cancer [10]. It is widely accepted that the inhibitor of apoptosis proteins (IAP) functions as a key negative regulator in TRAIL resistance [11, 12]. Mounting evidence confirms that XIAP, the most potent anti-apoptotic protein among IAPs, is unequivocally responsible for primary or acquired TRAIL resistance in tumor cells [13-16]. Overexpression of XIAP increases resistance to TRAIL-induced apoptosis, while downregulation of XIAP

restores cell response to TRAIL [17, 18]. At the transcriptional level, almost all IAP proteins are driven by the upstream transcription factor -- NF-kappa B (NF-κB), which can be stimulated by multiple stimuli, including TRAIL [19]. TRAIL-induced NF-κB activation attenuates apoptosis, predominantly by upregulating various anti-apoptotic proteins, including IAPs [20, 21]. Therefore, NF-κB functions as an upstream regulator of IAPs and negatively regulates TRAIL signaling. The role of NF-κB in the anti-apoptotic process has been studied in prostate cancer cells both *in vitro* and *in vivo*. In prostate cancer cell lines, there seems to be an inverse correlation between androgen receptor (AR) status and constitutive NF-κB activity [22]. Thus it is tempting to speculate that the constitutive activation of NF-κB may contribute to prostate cancer cell survival following androgen ablation and, consequently, become resistant to treatment [22].

Smac is identified as a pro-apoptotic factor released from mitochondria into the cytosol triggered by TRAIL [23]. Upon stimulation, the released Smac physically interacts with XIAP through the N-terminal four conserved amino acid residues (AVPI) that bind to the baculoviral IAP repeat 3 (BIR3) domain of XIAP, and eliminate the inhibitory effect of XIAP on caspase activation [24-26]. Therefore, Smac functions as an endogenous IAP-antagonist. Due to the impressive pro-apoptotic role of Smac, synthetic small molecule Smac-mimicking compounds (Smac-mimetics) are being developed to sensitize apoptosis-resistant cancer cells to various apoptotic stimuli [3, 27]. Smac-mimetic IAP-antagonists induce TNFα-dependent apoptosis in several transformed cell lines [28-30]. Other reports show that small molecule Smac-mimetics successfully sensitize TRAIL-induced apoptosis by blocking functions of IAPs in multiple cancer cells [11, 16, 31, 32]. These studies provide a solid foundation for our assertion that mimicking Smac may represent a promising strategy for restoring defective apoptosis signaling triggered by TRAIL in human prostate cancer therapy.

Based on the high-resolution experimental 3D structure of Smac in complex with the XIAP BIR3 domain, we have designed and synthesized a group of potent non-peptidic mimetics of Smac that mimic the tetra-peptide at the N-terminal of the Smac protein, called SH-compounds [33, 34]. These cell-permeable

compounds show at least 20-fold more potential than the natural Smac peptide binding to the XIAP BIR3 domain in a cell-free system [33-35]. In the current study, we evaluated the sensitizing potential of one of these compounds, SH122, on TRAIL-mediated cell death in several human prostate cancer cell lines. We also investigated potential molecular targets and the mechanism of action involved in SH122-mediated TRAIL sensitization.

Methods

Cell Culture and Reagents

Human prostate cancer DU145 and LNCaP cells were obtained from the American Type Culture Collection. Androgen-independent prostate cancer cell line CL1 derived from its androgen-dependent cell line LNCaP was kindly provided by Dr. Arie Belldegrun (University of California, Los Angeles). Cells were routinely maintained in Dulbecco's Modified Eagle Medium (DMEM, Gibco) with 10% fetal bovine serum (FBS) and 2 mM L-glutamine. Cultures were maintained in a humidified incubator at 37^{o}C with 5% CO_2.

Small molecule Smac-mimetic SH122 as well as its inactive analogs SH123 and SH110 were kindly provided by Dr. Shaomeng Wang (University of Michigan). TRAIL was purchased from Cell Sciences (Canton, MA). Antibodies against XIAP and cIAP-1 were purchased from BD Biosciences (San Jose, CA). Antibodies against PARP, RelA and IkappaBalpha (IκBα) were purchased from Santa Cruz (Santa Cruz, CA). Other antibodies include: anti-caspase-3 (BioVision, Mountain View, CA), anti-caspase-8 (Calbiochem, San Diego, CA), anti-caspase-9 (Novus Biologicals, Littleton, CO), anti-Bid (Cell Signaling, MA), and anti-β-actin (Sigma, MO). Chemicals were from Sigma unless otherwise indicated.

Cytotoxicity Assay

To detect the survival of cells after treatment, a standard cell growth assay was performed using the CCK-8 detection kit (Dojindo Molecular Technologies, Gaithersburg, MD) following the manufacturer's instructions. Absorbance was detected at 450 nm and 650 nm respectively, using a microplate reader (TECAN ULTRA, Research Triangle Park, NC). Cell viability (%) was normalized by dividing normalized absorbance of treated samples by that of the untreated control. Inhibitory concentration 50% (IC_{50}) was calculated by GraphPad Prism 5.0 (San Diego, CA).

Pull-down Assay

Cells (1.0×10^7) were disrupted in a lysis buffer (50 mM Tris-HCl, pH 7.5, 150 mM NaCl, 1% Nonidet P-40, 0.5% sodium deoxycholate), with freshly added protease inhibitor cocktail (Roche). Cells lysates were homogenized by passing through a 27-1/2G syringe needle (BD). After centrifugation at 10,000×g for 15 min at 4^{o}C, the supernatant was harvested and incubated with biotin-labeled Smac-mimetic compounds with or without non-labeled compounds, for 1 hour at 4^{o}C. Lysates were incubated with pre-cleared Streptavidin-Agarose beads (Invitrogen) by gently rotating for 2 hours at 4 ^{o}C. The beads were collected and washed with washing buffer (Roche) and eluted in 60 μl of loading buffer (Bio-Rad). After boiling for 5 min, the eluents were analyzed by immunoblotting to detect proteins that interacted with the compounds.

Apoptosis Assay

For apoptosis analysis by flow cytometry, DU145 cells were treated with SH122 and TRAIL, alone or in combination, with SH110 used as a negative control. Cells were harvested by trypsinization and washed twice with ice-cold PBS. After centrifuge, cells were stained with 100 μl Annexin V-FITC diluted in binding buffer (10 mM HEPES,100 mM NaCl, 10 mM KCl, 1mM $MgCl_2$, 1.8 mM $CaCl_2$) containing propidium iodide (50 μg/ml). Cells were incubated for 15 min at room temperature before analyzed by flow

cytometry with FACScan (BD) using 488-nm laser line. Data were analyzed using WinMDI 2.8 software (Purdue University Cytometry Laboratory).

shRNA Transfection

The shRNA specific for XIAP in plasmid pRS-shXIAP29 was purchased from OriGene (Rockville, MD). The shRNA specific for cIAP-1 in plasmid pGB-shcIAP-1 was purchased from BioVision (Mountain View, CA). shRNA plasmids (2.0 μg) were transfected into DU145 cells using LipofectAMINE 2000 (Invitrogen, Carlsbad, CA), following the manufacturer's instruction. Forty-eight hours after transfection, cells were treated with Smac-mimetic compounds and/or TRAIL and processed for cytotoxicity analysis. Knockdown effect was detected by Western blot.

Western Blot Analysis

Whole cell proteins were isolated by RIPA buffer (50 mM Tris-HCl, pH 8.0, 150 mM NaCl, 0.1% SDS, 1% NP-40, 0.25% Sodium deoxycholate and 1 mM EDTA) with freshly added protease inhibitor cocktail (Roche). Whole cell lysates were clarified by centrifugation at 10,000×g for 10 minutes at 4^{o}C. Total protein concentrations were determined by BCA Protein assay (Pierce, Rockford, IL). Equal amounts of proteins were loaded to pre-cast 4-20% SDS-PAGE gels (Invitrogen). Proteins resolved on gels were transferred to PVDF membranes (Bio-Rad). After electro-transfer, membranes were blocked with 5% nonfat milk in TBS-T buffer (20 mM Tris-HCl, pH 8.0, 150 mM NaCl, 0.05% Tween 20), and probed with the desired primary antibodies. Blots were then incubated with horseradish-conjugated secondary antibodies and detected with the SuperSignal West Pico chemiluminescence substrate (Pierce), and exposed to an X-ray film (Kodak, Rochester, NY). Intensity of the desired bands was analyzed using TotalLab software (Nonlinear Dynamics, Durham, NC).

Cytosol and Nuclei Fractionation

To detect subcellular redistribution of NF-κB proteins, cytoplasmic and nuclear fractions were prepared according to the method reported [36] with modifications. Briefly, treated cells (5×10^6 cells) were resuspended in 200 μl of hypotonic buffer (10 mM HEPES, 5 mM KCl, 1.5 mM $MgCl_2$, 1 mM phenylmethylsulfonyl fluoride (PMSF), 1 mM dithiothreitol (DTT), and protease inhibitors), mixed well, and incubated with constant rotation at 4°C for 15 min. Nonidet P-40 (10%) was then added to reach the final concentration of 0.5%. Cytosolic extract were cleared by centrifugation at 12,000 rpm for 1 min. The pellets were washed once with hypotonic buffer, and resolved in nucleus extraction buffer (20 mM HEPES, 50 mM KCl, 300 mM NaCl, 1 mM PMSF, 1 mM DTT, and protease inhibitors), with constant rotation at 4 °C for 45 min. Nuclear extracts were harvested after centrifuging for 10 min at 12,000 rpm. Subcellular proteins were quantified by BCA assay before employed to Western blot analysis.

Quantitative Real-time PCR (qRT-PCR)

qRT-PCR was performed to determine the NF-κB target gene expression level [37]. Total RNA was extracted from DU145 cells using TRIzol (Invitrogen). Reverse transcription reaction with 1 μg of total RNA in 100 μl was carried out following the instructions of the TaqMan Reverse Transcription Kit (Applied Biosystems, Foster City, CA). For quantitative PCR, 1 μl of gene primers with SYBR Green (Applied Biosystems) in 20 μl of reaction volume was applied. Primers were designed as: TNF, forward, 5'CCAGGGACCTCTCTCTAATCAGC3', reverse, 5'CTCAGCTTGAGGGTTTGCTACAA3'; IL8, forward, 5'CGTGGCTCTCTTGGCAGC3', reverse, 5'TCTTTAGCACTCCTTGGCAAAAC3'; Actin (as an internal control): forward, 5'ATGCAGAAGGAGATCACTGC3', reverse, 5'TCATAGTCCGCCTAGAAGCA3'. BIRC4, forward, 5'AGTGGTAGTCCTGTTTCAGCATCA3', reverse, 5'CCGCACGGTATCTCCTTCA3'. FAM probed ICAM-1 primers were commercially obtained

from Applied Biosystems. All reactions with TaqMan PCR Master Mix (Applied Biosystems) were performed on the Mastercycler *realplex*^{2} S (Eppendorf, Westbury, NY). Target gene mRNA levels were normalized to Actin mRNA according to the following formula: [2^ –(C_T target – C_T Actin)] × 100%, where CT is the threshold cycle. Fold increase was calculated by dividing the normalized target gene expression of the treated sample with that of the untreated control.

Statistical Analysis

Two-tailed Student's *t*-test was employed, using GraphPad Prism 5.0 software (San Diego, CA). A threshold of $P < 0.05$ was defined as statistically significant.

Results

Validation of interactions between Smac-mimetic compound SH122 and IAPs

Based on 3-D rational design and computational modeling, SH122 (Fig. 1A) was synthesized and developed as a non-peptide small molecule IAP-antagonist that is 20~30-fold more potent than the N-terminal tetrapeptide of Smac in binding to IAPs, while inactive analogs SH123 and SH110 showed 200 folds less potent [34]. To verify the specific binding of SH122 to IAPs, we employed a pull-down assay with biotin-labeled SH122 (SH122BL) in human prostate cancer cells. As shown in Fig. 1B, both XIAP and cIAP-1 were pulled down by SH122 in DU145 cells. Furthermore, pre-incubation with 10-fold excess of non-biotin-labeled SH122 blocked the binding of SH122BL to XIAP/cIAP-1 for more than 90%, suggesting that the binding was specific. In other androgen-independent prostate cancer CL1 cells, 1 μM of SH122 was sufficient to pull down both XIAP and cIAP-1 (Fig. 1C), and similar as DU145, the binding effect was effectively competed by a 10-fold excess of non-labeled SH122. By contrast, negative control compound SH123BL hardly showed binding effect on either XIAP or cIAP-1, as evidenced in the previous report [38].

These results demonstrate that Smac-mimetic SH122 potently and specifically interacts with XIAP and cIAP-1 in human prostate cancer cells.

SH122 sensitizes TRAIL-induced prostate cancer cell growth inhibition

To detect the combination effects of a Smac-mimetic and TRAIL, cytotoxicity was tested after concurrent treatment of TRAIL with SH122. In DU145 cells, while TRAIL alone showed a minor effect on decreasing cell viability, 5 μM and 10 μM of SH122 showed 100- and 600-fold sensitization comparing to TRAIL alone, respectively (Fig. 2A). By contrast, the negative compound SH110 did not produce sensitization. Similar results were observed in two other prostate cancer cell lines. As shown in Fig. 2B, SH122, but not SH110, potentiated TRAIL-induced cell growth inhibition in LNCaP cells. In CL1 cells that were derived from LNCaP, SH122 showed dose-dependent effects on TRAIL sensitization, although the dose used was approximately 10-fold less than that for LNCaP cells (Fig. 2C). Notably, CL1 seemed to be more sensitive to TRAIL compared with LNCaP, as shown by IC_{50}, suggesting that ablation of androgen-receptor may result in upregulation of TRAIL receptor expression. These data demonstrate that the Smac-mimetic compound SH122 potentiates TRAIL-mediated cytotoxicity in both TRAIL-resistant and TRAIL-sensitive prostate cancer cell lines and shows a synergistic effect in combination with TRAIL.

SH122 enhances TRAIL-induced apoptosis

To determine whether apoptosis was involved in TRAIL-induced cell death, we examined apoptosis induced by TRAIL in combination with SH122, with Annexin V-FITC and PI staining by flow cytometry analysis. As shown in Fig. 3, SH122 increased TRAIL-induced apoptosis in a dose-dependent manner. Even at a lower dose (2.5 μM), SH122 enhanced TRAIL-induced total apoptosis as compared with TRAIL and SH122 alone (Fig. 3). In contrast, TRAIL alone (50 ng/ml) moderately induced apoptosis, and SH122 alone showed a minor effect on apoptosis, with a slightly increased apoptotic cell population compared with the control even at the highest dose (Fig. 3).

Both the death receptor pathway and mitochondrial pathway are involved in SH122-sensitized, TRAIL-induced apoptosis

Based on TRAIL-induced apoptotic signaling, we examined the expression of caspases treated with SH122 and TRAIL. Casapase-8 was cleaved into fragments (p43/41 and p18) as early as 4 h with TRAIL alone, while cleavage of caspase-8 became more intense with increased doses of SH122, especially at 6 h after treatment (Fig. 4A). Similar tendency was observed on casapse-3. Activation of caspase-3 was further confirmed by poly(ADP-Ribose) polymerase (PARP) cleavage, a typical feature of caspase-dependent apoptosis. PARP was cleaved by TRAIL alone at 4 h (Fig. 4A), while in combination with SH122, cleaved PARP lasted up to 8 h. These results suggest that SH122 enhances TRAIL-induced apoptosis by activating caspases and promoting PARP cleavage.

To determine the combination effect of TRAIL and SH122 on the mitochondrial pathway, caspase-9 and Bid activation were examined. As shown in Fig. 4B, Bid levels did not change at 4 h or 6 h, while at 8 h, Bid levels decreased in combination treatment, but not by TRAIL alone. Furthermore, caspase-9 cleavage could be detected as early as 4 h by either TRAIL alone or in combination with SH122, as evidenced by the appearance of its cleaved forms, p35 and p17. Interestingly, both pro- and cleaved caspase-9 were diminished at 8 h, indicating that caspase-9 activation was an early event with Bid cleavage (Fig. 4B). These data suggest that the mitochondria pathway is also involved in TRAIL-induced, SH122-mediated apoptosis. Taken together, these *in vitro* apoptosis data reveal that SH122 potentiates TRAIL-induced apoptosis by activating both the extrinsic death receptor pathway and the intrinsic mitochondrial pathway, typically through activation of caspase cascade. More importantly, SH-122 combined with TRAIL induced apoptosis in a longer term than TRAIL alone (8 h *vs.* 4 h), showing an enhanced effect on TRAIL treatment.

Downregulation of XIAP and cIAP-1 sensitizes TRAIL-induced cell death

It is well established that IAPs (especially XIAP) are responsible for blocking TRAIL-induced apoptosis by inhibiting caspases functions [11, 14, 39]. To investigate the potential link between the IAPs and TRAIL-resistance, short-hairpin RNA (shRNA) of XIAP or cIAP-1 was transfected into DU145 cells, and cytoxicity was examined. As shown in Fig. 5, XIAP or cIAP-1 knockdown shifted the cytotoxicity curve to the left, i.e., sensitized the cells to TRAIL. Based on IC_{50}, a more than 300-fold sensitization was observed in the cells transfected with XIAP shRNA as compared with vector control (Fig. 5A and B). Similarly, in cIAP-1-shRNA transfected cells, an approximately 100-fold sensitization was achieved as compared with that of vector control (Fig. 5C and D). These results demonstrate that knockdown of XIAP and cIAP-1 effectively sensitizes the cells to TRAIL, indicating that both XIAP and cIAP-1 are involved in TRAIL-resistance, and silencing XIAP and/or c-IAP1 can overcome such resistance in prostate cancer cells.

Downregulation of XIAP attenuates sensitization potential of SH122 on TRAIL-induced cell death

It had been shown that both XIAP and cIAP-1 are specific targets of SH122 (Fig. 1B and C), and knockdown XIAP/cIAP-1 resulted in significant TRAIL-sensitization (Fig. 5). To evaluate the role of XIAP in SH122-mediated TRAIL sensitization, we treated XIAP-knockdown cells with SH122 and TRAIL. In vector shRNA (shControl) -transfected cells, although negative compound SH110 showed moderate sensitive effect, SH122 dramatically synergized TRAIL-induced cell death in a dose-dependent manner. Even at the lowest dose (0.1 μM), SH122 exhibited 22-fold more potent in sensitizing TRAIL comparing with high dose of SH110 (10 μM) (Fig. 6A). However, in XIAP shRNA-transfected cells, sensitizing potential of SH122 showed 10^2~10^4 folds less potent than that in shControl cells (Fig. 6B). These results demonstrate that silencing XIAP dramatically attenuates SH122-mediated sensitization of TRAIL-induced cytotoxicity, suggesting that XIAP is an important target of IAP-inhibitor involved in TRAIL sensitization.

SH122 inhibits TRAIL-induced NF-κB activation

Because NF-κB activation is known to play a crucial role in inhibiting apoptosis [19, 21], we thought it was important to evaluate the effect of SH122 on NF-κB activity by TRAIL. First, we treated cells with TRAIL alone in the dose that achieved apoptosis, to create optimal conditions for NF-κB activation in our system. TRAIL induced IκBα degradation by 60% at 40 min post-treatment, and concomitantly, nuclear RelA expression increased over 3-fold at 40 min and lasted for 3 h treatment (Fig. 7A). This revealed that TRAIL induced NF-κB activation via classic pathway by degrading cytosolic IκBα and promoting RelA nuclear translocation. It is worth noting that at 120 min post treatment, cleaved PARP was observed in the nuclei extracts, suggesting a quick apoptosis induced by TRAIL along with NF-κB activation, also reflecting a balance of cell death and cell survival triggered by the same stimuli (Fig. 7A). Consistently, TRAIL induced multiple NF-κB target gene expression. For the four target genes examined, TNF and IL8 expression reached their peaks at 2 h post treatment, while ICAM-1 and BIRC4 expression keep increasing during treatment (Fig. 7B).

Next, we pretreated DU145 cells with different doses of SH122 or SH-123 to evaluate the effect of the IAP-antagonist on TRAIL-induced NF-κB activation. Pre-treatment of SH122 potently suppressed IκBα degradation and RelA translocation in a dose-dependent manner (Fig. 7C). Consistently, at the same time point, SH122 was shown to suppress expression of all three NF-κB target genes by 30-80% (P<0.01 vs. control) even at a lower dose (Fig. 7D). In comparison, even high concentrations of the negative compound SH123 altered neither NF-κB protein redistribution (Fig. 7C) nor NF-κB target gene expression (Fig. 7D). These results demonstrate that SH-122 exhibits a promising effect on blocking TRAIL-induced NF-κB activation.

Discussion

In this study, we found that small molecule Smac-mimetic SH122 potently sensitized TRAIL-induced apoptosis in multiple human prostate cancer cell lines. We also found that although downregulation of either XIAP or cIAP-1 sensitized TRAIL-mediated cytotoxicity, XIAP-knockdown attenuated SH122-mediated TRAIL sensitization. Our results demonstrate that IAPs are valid molecular targets for modulating TRAIL sensitivity in prostate cancer cells, and blocking IAPs achieves improved efficacy and overcomes resistance to TRAIL. In addition, our results disclose that NF-κB is involved in regulating sensitivity of prostate cancer cells to TRAIL, and Smac-mimetic can augment TRAIL-induced apoptosis by blocking both IAPs and NF-κB (Fig. 8).

Smac-mimic IAP-antagonists sensitize TRAIL-induced apoptosis by blocking XIAP function in multiple tumor models, including breast cancer [31], multiple myeloma [16], glioblastoma [11] and ovarian cancer [32]. Embelin, a natural XIAP inhibitor [40], sensitized TRAIL-induced apoptosis in pancreatic cancer cells [41]. These findings provide a strong rationale that downmodulation of overexpressed XIAP by Smac-mimetics will achieve TRAIL-sensitization. To our knowledge, there are limited reports on combining small molecule Smac-mimetic candidates with TRAIL in prostate cancer therapy. Interestingly, in prostate cancer cell lines, no strict correlation has been observed between XIAP expression and TRAIL responsiveness [3]. This discrepancy indicates that XIAP is not the only determinant of TRAIL-resistance in prostate cancer. Nevertheless, blocking XIAP function by transient overexpression of Smac achieved promising enhanced efficacy in combination with TRAIL in prostate cancer cell lines [42], indicating that XIAP is a predominant target for TRAIL sensitivity. In our system, we found that the IAP-antagonist alone did not induce apoptosis [34], however potently sensitized TRAIL-induced cytotoxicity in TRAIL-resistant DU145 and LNCaP cells, as well as in relatively TRAIL-sensitive CL1 cells. Our finding, consistent with other reports [17, 43, 44], suggests that the IAP-antagonist exerts a potent sensitization effect independent of

cell responsiveness to TRAIL, and provides an attractive strategy for using IAP-antagonists in the combination modality in human cancer therapy.

NF-κB is another well documented pro-survival factor that is involved in mediating resistance to TRAIL-induced apoptosis in tumor cells, in addition to IAPs [45]. It has been reported that constitutively active NF-κB signaling leads to TRAIL-resistance by upregulating XIAP in multiple human cancer cells [46], and in a certain tumor cell types, NF-κB is the primary cause for TRAIL resistance [10]. Moreover, there is mounting evidence that cIAP-1 physically interacts with adaptor proteins in TNFα/TRAIL-mediated NF-κB signaling [47-49], suggesting that IAPs appears to be a "bridging" molecule between apoptosis pathway and NF-κB pathway triggered by TRAIL (Fig. 8). Thus it is reasonable to postulate that the pro-apoptotic IAP-antagonists may modulate NF-κB. Indeed, several recent studies reveal that Smac-mimetics (IAP-antagonists) can induce TNFα-dependent apoptosis in Smac-sensitive cell lines by degrading cIAPs and regulating NF-κB signaling [28-30]. These findings indicate that in cell lines that are sensitive to both Smac and TNFα, an IAP-antagonist itself is sufficient to induce cell death, at least by autocrine TNFα signaling and caspase-8-dependent apoptosis [30, 49].

Apart from these findings, our study show that Smac-mimetics as a single agent induce neither cell death nor NF-κB activation in androgen-independent prostate cancer cells [38], suggesting that both apoptosis and NF-κB failed to be activated by Smac-mimetic alone in chemo- or radioresistant cells with constitutively active NF-κB signaling. The mechanism underlying such a discrepancy in different cell types remains to be investigated. However, our data provide the first evidence that a potent Smac-mimetic IAP-antagonist directly blocks TRAIL-induced NF-κB activation in prostate cancer cells. In fact, at the same doses that efficiently suppressed NF-κB activation, SH-122 significantly sensitized TRAIL potential by hundreds of folds, suggesting that blocking NF-κB by Smac-mimetic is sufficient for TRAIL sensitization. Additionally, SH122-mediated inhibition of IκBα degradation reflects an effect at the level of the IκBα kinase (IKK) complex that is in agreement with others' observation in different systems [11, 50], indicating

the activation of the canonical NF-κB pathway. Furthermore, SH122 was indeed shown to suppress XIAP mRNA (BIRC4) expression driven by NF-κB, demonstrating that TRAIL-mediated sensitization by small molecule Smac-mimetic is associated with functional inhibition of both XIAP and NF-κB, especially in androgen-independent prostate cancer. Future work will focus on evaluating the response to TRAIL and IAP-antagonist in androgen-dependent (AD) LNCaP cells and their androgen-independent (AI) derivative CL1 cells. Expected data on this isogenic (for hormone dependence) cell model will further support our assertion that NF-κB may play an essential role in the transition from AD to AI prostate cancer, and that overcoming resistance of TRAIL-induced apoptosis can be achieved by downregulating NF-κB –IAP signaling pathway.

Conclusions

Resistance to chemo- or radiotherapy, which is often associated with recurrence after prior androgen deprivation therapy in human prostate cancer, remains a severe clinical problem [51]. TRAIL is currently evaluated in phase I/II clinical trials, alone or in combination with other therapies for the treatment of prostate cancer [3, 10]. Our study indicates that blockade of IAPs by a small molecule Smac-mimetic promotes TRAIL-induced apoptosis in prostate cancer cells via modulating both the apoptosis pathway and NF-κB pathway. As IAPs are key molecular targets for the development of cancer cell-selective therapeutics, our findings reveal a potential mechanism for a Smac-mimetic IAP-antagonist on TRAIL-mediated signaling, and suggest that modulating IAPs may contribute to enhanced TRAIL efficacy, especially in androgen-independent prostate cancer with high levels of IAPs and constitutively active NF-κB. Therefore, small molecule Smac-mimetics that specifically target IAPs may yield a potential therapeutic benefit with TRAIL-based therapy in chemo- or radioresistant prostate cancer.

Competing interests

The author(s) declare that they have no competing interests.

Author's contributions

Y.D. and M.L. contributed equally to this study. Y.D. participated in the design of the study, performed NF-κB assay and drafted the manuscript. M.L. carried out cell culture, MTT assay, apoptosis assay, transfection, Western Blot, and prepared the manuscript. W.T. helped Western Blot. K.J.P. and T.S.L. are clinicians participated in the project and helped to review the manuscript. L.X. supervised the study and assisted with experimental design, data analysis, and revision of the manuscript. All authors read and approved the final manuscript.

Acknowledgements

We thank Dr. Arie Belldegrun at University of California Los Angeles for kindly providing the androgen-independent prostate cancer cell line CL1; Dr. Susan Harris for help with the manuscript; the University of Michigan Comprehensive Cancer Center (UMCCC) Flow Cytometry Core for flow cytometry analysis. This study was supported in part by Department of Defense Prostate Cancer Research Program W81XWH-06-1-0010 (to L. X.), NIH grants R01 CA121830-01 and R21 CA128220-01 (to L. X.), and by NIH through the University of Michigan's Cancer Center Support Grant (5 P30 CA46592).

Figure Legends

Figure 1. Smac-mimetic compound interacted with XIAP and cIAP-1 in human prostate cancer cells. **A.** structure of the Smac-mimetic compound SH122, and its inactive control compounds SH123 and SH110. **B.** DU145 cells were colleted and disrupted in a lysis buffer. Biotin-labeled SH122 (SH122BL, 20 μM) was incubated with whole cell lysates with or without 10-fold excess of non-labeled SH122, followed by incubation with precleared Streptavidin agarose beads. Eluted beads were employed to Western blot analysis. Samples were incubated with anti-XIAP or cIAP-1 antibody. Data shown represent one of at least three independent experiments. SH122BL, Biotin-labeled SH122. **C.** CL1 cell lysate was incubated with 1 μM and 2.5 μM of SH122BL, or 2.5 μM of SH-123BL, with or without 10-fold excess of their unlabeled forms. Pull-down assay was performed as **B**. SH123BL, Biotin-labeled SH123.

Figure 2. SH122 promoted TRAIL-induced cell death in prostate cancer cell line DU145 (A), LNCaP (B) and CL1 (C). Cells (5,000 cells/well in 96-well plates) were treated with different concentrations of TRAIL and SH122, alone or in combination, with SH110 as a negative control. After incubation for 96 h, cells were stained with Cell Counting kit-8 reagent. The optical density of each sample was measured. Data were normalized as described in *Materials and Methods*. Data were presented as mean± SD (*n*=3).

Figure 3. SH122 enhanced TRAIL-induced apoptosis. DU145 cells were seeded into 6-well plates at the concentration of 2×10^5/ml, and exposed by 2.5, 5 and 10 μM of SH122, with or without TRAIL (50 ng/ml). Eighteen hours after incubation, cells were harvested and processed for Annexin V-FITC and PI (Trevigen) staining by flow cytometry. Numbers represented total apoptosis (Annexin V positive cell population). Data represented one of three independent experiments.

Figure 4. SH122 potentiated TRAIL-induced apoptosis by activating both the death-receptor pathway (A) and mitochondrial pathway (B). DU145 cells were treated with 10 and 20 μM of SH122, in

the presence or absence of 300 ng/ml of TRAIL, with or without pretreatment with zVAD (2 μM), for 4 h, 6 h, and 8 h, respectively. Whole-cell lysates (30 μg) were subjected to Western blot analysis, and membranes were probed with antibodies against caspase-8, caspase-3, caspase-9, PARP and Bid. Actin was shown as a loading control.

Figure 5. Downregulation of XIAP or cIAP-1 sensitized TRAIL-induced cell death. DU145 cells were transfected with shRNA of XIAP (shXIAP) (**A, B**) or cIAP-1 (shcIAP-1) (**C, D**), or the vector control (shVector), and knockdown effect was measured 48 h after transfection (**A, C**). Transfected cells were treated with TRAIL, and cytotoxicity was determined by CCK-8 detection kit (**B, D**). Normalized data were presented as mean±SD (*n*=3).

Figure 6. Downregulation of XIAP attenuated sensitization effect of SH122 on TRAIL-induced cell death. Cells transfected with either XIAP shRNA (**A**) or the vector control shRNA (**B**) were treated with serial diluted TRAIL, alone or in combination with 0.1, 1 and 10 μM of SH122, respectively, with 10 μM of SH110 as a negative control. Cytotoxicity was determined by CCK-8 detection kit. Normalized data were presented as mean±SD (*n*=3). Sensitization fold was calculated by dividing IC_{50} of compound-treated group by that of DMSO control.

Figure 7. SH122 suppressed TRAIL-induced NF-κB activation. A. DU145 cells were continuously treated with 300 ng/ml of TRAIL for 20, 40, 60, 120, and 180 min. Cytosol and nuclei subcompartments were fractionated for detection of IκBα and RelA, with Actin and PARP used as markers of cytosolic and nuclear extracts, respectively. Relative expression of IκBα and RelA was shown by dividing band intensity by that of Actin and PARP, respectively. CE, cytosolic extract; NE, nuclear extract. **B.** After treatment as described in **A**, cells were harvested for total RNA extraction. cDNA was synthesized and quantitative PCR was performed to detect four NF-κB target genes: TNF, IL8, ICAM-1 and BIRC4. Fold increase of gene

expression was calculated by dividing the normalized gene expression activity by that of the untreated control. *Columns*, mean; *bars*, SD (*n*=3). **C.** Cells were pre-treated with compounds [SH122: 1, 5, and 10 μM; SH-123: 10 μM; MG132 (10 μM): positive control] for 1 h, and challenged with TRAIL (300 ng/ml) for 40 min. Cytosol and nuclei subcellular compartments were fractionated for detection of IκBα and RelA, respectively, as described in **A**. C, vehicle control. **D.** After treatment as described in **C**, cells were harvested for total RNA extraction. cDNA was synthesized and quantitative PCR was performed to detect three NF-κB target genes: TNF, IL8 and BIRC4. C, vehicle control. *Columns*, mean; *bars*, SD (*n*=3).

Figure 8. Working model of Smac-mimetic IAP-antagonist sensitizing TRAIL-induced apoptosis by suppressing NF-κB. TRAIL triggers apoptosis via both death-receptor (DR4/DR5) and mitochondrial pathway, by activating initiator caspase-8 and -9, and effector caspase-3. Furthermore, both Bid and PARP are cleaved by caspases, which are typical predictors of TRAIL-mediated apoptosis. A Smac-mimetic effectively blocks IAPs (XIAP/cIAP-1) function and facilitates caspase activation. Simultaneously, the Smac-mimetic suppresses TRAIL-induced classical NF-κB activation by preventing IκBα degradation and RelA nuclear translocation. Blockade of NF-κB – XIAP signaling by small molecule Smac-mimetic abolishes counteraction of pro-survival factors on TRAIL-mediated apoptosis.

References

1. DiPaola RS, Patel J, Rafi MM: **Targeting apoptosis in prostate cancer**. *Hematol Oncol Clin North Am* 2001, **15**(3):509-524.
2. Xu L, Frederik P, Pirollo KF, Tang WH, Rait A, Xiang LM, Huang W, Cruz I, Yin Y, Chang EH: **Self-assembly of a virus-mimicking nanostructure system for efficient tumor-targeted gene delivery**. *Hum Gene Ther* 2002, **13**(3):469-481.
3. Bucur O, Ray S, Bucur MC, Almasan A: **APO2 ligand/tumor necrosis factor-related apoptosis-inducing ligand in prostate cancer therapy**. *Front Biosci* 2006, **11**:1549-1568.
4. Shankar S, Siddiqui I, Srivastava RK: **Molecular mechanisms of resveratrol (3,4,5-trihydroxy-trans-stilbene) and its interaction with TNF-related apoptosis inducing ligand (TRAIL) in androgen-insensitive prostate cancer cells**. *Mol Cell Biochem* 2007, **304**(1-2):273-285.
5. Steele LP, Georgopoulos NT, Southgate J, Selby PJ, Trejdosiewicz LK: **Differential susceptibility to TRAIL of normal versus malignant human urothelial cells**. *Cell Death Differ* 2006, **13**(9):1564-1576.
6. Almasan A, Ashkenazi A: **Apo2L/TRAIL: apoptosis signaling, biology, and potential for cancer therapy**. *Cytokine Growth Factor Rev* 2003, **14**(3-4):337-348.
7. Ng CP, Zisman A, Bonavida B: **Synergy is achieved by complementation with Apo2L/TRAIL and actinomycin D in Apo2L/TRAIL-mediated apoptosis of prostate cancer cells: role of XIAP in resistance**. *Prostate* 2002, **53**(4):286-299.
8. Knight MJ, Riffkin CD, Ekert PG, Ashley DM, Hawkins CJ: **Caspase-8 levels affect necessity for mitochondrial amplification in death ligand-induced glioma cell apoptosis**. *Mol Carcinog* 2004, **39**(3):173-182.
9. Fulda S, Meyer E, Debatin KM: **Inhibition of TRAIL-induced apoptosis by Bcl-2 overexpression**. *Oncogene* 2002, **21**(15):2283-2294.
10. Kruyt FA: **TRAIL and cancer therapy**. *Cancer Lett* 2008, **263**(1):14-25.
11. Li L, Thomas RM, Suzuki H, De Brabander JK, Wang X, Harran PG: **A small molecule Smac mimic potentiates TRAIL- and TNFalpha-mediated cell death**. *Science* 2004, **305**(5689):1471-1474.
12. Cummins JM, Kohli M, Rago C, Kinzler KW, Vogelstein B, Bunz F: **X-linked inhibitor of apoptosis protein (XIAP) is a nonredundant modulator of tumor necrosis factor-related apoptosis-inducing ligand (TRAIL)-mediated apoptosis in human cancer cells**. *Cancer Res* 2004, **64**(9):3006-3008.
13. Fulda S, Wick W, Weller M, Debatin KM: **Smac agonists sensitize for Apo2L/TRAIL- or anticancer drug-induced apoptosis and induce regression of malignant glioma in vivo**. *Nat Med* 2002, **8**(8):808-815.
14. Schimmer AD, Welsh K, Pinilla C, Wang Z, Krajewska M, Bonneau MJ, Pedersen IM, Kitada S, Scott FL, Bailly-Maitre B *et al*: **Small-molecule antagonists of apoptosis suppressor XIAP exhibit broad antitumor activity**. *Cancer Cell* 2004, **5**(1):25-35.
15. Gaither A, Porter D, Yao Y, Borawski J, Yang G, Donovan J, Sage D, Slisz J, Tran M, Straub C *et al*: **A Smac mimetic rescue screen reveals roles for inhibitor of apoptosis proteins in tumor necrosis factor-alpha signaling**. *Cancer Res* 2007, **67**(24):11493-11498.
16. Chauhan D, Neri P, Velankar M, Podar K, Hideshima T, Fulciniti M, Tassone P, Raje N, Mitsiades C, Mitsiades N *et al*: **Targeting mitochondrial factor Smac/DIABLO as therapy for multiple myeloma (MM)**. *Blood* 2007, **109**(3):1220-1227.
17. Chawla-Sarkar M, Bae SI, Reu FJ, Jacobs BS, Lindner DJ, Borden EC: **Downregulation of Bcl-2, FLIP or IAPs (XIAP and survivin) by siRNAs sensitizes resistant melanoma cells to Apo2L/TRAIL-induced apoptosis**. *Cell Death Differ* 2004, **11**(8):915-923.
18. Zhang L, Fang B: **Mechanisms of resistance to TRAIL-induced apoptosis in cancer**. *Cancer Gene Ther* 2005, **12**(3):228-237.

19. Sarkar FH, Li Y: **NF-kappaB: a potential target for cancer chemoprevention and therapy**. *Front Biosci* 2008, **13**:2950-2959.
20. Pahl HL: **Activators and target genes of Rel/NF-kappaB transcription factors**. *Oncogene* 1999, **18**(49):6853-6866.
21. Falschlehner C, Emmerich CH, Gerlach B, Walczak H: **TRAIL signalling: decisions between life and death**. *Int J Biochem Cell Biol* 2007, **39**(7-8):1462-1475.
22. Suh J, Rabson AB: **NF-kappaB activation in human prostate cancer: important mediator or epiphenomenon?** *J Cell Biochem* 2004, **91**(1):100-117.
23. Irmler M, Steiner V, Ruegg C, Wajant H, Tschopp J: **Caspase-induced inactivation of the anti-apoptotic TRAF1 during Fas ligand-mediated apoptosis**. *FEBS Lett* 2000, **468**(2-3):129-133.
24. Holcik M, Gibson H, Korneluk RG: **XIAP: apoptotic brake and promising therapeutic target**. *Apoptosis* 2001, **6**(4):253-261.
25. Wu G, Chai J, Suber TL, Wu JW, Du C, Wang X, Shi Y: **Structural basis of IAP recognition by Smac/DIABLO**. *Nature* 2000, **408**(6815):1008-1012.
26. Liu Z, Sun C, Olejniczak ET, Meadows RP, Betz SF, Oost T, Herrmann J, Wu JC, Fesik SW: **Structural basis for binding of Smac/DIABLO to the XIAP BIR3 domain**. *Nature* 2000, **408**(6815):1004-1008.
27. Srinivasula SM, Ashwell JD: **IAPs: What's in a Name?** *Mol Cell* 2008, **30**:123-135.
28. Varfolomeev E, Blankenship JW, Wayson SM, Fedorova AV, Kayagaki N, Garg P, Zobel K, Dynek JN, Elliott LO, Wallweber HJ *et al*: **IAP antagonists induce autoubiquitination of c-IAPs, NF-kappaB activation, and TNFalpha-dependent apoptosis**. *Cell* 2007, **131**(4):669-681.
29. Vince JE, Wong WW, Khan N, Feltham R, Chau D, Ahmed AU, Benetatos CA, Chunduru SK, Condon SM, McKinlay M *et al*: **IAP antagonists target cIAP1 to induce TNFalpha-dependent apoptosis**. *Cell* 2007, **131**(4):682-693.
30. Petersen SL, Wang L, Yalcin-Chin A, Li L, Peyton M, Minna J, Harran P, Wang X: **Autocrine TNFalpha signaling renders human cancer cells susceptible to Smac-mimetic-induced apoptosis**. *Cancer Cell* 2007, **12**(5):445-456.
31. Bockbrader KM, Tan M, Sun Y: **A small molecule Smac-mimic compound induces apoptosis and sensitizes TRAIL- and etoposide-induced apoptosis in breast cancer cells**. *Oncogene* 2005, **24**(49):7381-7388.
32. Petrucci E, Pasquini L, Petronelli A, Saulle E, Mariani G, Riccioni R, Biffoni M, Ferretti G, Benedetti-Panici P, Cognetti F *et al*: **A small molecule Smac mimic potentiates TRAIL-mediated cell death of ovarian cancer cells**. *Gynecol Oncol* 2007, **105**(2):481-492.
33. Sun H, Nikolovska-Coleska Z, Yang CY, Xu L, Liu M, Tomita Y, Pan H, Yoshioka Y, Krajewski K, Roller PP *et al*: **Structure-based design of potent, conformationally constrained Smac mimetics**. *J Am Chem Soc* 2004, **126**(51):16686-16687.
34. Sun H, Nikolovska-Coleska Z, Yang CY, Xu L, Tomita Y, Krajewski K, Roller PP, Wang S: **Structure-based design, synthesis, and evaluation of conformationally constrained mimetics of the second mitochondria-derived activator of caspase that target the X-linked inhibitor of apoptosis protein/caspase-9 interaction site**. *J Med Chem* 2004, **47**(17):4147-4150.
35. Sun H, Nikolovska-Coleska Z, Lu J, Qiu S, Yang CY, Gao W, Meagher J, Stuckey J, Wang S: **Design, synthesis, and evaluation of a potent, cell-permeable, conformationally constrained second mitochondria derived activator of caspase (Smac) mimetic**. *J Med Chem* 2006, **49**(26):7916-7920.
36. Burstein E, Hoberg JE, Wilkinson AS, Rumble JM, Csomos RA, Komarck CM, Maine GN, Wilkinson JC, Mayo MW, Duckett CS: **COMMD proteins, a novel family of structural and functional homologs of MURR1**. *J Biol Chem* 2005, **280**(23):22222-22232.
37. Maine GN, Burstein E: **COMMD proteins and the control of the NF kappa B pathway**. *Cell Cycle* 2007, **6**(6):672-676.

38. Dai Y, Liu ML, Tang WH, Desano J, Burstein E, Davis M, Pienta KJ, Lawrence TS, Xu L: **Molecularly Targeted Radiosensitization of Human Prostate Cancer by Modulating Inhibitor of Apoptosis**. *Clin Cancer Res (in press)* 2008.
39. Ng CP, Bonavida B: **X-linked inhibitor of apoptosis (XIAP) blocks Apo2 ligand/tumor necrosis factor-related apoptosis-inducing ligand-mediated apoptosis of prostate cancer cells in the presence of mitochondrial activation: sensitization by overexpression of second mitochondria-derived activator of caspase/direct IAP-binding protein with low pl (Smac/DIABLO)**. *Mol Cancer Ther* 2002, **1**(12):1051-1058.
40. Nikolovska-Coleska Z, Xu L, Hu Z, Tomita Y, Li P, Roller PP, Wang R, Fang X, Guo R, Zhang M *et al*: **Discovery of embelin as a cell-permeable, small-molecular weight inhibitor of XIAP through structure-based computational screening of a traditional herbal medicine three-dimensional structure database**. *J Med Chem* 2004, **47**(10):2430-2440.
41. Naumann U, Bahr O, Wolburg H, Altenberend S, Wick W, Liston P, Ashkenazi A, Weller M: **Adenoviral expression of XIAP antisense RNA induces apoptosis in glioma cells and suppresses the growth of xenografts in nude mice**. *Gene Ther* 2007, **14**(2):147-161.
42. Mitsiades CS, Mitsiades N, Poulaki V, Schlossman R, Akiyama M, Chauhan D, Hideshima T, Treon SP, Munshi NC, Richardson PG *et al*: **Activation of NF-kappaB and upregulation of intracellular anti-apoptotic proteins via the IGF-1/Akt signaling in human multiple myeloma cells: therapeutic implications**. *Oncogene* 2002, **21**(37):5673-5683.
43. Amantana A, London CA, Iversen PL, Devi GR: **X-linked inhibitor of apoptosis protein inhibition induces apoptosis and enhances chemotherapy sensitivity in human prostate cancer cells**. *Mol Cancer Ther* 2004, **3**(6):699-707.
44. Mao HL, Liu PS, Zheng JF, Zhang PH, Zhou LG, Xin G, Liu C: **Transfection of Smac/DIABLO sensitizes drug-resistant tumor cells to TRAIL or paclitaxel-induced apoptosis in vitro**. *Pharmacol Res* 2007, **56**(6):483-492.
45. Morales JC, Ruiz-Magana MJ, Ruiz-Ruiz C: **Regulation of the resistance to TRAIL-induced apoptosis in human primary T lymphocytes: role of NF-kappaB inhibition**. *Mol Immunol* 2007, **44**(10):2587-2597.
46. Braeuer SJ, Buneker C, Mohr A, Zwacka RM: **Constitutively activated nuclear factor-kappaB, but not induced NF-kappaB, leads to TRAIL resistance by up-regulation of X-linked inhibitor of apoptosis protein in human cancer cells**. *Mol Cancer Res* 2006, **4**(10):715-728.
47. Kuai J, Nickbarg E, Wooters J, Qiu Y, Wang J, Lin LL: **Endogenous association of TRAF2, TRAF3, cIAP1, and Smac with lymphotoxin beta receptor reveals a novel mechanism of apoptosis**. *J Biol Chem* 2003, **278**(16):14363-14369.
48. Samuel T, Welsh K, Lober T, Togo SH, Zapata JM, Reed JC: **Distinct BIR domains of cIAP1 mediate binding to and ubiquitination of tumor necrosis factor receptor-associated factor 2 and second mitochondrial activator of caspases**. *J Biol Chem* 2006, **281**(2):1080-1090.
49. Bertrand MJ, Milutinovic S, Dickson KM, Ho WC, Boudreault A, Durkin J, Gillard JW, Jaquith JB, Morris SJ, Barker PA: **cIAP1 and cIAP2 facilitate cancer cell survival by functioning as E3 ligases that promote RIP1 ubiquitination**. *Mol Cell* 2008, **30**(6):689-700.
50. Ahn KS, Sethi G, Aggarwal BB: **Embelin, an inhibitor of X chromosome-linked inhibitor-of-apoptosis protein, blocks nuclear factor-kappaB (NF-kappaB) signaling pathway leading to suppression of NF-kappaB-regulated antiapoptotic and metastatic gene products**. *Mol Pharmacol* 2007, **71**(1):209-219.
51. Johnstone RW, Ruefli AA, Lowe SW: **Apoptosis: a link between cancer genetics and chemotherapy**. *Cell* 2002, **108**(2):153-164.

Fig. 1

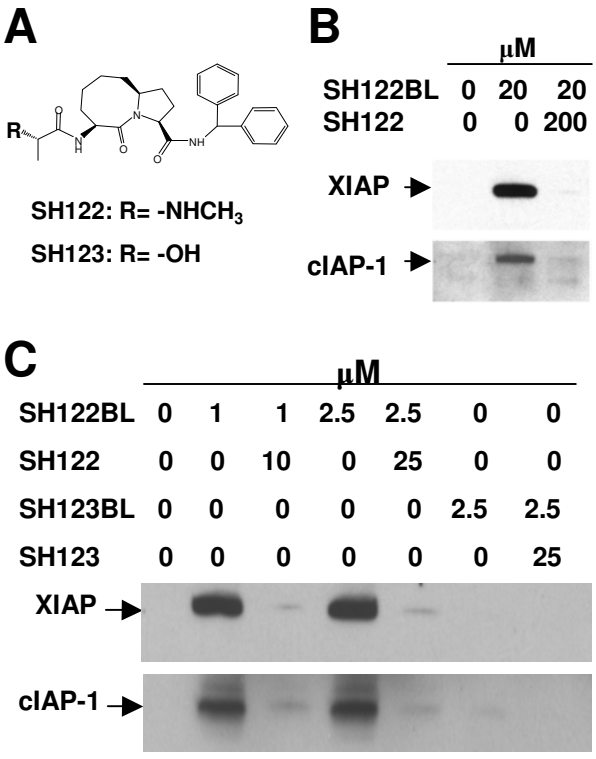

Figure 1

Fig. 2

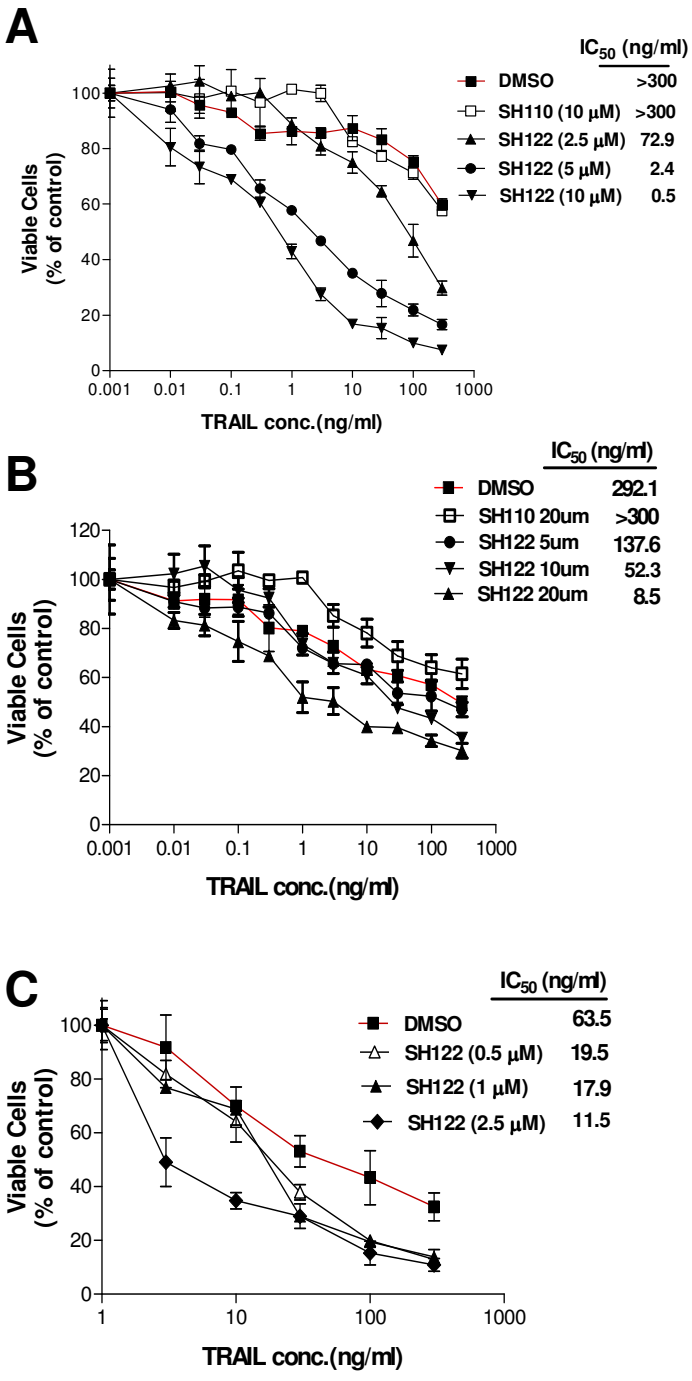

Figure 2

Fig. 3

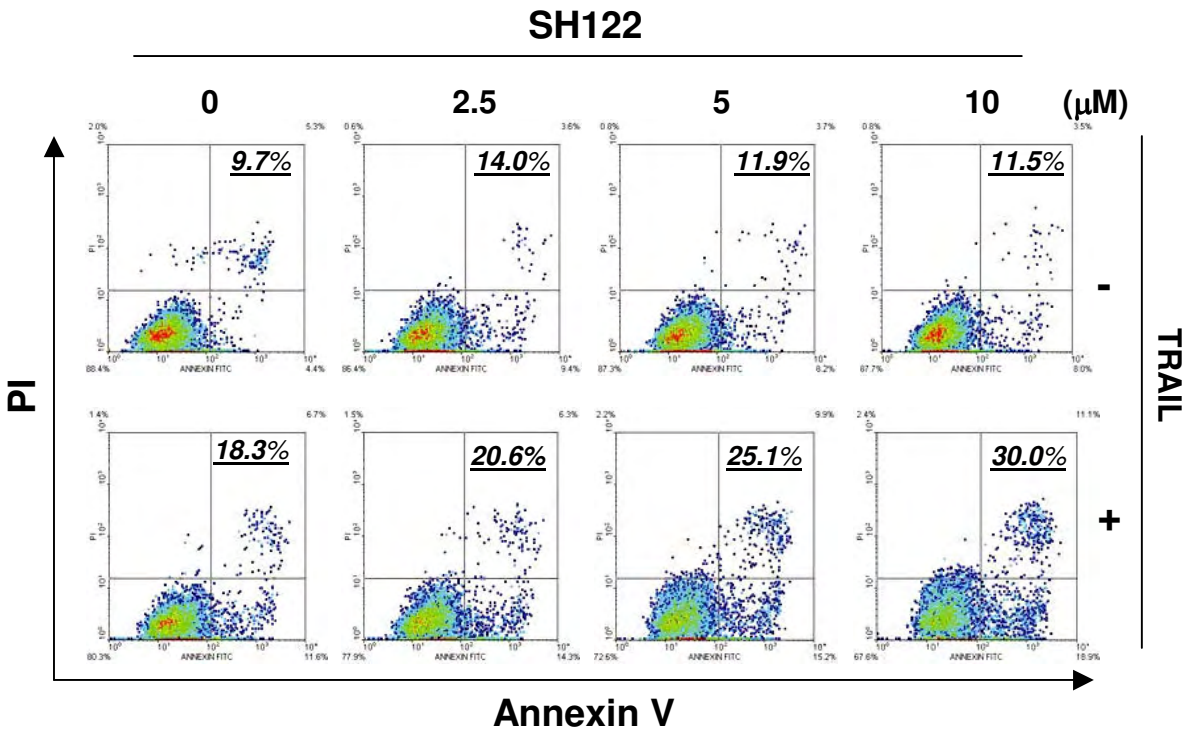

Figure 3

Fig. 4

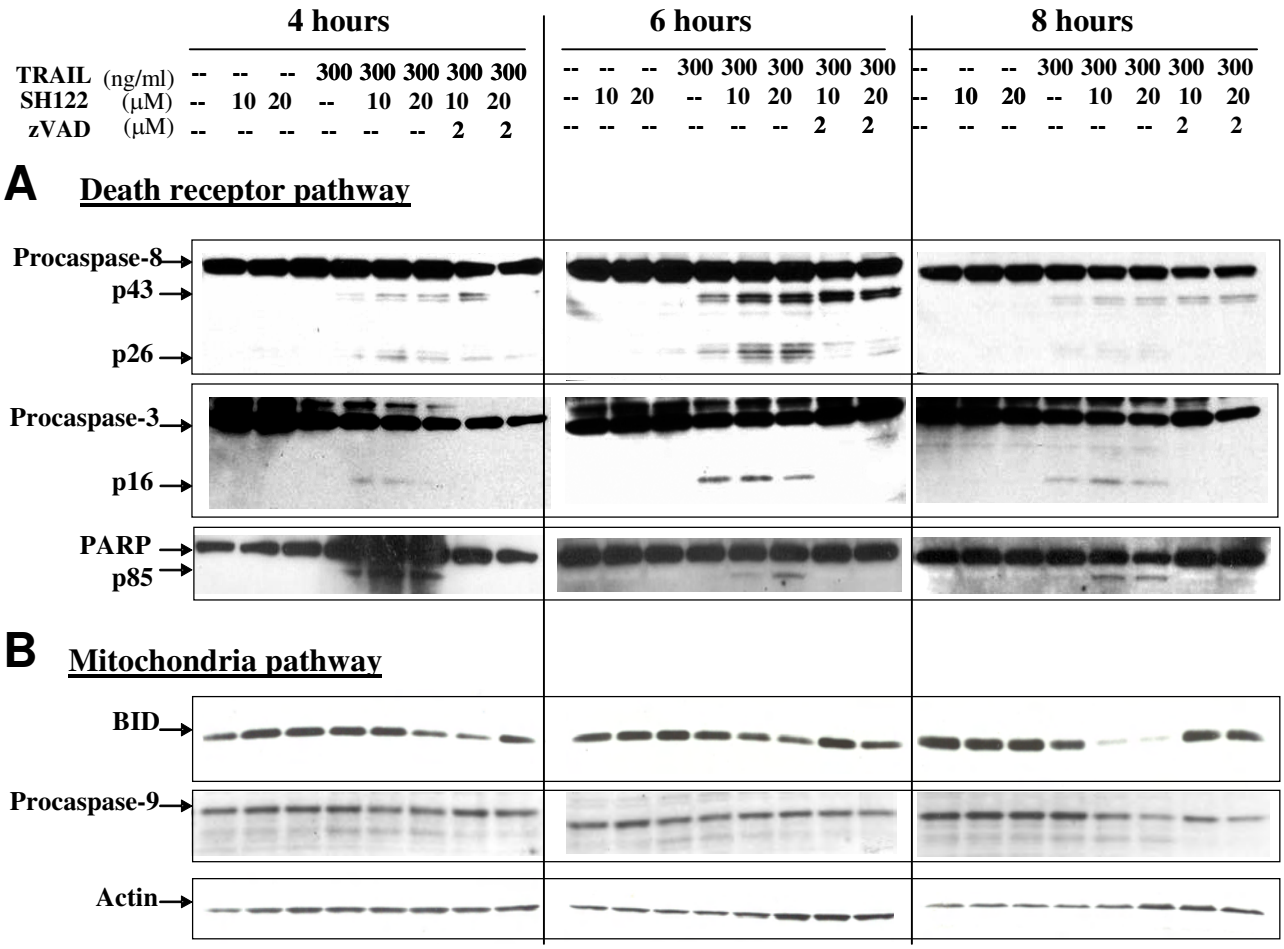

Figure 4

Fig. 5

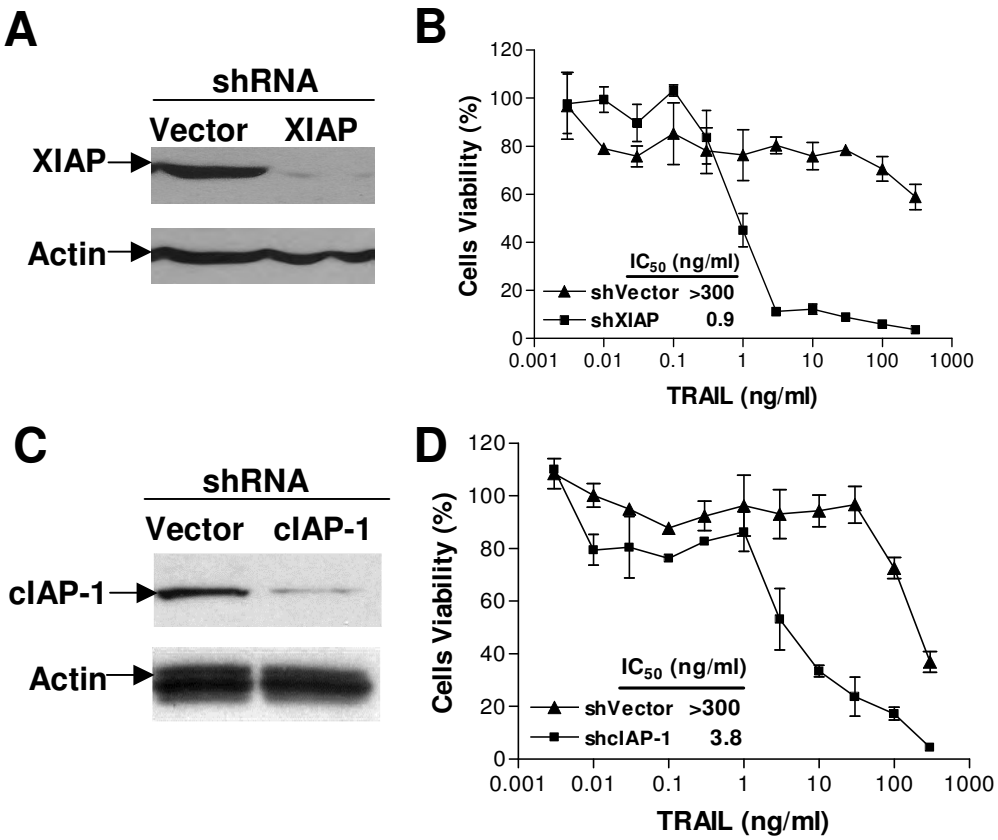

Figure 5

Fig. 6

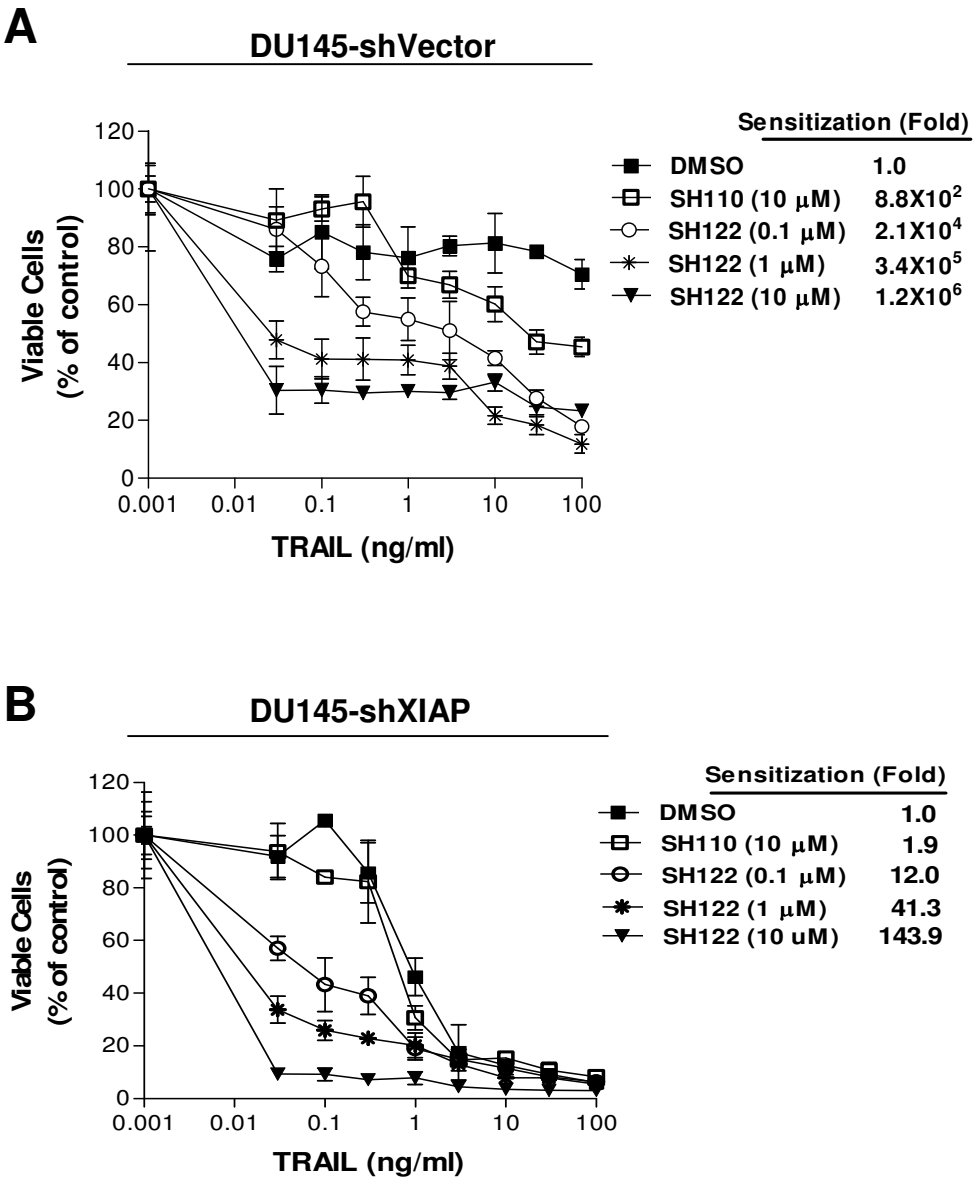

Figure 6

Fig. 7

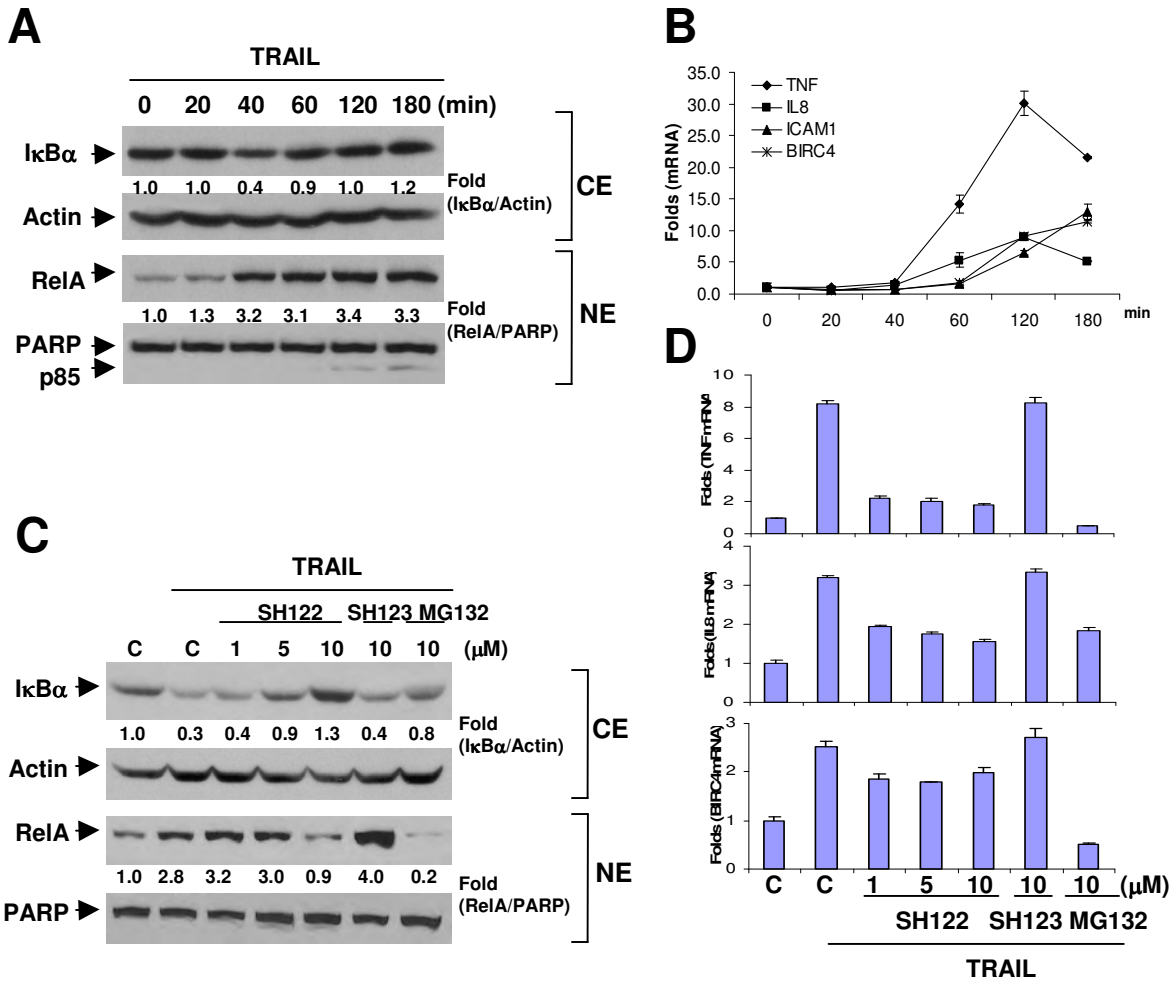
A
TRAIL
0 20 40 60 120 180 (min)
IκBα
1.0 1.0 0.4 0.9 1.0 1.2
Actin
Fold (IκBα/Actin)
CE
RelA
1.0 1.3 3.2 3.1 3.4 3.3
PARP
p85
Fold (RelA/PARP)
NE
B
TNF
IL8
ICAM1
BIRC4
Folds (mRNA)
min
C
TRAIL
SH122 SH123 MG132
C C 1 5 10 10 10 (μM)
IκBα
1.0 0.3 0.4 0.9 1.3 0.4 0.8
Actin
Fold (IκBα/Actin)
CE
RelA
1.0 2.8 3.2 3.0 0.9 4.0 0.2
PARP
Fold (RelA/PARP)
NE
D
C C 1 5 10 10 10 (μM)
SH122 SH123 MG132
TRAIL

Fig. 8

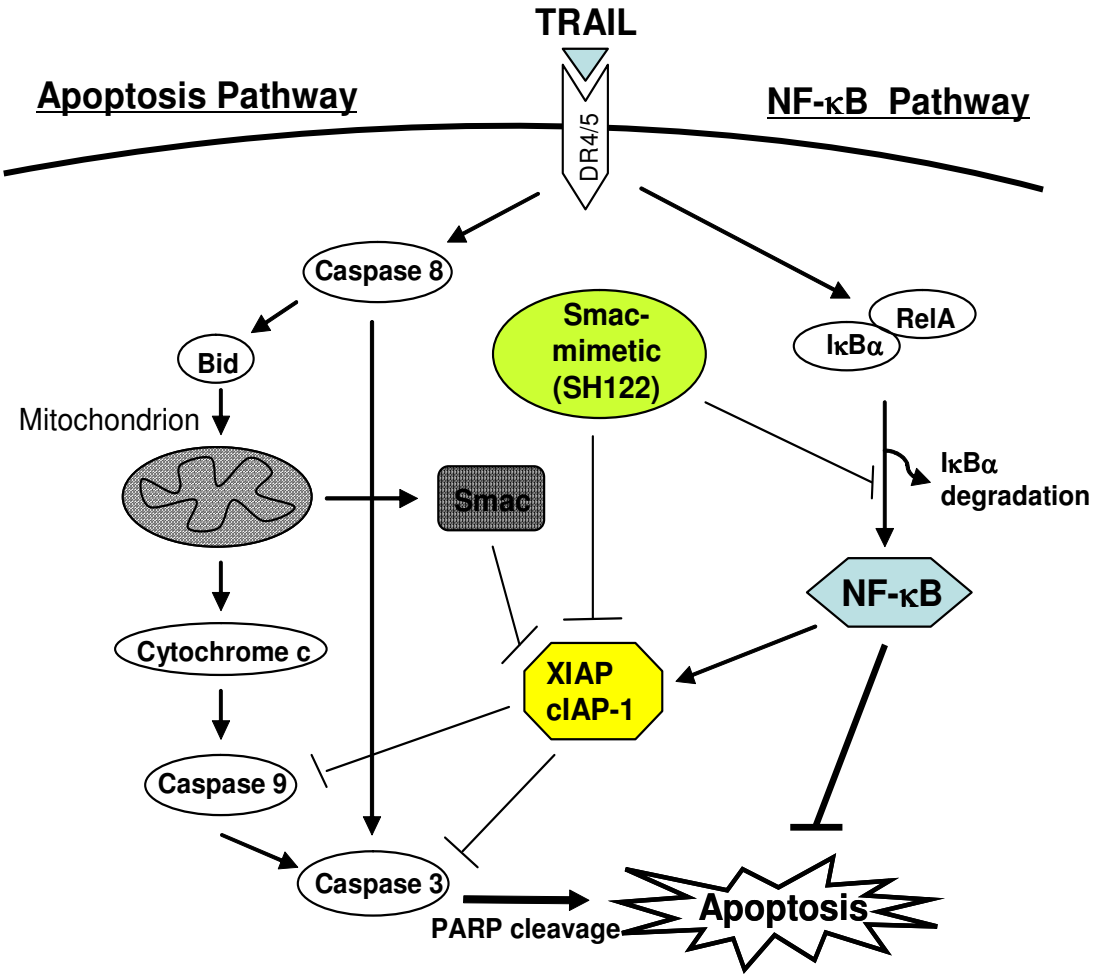

Figure 8